UNIVERSITY OF CALIFORNIA, SAN DIEGO

Sec24 phosphorylation regulates COPII vesicles during autophagy

A dissertation submitted in partial satisfaction of the
requirements for the degree Doctor of Philosophy

in

Biomedical Sciences

by

Saralin Morgan Davis

Committee in charge:

Professor Susan Ferro-Novick, Chair
Professor Seth Field
Professor Amy Kiger
Professor Peter Novick
Professor Karen Oegema

2016

The Dissertation of Saralin Morgan Davis is approved, and it is acceptable in quality and form for publication on microfilm and electronically:

Chair

University of California, San Diego

2016

DEDICATION

I dedicate this dissertation to my family for their continual support and for reminding me what is important in life.

TABLE OF CONTENTS

LIST OF ABBREVIATIONS

AMP	ampicillin
AP	adaptor protein
ATG	autophagy related
BSA	bovine serum albumin
CC	coiled-coil domain
CIP	calf intestine phosphatase
CK1∂	casein kinase 1 delta
COG	conserved oligmeric Golgi
COPI	coat protein complex I
COPII	coat protein complex II
CPY	carboxypeptidase Y
DFCP1	double FYVE domain-containing protein 1
DTT	dithiothreitol
ER	endoplasmic reticulum
ERES	ER exit sites
ERGIC	ER-Golgi intermediate compartment
ERMES	ER-mitochondria encounter structure
FOA	fluoroorotic acid
GAP	GTPase-activating protein
GDP	guanosine diphosphate
GEF	guanine nucleotide exchange factor

GFP	green fluorescent protein
GTP	guanosine-5’-triphosphate
HOPS	homotypic fusion and protein sorting
MBP	myelin basic protein
PACS2	phosphofurin acidic cluster sorting protein 2
PAS	pre-autophagosomal structure
PBS	phosphate buffered saline
PE	phosphatidylethanolamine
PI(3)P	phosphatidylinositol 4-phosphate
PIC	protease inhibitor cocktail
PMSF	phenylmethylsulfonyl
PtdIns	phosphatidylinositol
SD-N	synthetic minimal media lacking nitrogen
SIM	structured illumination microscopy
SMD	synthetic complete media
SNX	sorting nexin
SNARE	soluble N-ethylmaleimide sensitive factor attachment protein receptor
TBC1D5	TBC1 domain family member 5
TECPR2	tectonin beta-propeller containing protein 2
TGN	trans Golgi network
TOR	target of rapamycin
TRAPP	transport particle protein
TS	temperature sensitive

YCK	yeast casein kinase
WIPI	WD-repeat domain phosphoinositide-interacting

LIST OF FIGURES

LIST OF TABLES

ACKNOWLEDGEMENTS

I would like to first thank Dr. Susan Ferro-Novick for accepting me into her laboratory and for her essential guidance and support throughout this dissertation project. I was also fortunate to have many talented and helpful colleagues in the Ferro-Novick lab whose advice and friendship were invaluable to me during my time in graduate school. These colleagues include Juan Wang, Christopher Lord, Shekar Menon, Deepali Bhandari, Wenyun Zhou, Andrea Lougheed, Serena Cervantes, Shuliang Chen, Yixian Cai, Ming Zhu, Jinzhong Zhang, Jingzhen Ding and Shuaipeng Ma. I would also like to thank my thesis committee members who offered insightful comments and feedback and pushed me to think more critically about my work. This includes Dr. Seth Field, Dr. Amy Kiger, Dr. Peter Novick and Dr. Karen Oegema.

I also could not have completed this dissertation without my friends and family. My boyfriend John has been incredibly supportive of my graduate work as well as my future career choices. His love of life and adventure has made all aspects of my life in the last four years more fulfilling. Additionally, I can't thank him enough for the many late Sunday nights stopping into lab with me to set up cultures as well as his generous donation of Adobe programs and PyMol. I also have to thank the rest of the Yamauchi family. They have been so welcoming and supportive of me and have become part of my LA family. Additionally, I was fortunate to have made great friends during graduate school who have made the last six years truly enjoyable.

Lastly, I can't thank my family enough for their encouragement and guidance. My brother always made sure to check in with me and give me perspective during challenging times. My father and stepmom have always been there to support and encourage me. My grandparents have given me unconditional love and life advice that I will forever carry with me. Finally, my mom always went out of her way to encourage my educational pursuits and I would not be the person I am without the sacrifices she made and the confidence she has given me.

Chapter 1 is being prepared for submission for publication in Developmental Cell, with co-author Susan Ferro-Novick. The dissertation author is the primary author of this paper.

Most of the work in Chapter 2 and Chapter 3 is taken from "Sec24 phosphorylation regulates autophagosome abundance during nutrient deprivation" which has been submitted for publication and is currently under review at Elife. Juan Wang, Ming Zhu, Kyle Stahmer, Ramya Lakshminarayan, Majid Ghassemian, Yu Jiang, Elizabeth Miller and Susan-Ferro-Novick are co-authors. The dissertation author is the primary researcher of this paper. Other non-published work in this section was performed by the dissertation author unless otherwise noted.

Some of the work in Chapter 4 was performed by other researchers. Hua Yuan is a co-author of this chapter.

VITA

2010 Bachelor of Arts, Colby College

2016 Doctor of Philosophy, University of California, San Diego

Publications

Davis, S., Wang, J., Stahmer, K., Lakshminarayan, R., Ghassemian, M., Jiang, Y., Miller, EA., and Ferro-Novick, S. "Sec24 phosphorylation regulates autophagosome abundance during nutrient deprivation." *Elife,* Under revision.

Wang, J., Davis, S., Menon, S., Zhang, J., Ding, J., Cervantes, S., Miller, EA, Jiang, Y., and Ferro-Novick, S. "Ypt1/Rab1 regulates Hrr25/CK1∂ kinase activity in ER-Golgi traffic and macroautophagy." *J Cell Biol* 2015 210(2): 273-285.

Wang, J., Cervantes, S., Davis, S. and Ferro-Novick, S. "Identifying a rab effector on the macroautophagy pathway." *Methods Mol. Biol.* 2015 198:117-25.

Davis, S. and Ferro-Novick, S. "Ypt1 and COPII vesicles act in autophagosome biogenesis and the early secretory pathway." *Biochem. Soc. Trans.* 2015 43(1): 92-6.

Holly, JE, Davis, SM, and Sullivan, KE. "Differences between perception and eye movements during complex motions." *J Vestb. Res.* 21(4):193-208.

ABSTRACT OF THE DISSERTATION

Sec24 phosphorylation regulates COPII vesicles during autophagy

by

Saralin Morgan Davis

Doctor of Philosophy in Biomedical Sciences

University of California, San Diego, 2016

Professor Susan Ferro-Novick, Chair

Macroautophagy is a process of bulk degradation initiated during cellular starvation or stress. When macroautophagy (hereafter referred to as autophagy) is induced there is a rapid upregulation in the formation of autophagosomes; double membrane vesicles, which engulf cytoplasmic materials and organelles. After formation, autophagosomes fuse with the vacuole releasing their contents for

degradation, which is essential to maintain homeostasis during nutrient deprivation. Although the membrane source and trafficking events leading to autophagosome formation are poorly understood, recent findings have implicated endoplasmic reticulum (ER)-derived COPII vesicles in autophagosome biogenesis. During nutrient rich conditions, COPII vesicles work on the secretory pathway by transporting cargo from the ER to the Golgi. How the function of COPII vesicles is regulated to balance their roles in secretion and autophagy is unclear. Moreover, the molecular mechanism of how COPII vesicles recognize autophagy machinery to aid in autophagosome formation is unknown. The current understanding of the function of COPII vesicles and other parts of the secretory pathway in autophagy is discussed in Chapter 1.

The work in this dissertation examines how phosphorylation of Sec24, a subunit of the inner COPII coat, regulates autophagosome formation. In Chapter 2 we rule out a major role for Sec24 phosphorylation in regulating the secretory pathway. We next screened for Sec24 phosphorylation sites that are required for autophagy and not ER-Golgi transport. This analysis identified a patch of conserved phosphorylation sites that are required for autophagosome formation during starvation. Phosphorylation of these residues regulates autophagosome frequency and enhances the interaction of the COPII coat with Atg9, a key regulator of autophagosome initiation. Chapter 3 discusses the role of the serine/threonine kinase Hrr25 in regulating the Sec24-Atg9 interaction through Sec24 phosphorylation. Chapter 4 discusses the interacting domains of Uso1, a long coil-coiled tether that links COPII vesicles to the Golgi on the secretory pathway. Chapter 5 places these findings into the broader context of COPII vesicle trafficking and autophagosome formation.

Additionally, this final chapter gives recommendations for future studies to further our knowledge of the membrane rearrangements required for autophagosome initiation.

CHAPTER 1

The role of the secretory pathway in autophagosome formation

1.1 Summary

The induction of autophagy by starvation leads to a rapid increase in the formation of autophagosomes, unique organelles that replenish the cellular pool of nutrients by sequestering cytoplasmic material for degradation. The urgent need for membrane to form autophagosomes leads to a dramatic rearrangement of intracellular membranes to maintain homeostasis. Here we discuss recent findings that have begun to uncover how different parts of the secretory pathway directly and indirectly contribute to autophagosome formation during starvation.

1.2 Introduction

Macroautophagy (hereafter referred to as autophagy) is a highly conserved bulk degradation process that is rapidly upregulated to maintain homeostasis when cells are starved for nutrients. During autophagy, large double-membrane vesicles called autophagosomes non-selectively deliver cytoplasmic components to the vacuole or lysosome for degradation. In addition to non-selective autophagy, there are a variety of types of selective autophagy, which target a specific cargo for degradation. This dissertation will focus on non-selective starvation induced autophagy. For a recent review of selective autophagy see (Sica et al., 2015; Stolz et al., 2014). Although the mechanism of autophagosome formation has remained elusive, recent

findings have begun to unravel some of the key events in the process, which require the activation and recruitment of both specific autophagy-related (Atg) proteins and membrane trafficking machinery from the secretory pathway. The secretory pathway traffics membrane-bound and secreted proteins through a complex network of intracellular compartments. Recent studies have highlighted the early secretory pathway as a key player in autophagosome biogenesis. This introduction will outline the role of the secretory pathway and its associated trafficking machinery in contributing to autophagosome formation during starvation.

There are four major stages of autophagosome formation; initiation, expansion, closure and fusion with the endolysomal system (Lamb et al., 2013) (Figure 1.1). Upon autophagy induction, formation of the autophagosome is initiated adjacent to a pre-autophagosomal structure (PAS). The PAS was originally identified in the yeast *Saccharomyces cerevisiae* as a location where Atg proteins are recruited (Nakatogawa et al., 2009). A double track membrane, called the phagophore, or isolation membrane, extends from the PAS engulfing cytoplasmic materials and organelles. In mammalian cells, there is not a single PAS, rather there are multiple sites of autophagosome formation. Additionally, Atg proteins in mammalian cells are recruited to a domain of the endoplasmic reticulum (ER) termed the omegasome, which cradles the developing phagophore and appears to be functionally similar to the PAS in yeast (Axe et al., 2008; Hayashi-Nishino et al., 2009). After sealing, the outer membrane of the fully formed autophagosome fuses with the vacuole or lysosome where hydrolases degrade the delivered cargo. This catabolic process is upregulated

during nutrient deprivation, resulting in a dramatic increase in the number of autophagosomes that are formed. Additionally, in higher eukaryotes autophagy plays an important role in the pathophysiology of various diseases and is essential for proper development and immune response (Hale et al., 2013; Schneider and Cuervo, 2014).

Genetic screens in yeast first identified Atg proteins that are necessary for autophagosome formation (Mizushima et al., 2011; Nakatogawa et al., 2009). The Atgs can be grouped into six major complexes that are recruited to sites of autophagosome formation in a hierarchical manner (Suzuki et al., 2007). These complexes are well conserved and mammalian homologues have been identified for all key Atg proteins. The most upstream complex is the Atg1/Ulk1 initiating complex, which contains the serine/threonine kinase Atg1/Ulk1. In yeast Atg1 forms a complex with Atg13, Atg17, Atg29 and Atg31 (Kawamata et al., 2008; Ragusa et al., 2012), while in mammalian cells Ulk1 complexes with Atg13, FIP200 (mammalian Atg17) and Atg101, which is absent in budding yeast (Hosokawa et al., 2009; Jung et al., 2009; Qi et al., 2015). When autophagy is induced, the initiating complex activates Atg1/Ulk1 kinase activity and recruits downstream Atg complexes, including the multispanning transmembrane protein Atg9, followed by the autophagy specific class III phosphatidylinositol 3-kinase (PI3K) complex (Rao et al., 2016; Suzuki et al., 2015). The PI3K complex generates phosphatidylinositol-3-phosphate (PI(3)P) at the PAS by phosphorylating phosphatidylinositol (PI) at the 3-position hydroxyl group. PI(3)P is needed for the recruitment of the PI(3)P-binding protein Atg18 (WIPI2 in

mammals) and its partner Atg2, which are involved in Atg9 recycling (Obara et al., 2008; Reggiori et al., 2004).

The most downstream Atg complexes are the two ubiquitin-like conjugation systems, Atg12 and Atg8. The Atg12 system results in the formation of the Atg16/Atg12/Atg5 complex, which is thought to act as an E3 ligase for the conjugation of Atg8 (LC3 in mammals) to phosphatidylethanolamine (PE) (Hanada et al., 2007; Noda et al., 2013). The Atg16/Atg5/Atg12 complex localizes to the outer membrane of the autophagosome and is released before vacuole fusion (Kuma et al., 2002). Conversely, Atg8-PE is embedded in both the inner and outer autophagosomal membrane and some Atg8 is delivered with the autophagosome to the vacuole (Kirisako et al., 1999). As a result, Atg8/LC3 is a commonly used marker for both the phagophore and mature autophagosome. Atg8 has been reported to regulate the later stages of autophagosome formation including expansion and closure (Nakatogawa et al., 2007; Xie et al., 2008). However, the mechanism of how Atg8 mediates membrane expansion remains unclear. Additionally, while the recruitment of the Atg complexes to sites of autophagosome formation is well defined, how these complexes work with trafficking machinery to coordinate the membrane rearrangements required for autophagosome formation is only beginning to emerge.

1.3 The Early Secretory pathway

The endoplasmic reticulum (ER) has been implicated as a critical organelle for the early stages of autophagosome formation. In mammalian cells Atg proteins are recruited to the ER upon autophagy induction and the growing phagophore or isolation

membrane is cradled between sheets of ER-associated membrane called the omegasome (Axe et al., 2008; Hayashi-Nishino et al., 2009). The omegasome is a PI(3)P enriched region of the ER that was originally identified by localization studies with the PI(3)P binding protein DFCP1 and named for its Ω-shape. Formation of the omegasome occurs de novo during starvation and is dependent on the PI3K complex (Axe et al., 2008). This PI(3)P enriched subdomain of the ER enwraps the phagophore as it expands, with occasional connections between the two membranes (Hayashi-Nishino et al., 2009). Before full maturation, the autophagosome is released and the omegasome contracts back to the ER. Recently, specific subdomains of the ER, ER Exit Sites (ERES) and ER-mitochondria contact sites, have been implicated as sites of autophagosome biogenesis.

1.3.1 ER Exit Sites

ERES are domains of the ER where COPII vesicles, that transport cargo between the ER and the Golgi, are formed (Budnik and Stephens, 2009). Assembly of the COPII coat is initiated at ERES by the GTPase Sar1. Activated Sar1 becomes anchored to the ER membrane to recruit the inner COPII coat (Sec23/Sec24), or coat adaptor, that sorts cargo into the vesicle. The coat adaptor recruits the outer shell (Sec13/Sec31), which leads to membrane deformation and vesicle budding (Lord et al., 2013; Zanetti et al., 2011). After vesicle budding, Sar1 is released from the vesicle (Barlowe et al. 1994), however, the adaptor and outer shell of the coat remain on the vesicle until it docks with its target membrane (Cai et al. 2007; Lord et al., 2011)

(Figure 1.2). The COPII coat adaptor plays an important role in targeting the vesicle to its acceptor membrane (Cai et al., 2007; Lord et al., 2011).

Proteomics has recently linked the ERES to the autophagy machinery (Graef et al., 2013), and Atg proteins were found to assemble adjacent to the ERES (Graef et al., 2013; Suzuki et al., 2013). In particular, the growing edge of the phagophore, where Atg9 and Atg2 localize, was shown to face the ERES (Graef et al., 2013; Suzuki et al., 2013). In mammalian cells, LC3 puncta colocalize with the ER-marker Sec61 and Sec16, a scaffold protein that interacts with multiple COPII coat subunits at the ERES to regulate coat assembly (Graef et al., 2013). Furthermore, loss of function temperature-sensitive mutations in genes that encode secretory machinery such as *SEC16* or *SEC12*, the guanine nucleotide exchange factor (GEF) for Sar1, inhibit autophagosome formation (Graef et al., 2013; Ishihara et al., 2001). Disruption of ERES by knockdown of Sar1 or TECPR2, a protein that is required for the stability of SEC24D in mammalian cells, also inhibits autophagosome formation at an early stage (Stadel et al., 2015; Zoppino et al., 2010). ERES have been proposed to function in autophagy through the production of COPII vesicles, which may directly provide membrane for the growing phagophore. Alternatively, ERES may act as a platform on which Atg proteins and the phagophore assemble (Sanchez-Wandelmer et al., 2015). Although these models are not entirely mutually exclusive, a growing body of evidence favors the former model.

1.3.2 COPII vesicles

Almost 15 years ago, mutants that block the early secretory pathway were also shown to block autophagy (Hamasaki et al., 2003; Ishihara et al., 2001). However, it was argued that these mutants were inhibiting autophagy indirectly by disrupting the flow of membrane traffic from the ER (Hamasaki et al., 2003). Recent work has begun to separate out the function of COPII vesicles in autophagy from their role in secretion, demonstrating that COPII vesicles directly act in autophagosome formation.

Supporting a direct role for COPII vesicles in autophagy, COPII coated structures accumulate at the PAS when autophagy is blocked (Tan et al., 2013). Although mutations in the COPII vesicle trafficking machinery broadly inhibit autophagy, a notable exception is the tether Uso1, which links COPII vesicles to the Golgi (Tan et al., 2013). This finding indicates that general ER-Golgi traffic is not required for autophagy. ER-Golgi SNAREs (type II membrane proteins required for fusion (Jahn and Scheller, 2006)), which are normally packaged into COPII vesicles, are also required for autophagy (Nair et al., 2011; Tan et al., 2013) as is the ER localized SNARE, Ufe1. A recent study suggested that Ufe1 might traffic to sites of autophagosome formation in a special class of COPII vesicles (Lemus et al., 2016).

While the findings described above are consistent with a role for COPII vesicles in autophagosome formation, how the vesicle recognizes the autophagy machinery is unclear. In line with previous findings showing that the COPII coat actively targets the vesicle to its final intracellular destination (Cai et al., 2007; Lord et al., 2013), a recent study has shown that during nutrient deprivation, Sec24 plays a

pivotal role in engaging the vesicle with the Atg machinery. In particular, phosphorylation of a cluster of amino acids on the membrane distal surface of Sec24 was shown to commit COPII vesicles to autophagy. Mutating these phosphorylation sites to alanine specifically disrupted autophagosome formation, but not ER-Golgi transport (Davis et al., In Revision). Furthermore, phosphorylation of this Sec24 regulatory surface was found to modulate autophagosome abundance during starvation via the ability of Sec24 to interact with Atg9. Casein kinase 1, Hrr25, is a key kinase that phosphorylates this Sec24 surface. These phosphorylation events were found to be independent of the assembly of the Atg hierarchy (Davis et al., In Revision). Together these findings show that phosphorylation regulates membrane rearrangements during starvation induced autophagy and the COPII coat is a target of this regulation.

Membrane fractionation also identified the mammalian ER-Golgi intermediate compartment (ERGIC) as required for LC3 lipidation in an in vitro reaction (Ge et al., 2013). The ERGIC is a site of both COPII vesicle fusion and COPI vesicle budding, COPI vesicles mediate multiple trafficking events including retrograde traffic from the ERGIC to the ER (Lorente-Rodriguez and Barlowe, 2011). While the relationship of the omegasome to this ERGIC fraction is unclear, the ERES were found to move to the ERGIC fraction when autophagy was induced. Interestingly, it was shown that the budding of COPII, but not COPI vesicles, from this ERGIC fraction is required for LC3 lipidation (Ge et al., 2014). COPII vesicles were also found to relocalize to the ERGIC during starvation and this event was dependent on PI3-kinase activity (Ge et

al., 2014). Other components required for autophagy also translocate to sites of autophagosome formation in a PI3K-dependent manner when autophagy is induced (Axe et al., 2008). The collective findings discussed above suggest that only those translocated COPII vesicles with phosphorylated Sec24, and the appropriate SNAREs, contribute to autophagosome formation (Figure 1.2).

1.3.3 ER-Mitochondria Contact Sites

ER-mitochondria contact sites are locations of non-vesicular lipid transfer (Phillips and Voeltz, 2014) that have also been proposed to be sites of autophagosome biogenesis. Key autophagy machinery such as Atg14, part of the PI3K complex, and Atg5 localize to ER-mitochondria contact sites during starvation in a manner dependent on the SNARE Stx17 (Hamasaki et al., 2013). Stx17 is required late in autophagy for autophagosome-lysosome fusion (Diao et al., 2015). Disruption of ER-mitochondria contact sites via knockdown of PACS2, a cytosolic-sorting protein that uncouples the mitochondria from the ER, or mitofusin 2, an ER-mitochondria tether, disrupts autophagosome formation at an early stage. Live cell imagining revealed that the ER is the dominant platform for autophagosome biogenesis with the mitochondria interacting more dynamically (Hamasaki et al., 2013). Interestingly, a significant fraction of the COPII coat subunit Sec31 was also reported to colocalize with ER-mitochondria markers during starvation, raising the possibility there could be a connection between COPII vesicles and ER-mitochondria contact sites (Tan et al., 2013).

As the basic mechanism of autophagy is well conserved from yeast to man, an essential role for mitochondria in the biogenesis of the autophagosome should be conserved. In yeast, however, a role for ER-mitochondria contact sites in autophagy has not been substantiated. ERMES, a critical tether for maintaining ER-mitochondria contact sites, is required for selective autophagy of the mitochondria (mitophagy), but not general autophagy (Bockler and Westermann, 2014). Additionally, mitochondria were not found to colocalize significantly with the PAS, phagophores or autophagosomes (Graef et al., 2013).

1.4 The Golgi/Endosome/Plasma Membrane

The Golgi, endosome and plasma membrane have all been implicated in autophagosome formation. Recent findings suggest the contribution of each of these organelles is largely through the regulation of Atg9 and Atg16 trafficking. In this section we will discuss the role that each of these organelles plays in the constitutive trafficking of Atg9 and Atg16 as well as the delivery of these Atg proteins to sites of autophagosome formation.

1.4.1 Atg9

As mentioned above, the multispanning Atg9 transmembrane protein is necessary for the recruitment of downstream Atg proteins, including the Atg2/Atg18 (WIPI2) complex and the PI3K complex (Suzuki et al., 2007; Suzuki et al., 2015). In yeast, Atg9 is incorporated into the autophagosomal membrane, but is recycled before the autophagosome fuses with the vacuole (Yamamoto et al., 2012). Although mammalian Atg9 (mAtg9) is required for formation of the omegasome (Orsi et al.,

2012), it does not appear to incorporate into the autophagosomal membrane, rather it localizes to tubular-vesicular clusters adjacent to sites of autophagosome formation (Orsi et al., 2012). More recent studies suggest that while mAtg9 has a complex trafficking route, it associates with Atg16L1 in Rab11 positive recycling endosomes, which may function as an autophagosome precursor (Puri et al., 2013).

Yeast Atg9 must pass through the early secretory pathway before it localizes to endosomal compartments (Ohashi and Munro, 2010). When cells are deprived of nutrients, however, Atg9 traffics from the endosome to the late Golgi, prior to its delivery to the PAS. The primary Atg9 trafficking pathway appears to be the early endosome-Golgi pathway (Shirahama-Noda et al., 2013), which is mediated by the sorting nexin Atg24 and the TRAPPIII complex that activates the Rab GTPase Ypt1 (Lynch-Day et al., 2010). During starvation, late endosome-Golgi bypass trafficking pathways may also exist to help ensure sufficient Atg9 is transported to sites of autophagosome formation during periods of stress (Ohashi and Munro, 2010; Shirahama-Noda et al., 2013) (Figure 1.3).

Upon autophagy induction, Atg9 vesicles form from the late-Golgi in an Atg23 and Atg27 dependent manner (Yamamoto et al., 2012). Atg23 is a peripheral membrane protein and Atg27 is a single-pass transmembrane protein. Atg23 and Atg27 form a complex with Atg9 (Legakis et al., 2007) and regulate the amount of Atg9 that is incorporated into vesicles (Backues et al., 2015). Atg9 vesicles are recruited to the PAS through the Atg1 initiating complex. Specifically, the N-terminal cytoplasmic domain of Atg9 was shown to interact with the HORMA domain of

Atg13, which is required for Atg9 PAS recruitment (Suzuki et al., 2015). Additionally, the Atg9 core was reported to interact with Atg17 (Rao et al., 2016). The Atg9 binding region of Atg17 is inhibited by Atg29-Atg31, but incorporation of Atg1-Atg13 into the complex relieves this inhibition, allowing Atg17 to interact with Atg9 (Rao et al., 2016). At the PAS, Atg1 phosphorylates the C-terminus of Atg9, which facilitates the recruitment of Atg18 (Papinski et al., 2014). Atg18 and its binding partner Atg2 regulate Atg9 recycling from the autophagosome through an unknown mechanism (Reggiori et al., 2004).

Multiple SNAREs have been implicated in Atg9 trafficking and autophagy. The exocytic SNARES Sso1/Sso1 and Sec9 as well as the late Golgi SNARE Tlg2 have been proposed to regulate Atg9 trafficking to the PAS (Nair et al., 2011). Tlg2, which is required for endosome to Golgi traffic, only displays a severe autophagy defect when combined with other endosome-Golgi mutants, consistent with the observation that Atg9 uses multiple trafficking pathways during nutrient deprivation (Ohashi and Munro, 2010). Interestingly, the functionally redundant exocytic SNAREs Snc1/2 are not required for autophagy (Nair et al., 2011). Currently, it is unknown which SNAREs are present on Atg9 vesicles that are delivered to the PAS and which are required for Atg9 traffic. In the future it will be important to distinguish those SNAREs which are directly required for autophagosome formation, from those needed for Atg9 transport.

mAtg9 follows a similar, albeit slightly more complex, trafficking network as it has been reported to localize to the trans-Golgi network (TGN) as well as early, late

and recycling endosomes (Young et al., 2006). When autophagy is induced, mAtg9 disperses from the TGN to peripheral endosome compartments (Young et al., 2006). mAtg9 is thought to traffic to the plasma membrane where it is endocytosed in AP2 vesicles and then transported through the early endosome to the recycling endosome (Popovic and Dikic, 2014; Puri et al., 2013). The RabGAP TBCD15 interacts with mAtg9 and AP2 during starvation to facilitate Atg9 trafficking from the plasma membrane (Popovic and Dikic, 2014). mAtg9 has been reported to form tubular-vesicular clusters from perinuclear Rab11-positive recycling endosomes. Tubulation of Rab11 recycling endosomes is induced upon nutrient deprivation and is dependent on the curvature inducing protein Bif-1 and dynamin 2 (Takahashi et al., 2016). Atg9 tubular-vesicular clusters are ultimately recruited adjacent to sites of autophagosome formation (Orsi et al., 2012), and this recruitment is independent of Ulk1 (Orsi et al., 2012) (Figure 1.3). Whether mAtg9 recruitment requires FIP200 or Atg13 is unknown. FIP200 shares little sequence similarity with Atg17 and the region of yeast Atg9 that interacts with Atg13 is not conserved, indicating mAtg9 may be recruited to sites of autophagosome formation through a different mechanism.

1.4.2 Atg16

Similar to Atg9, Atg16 relies on trafficking machinery for its proper localization and function. Atg16 is a peripheral membrane protein that forms a complex with Atg5-Atg12. Together Atg5-Atg12-Atg16 acts as an E3 like enzyme catalyzing the conjugation of Atg8/LC3 to PE. Thus, Atg16 has been proposed to be the key determinant for the location of Atg8 lipidation (Fujita et al., 2008). In

mammalian cells, Atg16L1 associates with clathrin coated pits and is endocytosed from the plasma membrane in distinct vesicles from mAtg9 (Puri et al., 2013; Ravikumar et al., 2010). After endocytosis, Atg16L1 may undergo homotypic fusion which is dependent on the SNARE VAMP7 (Moreau et al., 2011). Atg16L1 then coalesces with mAtg9 in Rab11-positive recycling endosomes. This fusion event is directed by another SNARE, VAMP3 (Puri et al., 2013). Recruitment of Atg16L1 to recycling endosomes is dependent on SNX18, a sorting nexin that binds PtdIns(4,5)P_2 (Knaevelsrud et al., 2013). During starvation, SNX18 recruits Rab11 to perinuclear recycling endosomes where together they recruit Atg16L1 (Knaevelsrud et al., 2013) (Figure 1.3). It is unknown if Atg16 is trafficked by a similar mechanism in lower eukaryotes. Additionally, the precise relationship between the omegasome and Atg16L1 recycling endosomes is unclear. While it has been proposed that SNX18 induces the tubulation of the recycling endosome to contribute membrane to the expanding phagophore (Knaevelsrud et al., 2013), it cannot be ruled out that the Atg16L1 recycling endosome mainly functions by facilitating Atg16L1 transport. A better understanding of the fusion events involved in delivering Atg16L1 to the omegasome would help clarify its contribution to autophagosome biogenesis. Furthermore, the relationship between the SNX18/Atg16L1 tubules and the recently described Bif-1/mAtg9 tubules, which both form from the perinuclear recycling endosome, has not been explored.

During starvation, Atg16L1 is recruited to sites of autophagosome formation. Atg16 recruitment to the PAS is dependent on its complex partner Atg5 and PI(3)P

(Suzuki et al., 2007). PI(3)P helps recruit Atg16 in part through Atg21, which interacts with both PI(3)P and Atg16, although additional factors likely help recruit Atg16 during starvation (Juris et al., 2015). In mammalian cells, after trafficking to the recycling endosome, Atg16L1 is recruited to the omegasome by the PI(3)P binding protein WIPI2b (Dooley et al., 2014). Although Atg16L1 also interacts with FIP200 (Nishimura et al., 2013), this interaction does not appear to be essential for autophagy and cannot explain the dependence of Atg16L1 recruitment on PI(3)P (Dooley et al., 2014).

1.5 Tethers and tethering factors

Tethers are essential membrane trafficking machinery that physically connect vesicles with their target membrane. They also facilitate the transition from vesicle tethering to fusion by binding to SNAREs and promoting SNARE complex assembly (Hong and Lev, 2014). Tethers are typically effectors of Rab GTPases, which act as molecular switches cycling between their inactive GDP-bound state and active GTP-bound state (Mizuno-Yamasaki et al., 2012). Tethers can be divided into two main subgroups; multisubunit complexes and long coiled-coil tethers. Long coiled-coil tethers include p115 (Uso1 in yeast) and the Golgins. The multisubunit complexes include COG (conserved oligomeric Golgi), the exocyst and HOPS (homotypic fusion and vacuole sorting protein), which will be discussed in this section. We will also discuss the TRAPP (transport particle protein) complexes here. While the TRAPP complexes are unlikely to directly tether membranes, they are tethering factors that participate in membrane tethering events (Lord et al., 2011). Some tethers and

tethering factors function directly in autophagosome formation and autophagosome-lysosome fusion, while others act indirectly by regulating the trafficking of Atg9 (Figure 1.4).

1.5.1 TRAPP

The guanine nucleotide exchange factor (GEF) for the Rab GTPase Ypt1, TRAPP, was originally identified in yeast where it forms 3 distinct complexes; TRAPPI, TRAPPII and TRAPPIII. TRAPPI is required for ER-Golgi transport, TRAPPII is needed for Golgi traffic, and TRAPPIII functions in autophagy (Barrowman et al., 2010). These three complexes share a core set of 6 subunits. In addition to the core subunits, TRAPPII and TRAPPIII contain adaptor subunits that target each of these complexes to different parts of the cell. Recent work has shown that TRAPPIII, which contains the unique subunit Trs85, is required for autophagy (Lynch-Day et al., 2010). Trs85 interacts with autophagy machinery at the PAS and maintains Golgi to endosome traffic, which is needed for constitutive Atg9 trafficking. The single-particle EM structure of TRAPPIII revealed that Trs85 caps one end of the elongated core TRAPPI structure (Tan et al., 2013). The Bet3 subunit, present in all three complexes, interacts with the COPII coat subunit Sec23 (Cai et al., 2007). The structure of TRAPPIII revealed that the addition of Trs85 to the complex does not obscure the Sec23 binding site on Bet3. In vitro binding studies confirmed that TRAPPIII binds to Sec23 (Tan et al., 2013). Therefore, similar to TRAPPI, TRAPPIII likely functions in part by activating Ypt1 on COPII vesicles. TRAPPIII, which is recruited to the PAS by Atg17, is needed for the PAS recruitment of Ypt1 and

autophagosome formation (Lynch-Day et al., 2010; Wang et al., 2013). Ypt1 functions at the PAS by recruiting effectors that include Atg1 and the CK1 kinase Hrr25 (Wang et al., 2015; Wang et al., 2013). Inhibiting Ypt1 function or COPII vesicle budding diminishes the recruitment of Hrr25 to the PAS, suggesting CK1 is delivered to the PAS by activated Ypt1 residing on COPII vesicles (Wang et al., 2015).

In addition to its role in regulating the recruitment of Ypt1 to the PAS, TRAPPIII also facilitates endosomal to Golgi transport and Atg9 trafficking (Shirahama-Noda et al., 2013). Supporting a role for TRAPPIII in Atg9 traffic, Trs85 was found on Atg9 vesicles and it partially colocalizes with Atg9 (Kakuta et al., 2012; Lynch-Day et al., 2010). Although TRAPPIII is essential for Atg9 trafficking during nutrient rich conditions, late endosome to Golgi bypass pathways exist during starvation that mask this requirement (Shirahama-Noda et al., 2013). Atg9 was also reported to recruit Trs85 to the PAS (Kakuta et al., 2012), however, others have found no effect on Trs85 recruitment in *atg9*Δ cells (Lynch-Day et al., 2010; Wang et al., 2013). Currently, it is unclear how TRAPPIII is recruited to the late-Golgi/early endosome to regulate early endosome traffic. Interactions with different vesicle coat complexes (COPII and COPI) have been shown to recruit TRAPPI and TRAPPII to the ER to Golgi (COPII) and Golgi (COPI) trafficking pathways respectively (Cai et al., 2007; Yamasaki et al., 2009). Whether TRAPPIII is engaged by a similar mechanism is unknown.

In mammalian cells, two forms of TRAPP have been identified: a TRAPPIII-like and TRAPPII-like complex (Bassik et al., 2013; Wang et al., 2013; Yamasaki et al., 2009). The mammalian TRAPPIII-like complex regulates both secretion and autophagy and contains TRAPPC8, the mammalian homologue of Trs85. Knockdown of TRAPPC8 disrupts Golgi integrity and general secretion (Lamb et al., 2016; Scrivens et al., 2011). Additionally, during starvation, knockdown of TRAPPC8 reduces the number of omegasomes, indicating it is required for autophagy at an early stage (Lamb et al., 2016). Similarly, Rab1a is required for autophagosome formation and in particular omegasome formation (Huang et al., 2011; Zoppino et al., 2010). TRAPPC8 was recently found to directly interact with the RAP GAP TBC1D14. TBC1D14 overexpression was previously shown to inhibit autophagy by inducing the formation of an enlarged, Ulk1-positive tubulated recycling endosome (Longatti et al., 2012). TBC1D14 and TRAPPC8 work together to regulate constitutive mAtg9 trafficking from Rab11-positive recycling endosomes to a Rab1-positive Golgi compartment (Lamb et al., 2016). While TRAPPC8 is critical for constitutive mAtg9 trafficking to the Golgi, it did not affect the co-localization of Atg9 with LC3 during starvation (Lamb et al., 2016). Although the roles of the mammalian TRAPP complexes are still being elucidated, thus far the general function of TRAPPIII in autophagosome formation and constitutive Atg9 trafficking appears to be largely conserved.

1.5.2 Cog

The conserved oligmeric Golgi complex (COG), which regulates intra-Golgi traffic via COPI coated vesicles (Willett et al., 2013), has been implicated in autophagy in yeast via its ability to regulate Atg9 traffic. COG is comprised of eight subunits, divided into two lobes, lobe A and lobe B. Disruptions in the essential lobe A COG subunits inhibit autophagosome formation (Yen et al., 2010). In particular, COG was found to affect the anterograde trafficking of Atg9 to the PAS. This is consistent with proper Golgi transport needed for Atg9 PAS delivery. COG was also suggested to play additional roles in tethering membranes at the PAS (Yen et al., 2010), although future work will be required to validate this model. The trafficking function of COG is well conserved in mammalian cells (Willett et al., 2013), but a role for COG in mammalian autophagy has not yet been identified.

1.5.3 Exocyst

The exocyst is an octameric complex that regulates the tethering of post-Golgi secretory vesicles to the plasma membrane (Munson and Novick, 2006). In mammalian cells two exocyst subunits, Exo84 and Sec5, are effectors of the Ras-like GTPase RalB (Moskalenko et al., 2002; Moskalenko et al., 2003). RalB was shown to be required for autophagosome formation and its activity was found to be enhanced during starvation. RalB promoted the assembly of Exo84 with the PI3K complex (Atg14L, Beclin1, Vps34), which assembles with activated Ulk1 (Bodemann et al., 2011). Beclin1 also formed a complex with another exocyst subunit, Sec5, which disassembles in a RalB dependent manner during starvation (Bodemann et al., 2011).

Therefore, RalB was hypothesized to function as a switch during autophagy to regulate the assembly of an Atg initiation complex, which employs an exocyst subcomplex as a platform. The role of the exocyst in autophagy, however, has recently been called into question. Findings in *Drosophila* show that the Ral GTPase and the exocyst are not needed for starvation-induced autophagy and only act during development in an autophagy pathway associated with cell death (Tracy et al., 2016). In yeast, there have been conflicting reports on whether exocyst subunits are required for autophagy (Geng et al., 2010; Ishihara et al., 2001; Nair et al., 2011). The GTPase Sec2 and its GEF Sec4, which associate with the exocyst, have been shown to contribute to autophagy by regulating Atg9 trafficking to the PAS.

1.5.4 HOPS

HOPS works with the Rab GTPase Ypt7/Rab7 to regulate multiple tethering and fusion events at the vacuole/lysosome. During autophagy, HOPS and Ypt7/Rab7 are required for autophagosome fusion with the vacuole/lysosome. In yeast, deletion of HOPS subunits and Ypt7 results in the accumulation of autophagosomes in the cytoplasm (Kirisako et al., 1999; Rieder and Emr, 1997). However, a clear role for HOPS in autophagosome fusion in higher eukaryotes has only recently emerged. Knockdown of multiple HOPS subunits leads to the accumulation of autophagosomes in both mammalian cells and *Drosophila* (Jiang et al., 2014; Takats et al., 2014). Additionally, HOPS subunits were shown to interact with the autophagosomal SNARE, Stx17, which helps recruit HOPS to the autophagosome (Jiang et al., 2014; Takats et al., 2014). A role for the HOPS-Stx17 interaction in autophagy has

subsequently been confirmed in a mouse model (Zhen and Li, 2015). HOPS has also been proposed to be linked to autophagosomes in mammalian cells by another Rab7 effector, Pleckstrin homology domain containing protein family member 1 (PLEKHM1). PLEKHM1 is thought to connect LC3 on autophagosomes with HOPS through binding the C-terminus of the VPS34 subunit (McEwan et al., 2015).

HOPS shares a core set of subunits with another tethering complex called CORVET, that regulates early to late endosome maturation (Balderhaar and Ungermann, 2013). HOPS and CORVET also contain additional unique subunits that interact with different Rabs, Rab7 (HOPS) and Rab5 (CORVET) (Balderhaar and Ungermann, 2013). Although subunits only present in CORVET have been implicated in autophagy in yeast (Chen et al., 2014), the Drosophilia CORVET specific subunit, *fob/Vps16B*, is not required for autophagy (Takats et al., 2014).

1.6 Concluding Remarks

Recent studies have highlighted the importance of the secretory and endocytic trafficking pathways in the transport of Atg proteins to sites of autophagosome formation during starvation. Additionally, the early secretory pathway has been shown to play a direct and critical role in contributing membrane to autophagosome formation. The COPII coat, in particular, facilitates the delivery of membrane and SNAREs to sites of autophagosome formation via its ability to recognize the Atg machinery. While it is not clear if the late secretory and endocytic pathways directly contribute membrane to autophagosome formation, key autophagy proteins, such as Atg9 and Atg16, use these pathways during nutrient deprivation. These Atgs proteins

have a complex tightly coordinated trafficking itinerary that regulates their delivery to sites of autophagosome formation.

Although significant progress has been made in understanding the initiation of autophagosome formation, the precise mechanism by which the autophagosomal membrane expands and closes has remained elusive. Additional studies will be needed to determine if the secretory pathway also contributes to this event. While this review has focused on autophagosome formation during starvation induced autophagy, recent work has highlighted the importance of other types of autophagy pathways that also use autophagosomes (Sica et al., 2015). These selective autophagy pathways target a particular cargo, often a damaged organelle or protein aggregate, for degradation. Future work will be required to determine if the secretory pathway also plays a role in forming autophagosomes on these less characterized pathways.

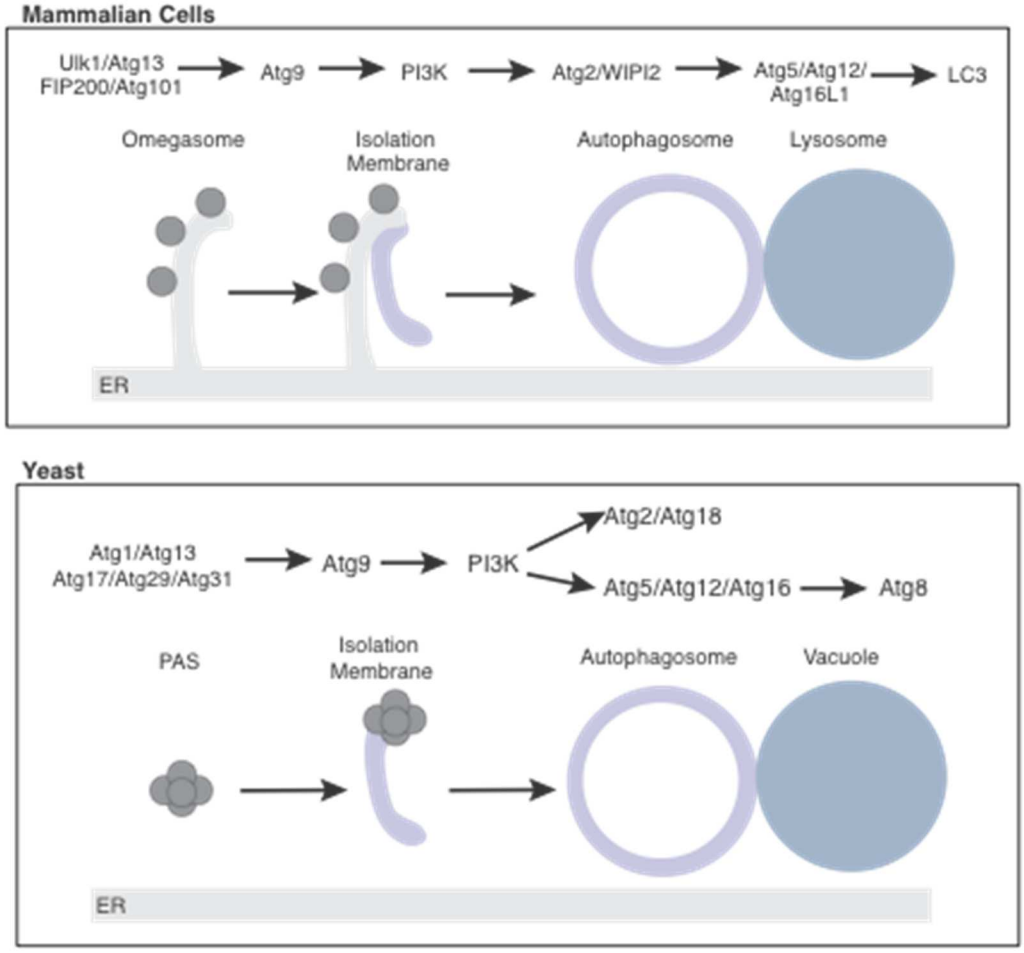

Figure 1.1. Overview of autophagosome formation.
Autophagy related (Atg) proteins are recruited in a hierarchical manner to the omegasome in mammals (top) or the pre-autophagosomal structure (PAS) in yeast (bottom). The Atgs can be grouped into six major complexes; the Atg1/Ulk1 initiating complex, Atg9, the phosphatidylionsital 3-kinase complex (PI3K), the Atg2/Atg18 (WIPI2 in mammals) complex, and the Atg12 and Atg8 conjugating systems. After Atgs are recruited to the omegasome or PAS a double membrane track called the isolation membrane forms that non-selectively engulfs proteins and organelles. The isolation membrane then seals to form the completed autophagosome. The autophagosome ultimately fuses with the lysosome or vacuole, releasing its contents for degradation.

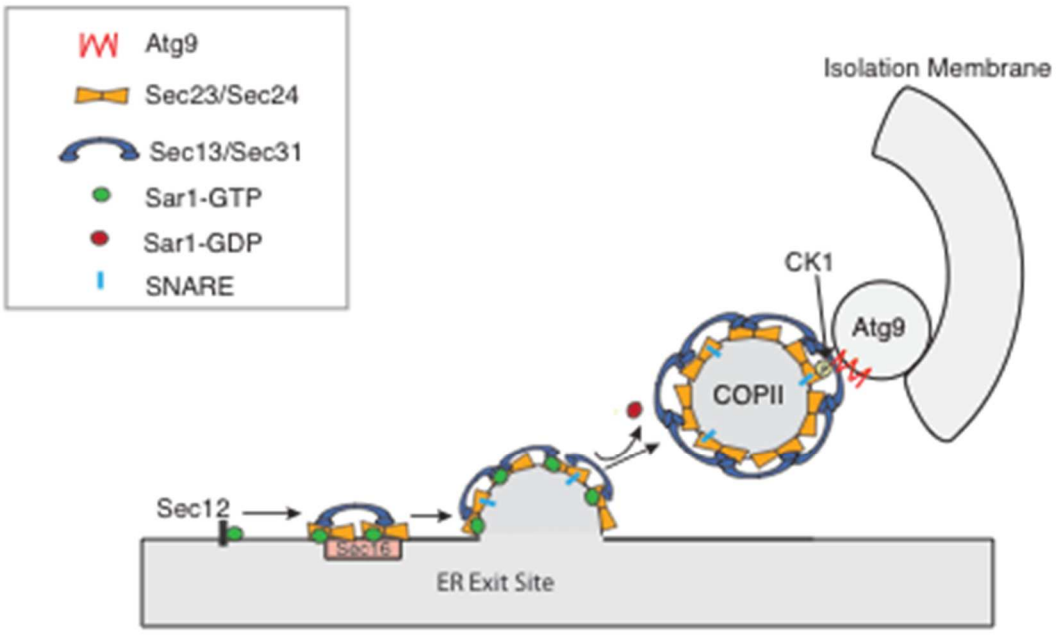

Figure 1.2. COPII vesicles in autophagosome formation.
Formation of the COPII coat is initiated at ER Exit Sites (ERES) by the guanine nucleotide exchange factor (GEF) Sec12. Sec12 activates the GTPase Sar1, which recruits the inner COPII coat, Sec23/Sec24, followed by the outer coat, Sec13/Sec31. Sec16 localizes to the ERES to facilitate coat assembly. After the coat has formed, Sar1 is inactivated and released from the vesicle. The COPII coat remains on the vesicle to aid in intracellular targeting. The casein kinase Hrr25 phosphorylates the COPII cargo adaptor Sec24, which enhances its interaction with Atg9. Atg9 localizes to the growing edge of the isolation membrane that faces the ERES.

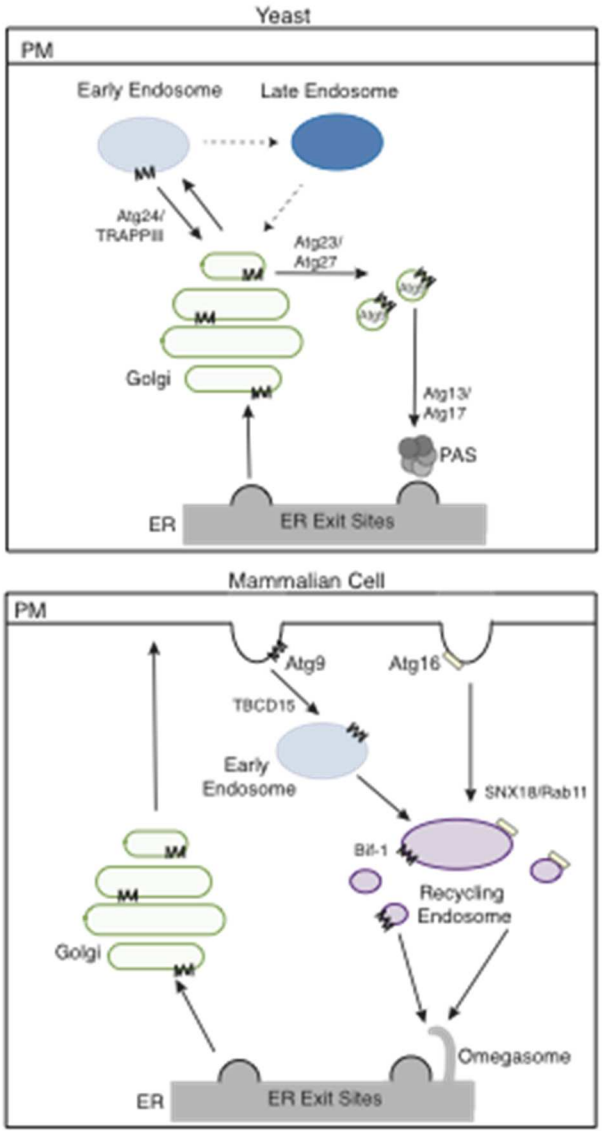

Figure 1.3. The Golgi and endosome system in autophagy.
Top, In yeast Atg9 traffics from the ER through the Golgi and localizes to endosome compartments. During starvation Atg9 traffics from the early endosome to the late Golgi where it is packaged into small vesicles. Bypass late endosome trafficking pathways likely exist during starvation (dotted arrows). Atg9 vesicles are recruited to the pre-autophagosome structure (PAS) by Atg13 and Atg17, which forms adjacent to ER exit sites. Bottom, In mammalian cells Atg9 traffics through the secretory pathway to the plasma membrane (PM) where it is endocytosed in AP2 vesicles, facilitated by the RAPGAP TBCD15. Atg9 then traffics through the early endosome to the recycling endosome, where it meets Atg16L1. Atg16L1 is packaged into separate clathrin vesicles from Atg9 at the PM and is recruited to the recycling endosome by Snx18/Rab11. The perinuclear recycling endosome is tubulated during starvation and Atg16L1 and Atg9 are subsequently recruited to the omegasome.

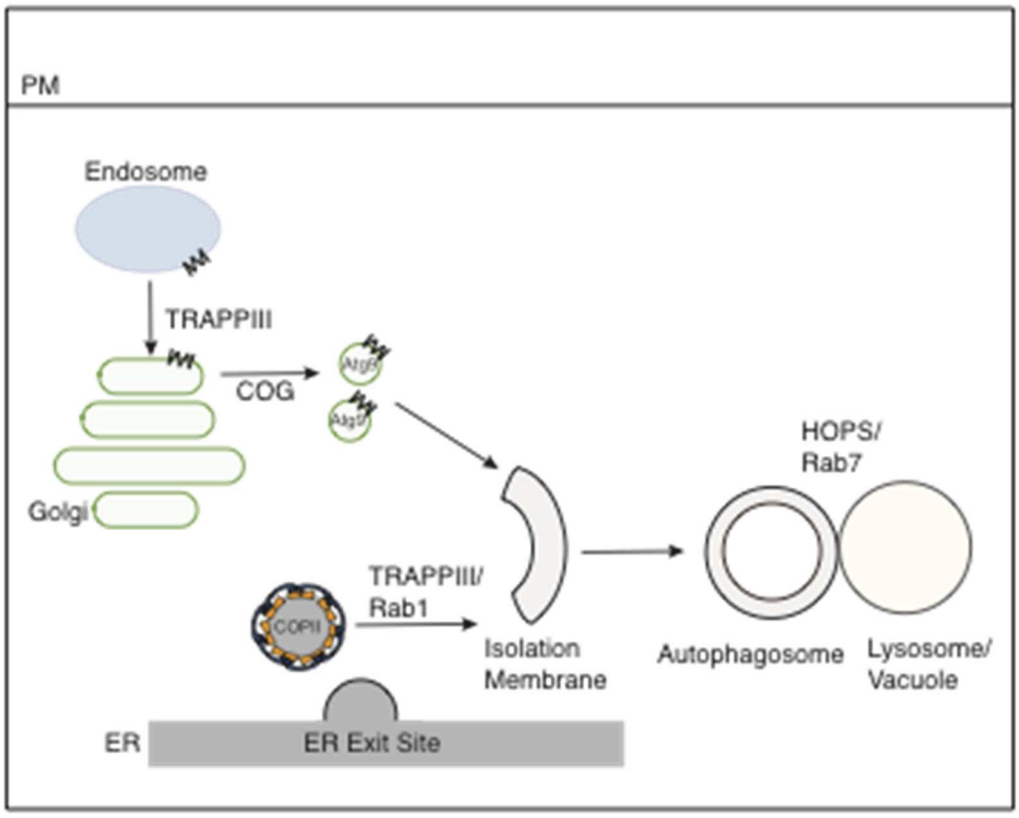

Figure 1.4. Tethers and tethering factors in autophagy.
Constitutive Atg9 trafficking requires the tethering factor TRAPPIII, for early endosome to Golgi transport in yeast or recycling endosome to Golgi transport in mammalian cells. Proper intra Golgi transport requires the tether COG and is needed before Atg9 vesicles are recruited adjacent to ER exit sites to initiate formation of the isolation membrane. TRAPPIII also binds the COPII coat where it likely activates the GTPase Rab1, which is required for autophagosome formation. The tether HOPS and Rab7 act after autophagosome formation in autophagosome-lysosome fusion.

1.7 Acknowledgments

Chapter 1 is being prepared for submission for publication in Developmental Cell, with co-author Susan Ferro-Novick. The dissertation author is the primary author of this paper.

CHAPTER 2

Phosphorylation of Sec24 regulates autophagosome abundance during nutrient deprivation

2.1 Summary

Endoplasmic Reticulum (ER)-derived COPII coated vesicles constitutively transport secretory cargo to the Golgi. However, when cells undergo starvation-induced stress, these vesicles are also required for formation of autophagosomes, distinct organelles that engulf cellular components for degradation by autophagy. How cells regulate COPII vesicles to fulfill dramatically different cellular roles in response to environmental cues is unknown. We hypothesized that phosphorylation of the COPII coat could regulate the function of COPII vesicles during starvation. Here we investigate the role of phosphorylation of the COPII cargo adaptor, Sec24, and find that phosphorylation of conserved amino acids on the membrane-distal surface of Sec24 is specifically required for autophagy, but not ER-Golgi transport. In particular, Sec24 phosphorylation regulates autophagosome abundance during starvation conditions.

We next sought to understand the mechanism through which Sec24 phosphorylation impacts autophagosome formation. Here we confirm an interaction between Sec24 and the essential Atg protein, Atg9 by co-immunoprecipitation. Moreover, Sec23/Sec24 directly interacts with the C-terminus of Atg9 and the Sec24-Atg9 interaction is regulated by Sec24 phosphorylation. We propose that the acute

need to produce autophagosomes during starvation drives the interaction of Sec24 with Atg9 to increase autophagosome abundance.

2.2 Introduction

Autophagy is a highly conserved catabolic process that uses membrane traffic to target proteins and organelles for degradation. Basal levels of autophagy continuously replenish the cellular pool of amino acids and other metabolites to maintain homeostasis. However, when cells are starved for nutrients, autophagy is quickly upregulated. This upregulation leads to a dramatic intracellular reorganization to meet the high demand for membrane required to form autophagosomes, distinct organelles that target cellular components for degradation (Nakatogawa et al., 2009). Induction of autophagy leads to the formation of a double-membrane structure, called the isolation membrane, that forms adjacent to a pre-autophagosome structure (PAS) where autophagy related proteins (Atg) are recruited in a hierarchical manner (Nakatogawa et al., 2009). As the isolation membrane expands, it engulfs cytoplasmic proteins and organelles targeted for degradation before it seals to form an autophagosome. The autophagosome then fuses with the vacuole/lysosome, releasing its contents for degradation (Lamb et al., 2013; Nakatogawa et al., 2009). Although the assembly pathway of the Atg proteins is known, the mechanism by which membranes are directed to the autophagy pathway remains a central unanswered question in the field.

Autophagosome biogenesis has been linked to COPII vesicles and an ER subdomain called the ER exit sites (ERES) where COPII vesicles are formed (Graef et

al., 2013; Suzuki et al., 2013; Tan et al., 2013; Ge et al., 2014; Wang et al., 2015; Lemus et al., 2016). How COPII vesicles, which are faithfully targeted to the Golgi under normal growth conditions, can be reprogrammed to function on an alternate trafficking pathway during nutrient deprivation remains enigmatic. COPII coated vesicle formation is initiated at the ER with the recruitment of an inner coat layer comprising the Sec23/Sec24 complex. Coat polymerization and vesicle budding occurs when Sec23/Sec24 recruits a second complex (Sec13/Sec31) that forms the outer shell of the coat. Sec24, the major cargo adaptor of the COPII coat, recruits biosynthetic cargo and SNAREs (which mediate vesicle fusion) into vesicles that are delivered to the Golgi (Lord et al., 2013). After vesicle fission, the coat lingers on the vesicle to facilitate vesicle targeting to the Golgi (Cai et al. 2007; Lord et al, 2011). COPII vesicle budding mutants, as well as other mutants that disrupt ER-Golgi traffic, also disrupt autophagy (Hamasaki et al., 2003). However, a direct functional link between COPII vesicles, the COPII coat and autophagy has been difficult to demonstrate.

Multiple COPII coat subunits, including Sec23 and Sec24, are phosphorylated by Hrr25 (Bhandari et al., 2013; Lord et al., 2011), a kinase required for ER-Golgi traffic and autophagy (Lord et al., 2011; Murakami et al., 1999; Wang et al., 2015; Yu and Roth, 2002). Previously, we showed that coat phosphorylation is required for COPII vesicle fusion (Lord et al., 2011; Wang et al., 2015). Given the recently identified role of COPII vesicles in autophagosome formation, and the observation that Hrr25 is required for autophagy, we asked if coat phosphorylation also functions to regulate vesicle traffic during autophagy. Here we find that phosphorylation of the

membrane distal surface of Sec24 promotes the interaction of Sec24 with the C-terminus of Atg9, which is needed for autophagy. Failure to phosphorylate this Sec24 site leads to a decrease in autophagosome number, but not autophagosome expansion. This phosphorylation event is independent of the assembly of the Atg machinery at the PAS. Together these studies reveal a surprising role for Sec24 phosphorylation in reprogramming core trafficking machinery to fulfill a distinct function during starvation.

2.3 Results

2.3.1 Identification of Sec24 phosphorylation sites

To address whether coat phosphorylation allows COPII vesicles to function in autophagy versus ER-Golgi traffic, we purified the COPII inner coat from yeast cells induced for autophagy. Our analysis initially focused on Sec24, as it is the major COPII cargo adaptor. Using mass spectrometry, we identified 27 high confidence Sec24 phosphorylation sites in vivo (Table 2.1). Many of the Sec24 phosphosites are conserved in the closely related paralog Iss1, which is also a cargo adaptor (Kurihara et al., 2000) (Table 2.1).

As Sec24 is an essential gene we first determined whether mutations in phosphorylated residues affect cell viability. Phosphorylated residues on Sec24 were mutated to either a phosphomimetic residue or to a non-phosphorylatable alanine and introduced as the sole copy in either a *sec24*Δ or *sec24*Δ*iss1*Δ background. As Iss1 can compensate for the function of Sec24 the *sec24*Δ*iss1*Δ background is more sensitive to Sec24 defects (Miller et al., 2003). Phosphorylated residues located

structurally near other sites were mutated as a group. This mutational analysis revealed phosphomimetic mutations in two different patches that resulted in cell inviabilty (Table 2.1). One of the patches is located on the membrane proximal surface of Sec24 (membrane proximal I) whereas the other is located on the membrane distal surface (Figure 2.1). Alanine mutations in the membrane proximal I patch were the only alanine mutations that affected cell viability (Figure 2.2; A).

2.3.2 Sec24 phosphorylation does not play a major role in regulating cargo packaging

Since Sec24 is the major cargo adaptor subunit of the COPII coat we initially focused on determining whether phosphorylation regulates Sec24-cargo interactions. We first analyzed the membrane proximal I patch, consisting of T635/S636/S638 as both the alanine and phosphomimetic mutants affected cell viability (Figure 2.2; A), these sites could regulate an essential function of Sec24. Additionally, these sites are located on the membrane proximal surface near other known cargo binding sites (Figure 2.1). To determine whether the phosphomimetic and alanine mutants affected Sec24 expression we tagged the Sec24 mutants with His_6 behind a galactose inducible promoter. Upon galactose induction WT Sec24-His_6 was expressed but Sec24-T635E/T636E/S638D-His_6 and Sec24-T635A/T636A/S638A-His_6 failed to express (Figure 2.2; B), indicating mutations in these sites affect the stability of Sec24 rather than the function of Sec24. As a result these sites were not studied further.

We next looked for phosphorylation sites near known cargo binding sites on Sec24. Two of the Sec24 phosphosites (S730 and S735) map to a region of the protein

that comprises one of the four well-characterized yeast cargo-binding sites (Miller et al., 2003; Miller et al., 2005; Pagant et al., 2015) (Figure 2.1). The so-called A-site packages a SNARE, Sed5, needed for ER-Golgi traffic and autophagy (Miller et al., 2005; Mossessova et al., 2003; Tan et al., 2013). COPII vesicles formed in vitro with Sec24-S730A/S735A showed normal capture of Sed5 and other cargo, whereas those formed with Sec24-S730D/S735D contained reduced amounts of Sed5 and were modestly impaired in their fusion efficiency with the Golgi (data not shown). Additionally, a strain harboring the Sec24-S730D/S735D mutations had reduced autophagic activity, whereas the Sec24-S730A/S735A mutation had no effect (data not shown). As phosphorylation of S730/S735 negatively regulated both ER-Golgi transport and autophagy, packaging of Sed5 into COPII vesicles is required on both pathways.

A second set of conserved phosphosites, S645/S678 (membrane proximal II) is located near a known cargo binding site in mammalian Sec24 (mSec24) (Figure 2.1). Sec23/Sec24 complexes with alanine and phosphomimetic mutations in these sites were purified from yeast and screened for their ability to package a variety of cargo. However, mutations in these sites did not disrupt the packaging of any cargo tested (data not shown). Therefore, although we did identify effects of S730/S735 phosphorylation on regulating the packaging of the SNARE Sed5, phosphorylation does not appear to be a commonly used mechanism for regulating Sec24-cargo interactions.

2.3.3 Phosphorylation of Sec24 is required for autophagy

As phosphorylation did not play a major role in regulating the cargo packaging function of Sec24, we next asked whether phosphorylation could regulate the function of Sec24 during autophagy. To test this hypothesis we screened a panel of alanine mutations in the phosphorylation sites conserved in Iss1. The effects of mutations in these sites on autophagy were monitored in a *sec24Δiss1Δ* double mutant background by assaying Pho8Δ60 activity. Pho8Δ60 is a cytosolic form of vacuolar alkaline phosphatase that is delivered to and activated in the vacuole when autophagy is induced (Klionsky, 2007). Only combinations of T324A, T325A and T328A were defective in autophagy (Table 2.2). These three sites form a patch located on the membrane distal surface of Sec24 (Figure 2.1), making them unlikely to regulate cargo packaging. Alanine mutations in the other 13 phosphosites tested showed no autophagy defects (Table 2.2).

When we dissected the role of individual residues on this membrane distal surface of Sec24, single and double mutant combinations of T324A/T325A/T328A showed a range of defects in Pho8Δ60 activity, with the triple alanine mutant showing the most dramatic defect (Figure 2.3; A). We were unable to test the full range of phosphomimetic combinations, as some caused lethality (Table 2.1, Figure 2.3; D). However, none of the viable phosphomimetic mutants showed a defect in autophagy (Figure 2.3; B, C). Sec24-T324A/T325A/T328A (hereafter referred to as Sec24-3A) was further characterized because it had the most dramatic defect in Pho8Δ60 activity. To confirm that phosphorylation of the Sec24 membrane distal surface is required for autophagy, we examined a second autophagy marker, Atg8. Cytosolic GFP-Atg8 is

lipidated and incorporated into membrane at the PAS before being delivered to the vacuole (Klionsky et al., 2007). Translocation of GFP-Atg8 to the vacuole following nitrogen starvation was significantly reduced in a strain expressing Sec24-3A (Figure 2.4; A). This defect was confirmed using western blot analysis by monitoring the cleavage of GFP-Atg8 to GFP (Figure 2.4; B). The GFP translocation defect was less severe in the presence of Iss1 (Figure 2.4; A right), suggesting functional complementation by the paralogous protein.

We next demonstrated that phosphorylation of the membrane distal sites on Sec24 is specifically required for autophagy by examining ER-Golgi traffic in cells containing Sec24-3A. The processing of carboxypeptidase Y (CPY), as it traffics from the ER (p1), Golgi (p2), and vacuole (m) is kinetically indistinguishable from wild-type (Figure 2.5), demonstrating that phosphorylation of the Sec24 membrane distal patch regulates a novel function of Sec24 that is specific to autophagy.

Since Sec24 robustly co-purifies with Sec23, our mass spectrometry data also included information on Sec23, which contained three phosphosites on an alpha helix structurally equivalent to the Sec24 membrane distal patch (Figure 2.6; A). Mutation of these Sec23 sites (T146/S147/S149) caused no defects in growth (data not shown), Pho8Δ60 activity (data not shown) or translocation of GFP-Atg8 to the vacuole (Figure 2.6; B), suggesting the effects we observed on autophagy are specific to Sec24 and its paralog, Iss1.

2.3.4 ER-Golgi transport is delayed during starvation

If COPII vesicles are diverted from the secretory pathway during autophagy induction, we hypothesized ER-Golgi transport may be decreased during starvation.

To test this idea the trafficking of CPY was monitored in cells grown in nutrient rich or starved for nitrogen for 1 h. After starvation the processing of CPY from its ER from (p1) to its Golgi form (p2) was significantly slowed (Figure 2.7; A), consistent with the model that some COPII vesicles are diverted from the secretory pathway. Expression of Sec24-3A did not rescue this delay even in an *iss1*Δ strain background (Figure 2.7; B), suggesting that additional sites and/or factors also participate in reprogramming COPII vesicles during starvation.

2.3.5 Phosphorylation of Sec24 regulates autophagosome frequency during starvation

We next wanted to determine whether Sec24-3A is required specifically for autophagosome formation during starvation-induced upregulation of autophagy. To compare autophagosome formation in nutrient rich and autophagy inducing conditions, structured illumination microscopy (SIM) was used to examine autophagosomes marked by GFP-Atg8 in the absence (nutrient rich) or presence of rapamycin. Rapamycin is an inhibitor of TOR, a key negative regulator of autophagy (Loewith and Hall, 2011). In nutrient-rich media, autophagosomes (also called Cvt vesicles) were smaller, less numerous, and dependent on Atg11 (Figure 2.8; A). As previously reported (He et al., 2006), Atg11 was only required for autophagosome formation in rich medium and not in rapamycin-treated cells (compare Figure 2.8; A and B).

Cells expressing Sec24-3A were not defective in autophagosome formation in nutrient rich medium (Figure 2.8; A), however, fewer autophagosomes formed in the

rapamycin-treated Sec24-3A cells (Figure 2.8; B). While Sec24-3A significantly reduced the number of autophagosomes, it did not significantly affect the size of autophagosomes that formed (Figure 2.8; C). Similar results were obtained when we blocked COPII vesicle budding at 37^{o}C in the temperature-sensitive mutant *sec12-4* mutant (data not shown) as well as in the ER-Golgi SNARE mutants *bet1-1* and *bos1-1* (Figure 2.9).

We also used a second assay to confirm the effect of Sec24-3A on the frequency of autophagosome formation during starvation. Autophagosome number and size can be indirectly assessed using transmission electron microscopy to measure the number and size of autophagic bodies. Upon deletion of the *PEP4* gene, which encodes a protease that is required for the activation of multiple vacuolar hydrolases, autophagic bodies accumulate in the vacuole (Backues et al., 2013). Two independent sets of electron microscopy were performed, after 90 min or 60 min of nitrogen starvation. At both time points, fewer autophagic bodies accumulated in cells expressing Sec24-3A compared to WT Sec24 (Figure 2.10; A, B, D). Although autophagic body number was significantly reduced, autophagic body size was not affected (Figure 2.10; C, E). Therefore, using two different approaches we could demonstrate that phosphorylation of the Sec24 membrane distal sites regulates autophagosome number, while autophagosome size or expansion is unaffected.

2.3.6 Phosphorylation of Sec24 regulates Sec24-Atg9 interaction

We previously proposed that COPII vesicles interact with Atg9 vesicles at the PAS (Tan et al., 2013). When autophagy is induced, Atg9 vesicles traffic from the

late Golgi to the PAS and localize adjacent to the ER exit sites that produce COPII vesicles (Graef et al., 2013; Suzuki et al., 2013; Yamamoto et al., 2012). Similar to our observations with Sec24, Atg9 was recently shown to regulate autophagosome number, but not size (Jin et al., 2014). Furthermore, proteomics revealed an interaction between multiple COPII coat subunits and Atg9 in detergent lysates (Graef et al., 2013). However, it remained unclear from these studies which coat subunit mediated this interaction and whether it was required for autophagy. Therefore, we first confirmed that Sec24 co-precipitates with Atg9 and tested whether this interaction is regulated by autophagy. Sec24 was immunoprecipitated from cells expressing Atg9-13myc that were grown in nutrient rich conditions (SMD) or starved for nitrogen (SD-N). The precipitate was then blotted with anti-myc antibody. Atg9-13myc co-immunoprecipitated with Sec24, but not the pre-immune control (Figure 2.11; A). Moreover, approximately 2.5-fold more Atg9-13myc co-immunoprecipitated with Sec24 from lysates prepared from nitrogen starved cells (Figure 2.11; A), demonstrating that this interaction is upregulated during autophagy.

Atg9 is a six transmembrane protein with N-terminal, C-terminal and Core cytoplasmic domains (Figure 2.11; B). While the middle and C-terminal domains are present in mammalian cells, the N-terminus is largely absent (Young et al., 2006). In order to determine which domain of Atg9 directly interacts with the COPII coat, the cytoplasmic domains of Atg9 were fused to GST and the purified fusion proteins were incubated with purified Sec23/Sec24 complex in vitro. The Sec23/Sec24 complex was used for these studies, since Sec24-His_6 is unstable in the absence of Sec23.

Sec24 was predominantly unphosphorylated as it was purified without phosphatase inhibitors and stored in the freezer following purification. A GST fusion to a Sec31 fragment (aa878-1114), which was previously shown to interact with the Sec23/Sec24 complex (Bi et al., 2007), served as a positive control. The C-terminus of Atg9 bound to Sec23/Sec24, while the N-terminal and middle hydrophilic Atg9 domains did not (Figure 2.11; C). Furthermore, binding of Sec23/Sec24 to the C-terminus increased with increasing concentrations of the complex and was saturable (data not shown). This interaction was dependent on Sec24, as Sec23 alone did not interact with GST-Atg9C (data not shown).

Next we used the phosphomimetic mutations to ask if the interaction between Sec24 and Atg9 is enhanced by phosphorylation of the membrane distal sites. While the most dramatic effects on autophagy were seen with the *sec24* triple alanine mutant (Figure 2.3; A), the *sec24* triple phosphomimetic mutant is inviable. Therefore, to cover all three phosphosites of interest in our binding studies, we used Sec23/Sec24-T325E and Sec23/Sec24-T324E/T328E. Consistent with the notion that phosphorylation enhances the Sec24-Atg9 interaction, both T325E and T324E/T328E increased the interaction of Sec24 with GST-Atg9C (Figure 2.12; A).

To determine whether the Sec24-Atg9 interaction is regulated by phosphorylation in vivo, wild-type or mutant Sec24 cells co-expressing Atg9-13myc were starved for nitrogen and Sec24 was immunoprecipitated in the presence of phosphatase inhibitors. Sec24-T324A/T325A (Figure 2.12; B, D), but not Sec24-T324E/T325E (Figure 2.12; E) disrupted the interaction of Sec24 with Atg9-13myc.

This defect was enhanced in Sec24-3A, where Sec24-T328 is also mutated (Figure 2.12; C, D). Sec24-3A did not impair the trafficking of Atg9 to the PAS (data not shown), indicating that Sec24 does not regulate Atg9 traffic. Together these findings imply that the C-terminus of Atg9 directly interacts with phosphorylated Sec24 via its membrane distal surface after Atg9 has been recruited to the PAS.

We next determined whether Sec24-3A affects recruitment of other Atg proteins to the PAS. For this study we examined the co-localization of a member of each of the remaining Atg complexes with the PAS marker Ape1 in WT Sec24 and Sec24-3A. Sec24-3A only affected the PAS localization of Atg8, the most downstream Atg, which showed a modest defect in PAS recruitment (Figure 2.13). The PAS localization of other Atgs was not affected (data not shown). These results indicate that a functional PAS is able to form in Sec24-3A and that Sec24 phosphorylation does not indirectly affect autophagy by disrupting the trafficking of Atg proteins to the PAS.

Microscopy-based studies have linked ERES to autophagosome formation (Graef et al., 2013; Suzuki et al., 2013), however, the ERES are also a subdomain of the ER where COPII vesicles bud (Budnik and Stephens, 2009). To ask if Sec24-3A disrupts the formation of ERES, the localization of Sec13-GFP was examined in cells expressing wild-type Sec24 or Sec24-3A. Sec13-GFP, a component of the outer COPII coat, predominantly localizes to ERES (Shindiapina and Barlowe, 2010). ERES localization of Sec13-GFP was not affected by Sec24-3A in nutrient rich or starvation conditions, suggesting Sec24-3A does not disrupt ERES formation (Figure

2.14). Thus, our findings imply that the major function of phosphorylation of the Sec24 membrane distal surface is to regulate the interaction of COPII vesicles with the Atg machinery.

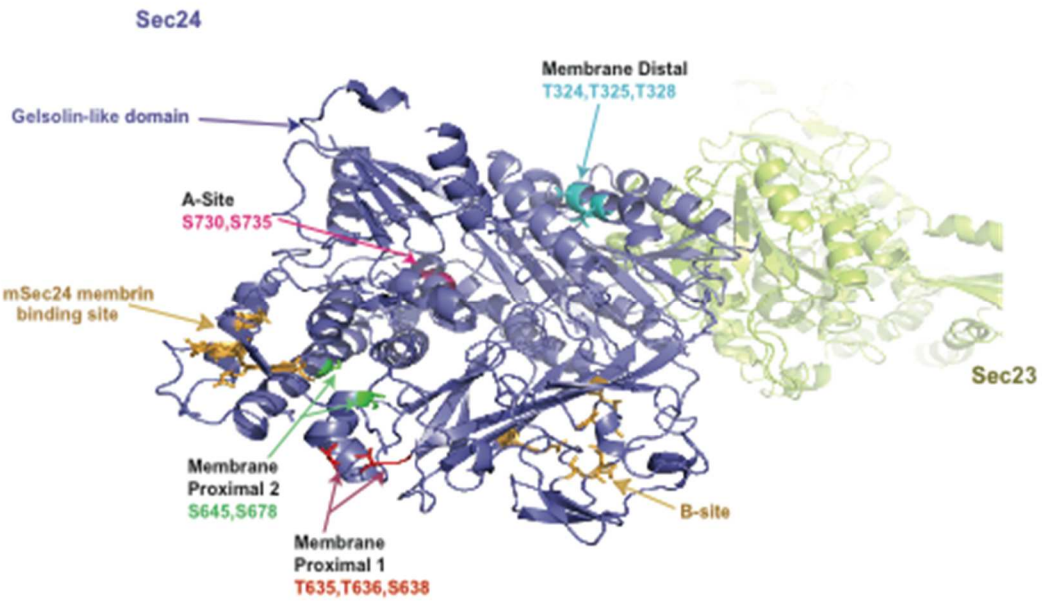

Figure 2.1. Location of key Sec24 phosphorylation sites.
Ribbon diagram of Sec23 (lime) and Sec24 (lavender) with groups of key Sec24 phosphorylation sites (green, pink, red, and teal). The mSec24 membrin-binding site and conserved cargo binding B-site are colored light brown.

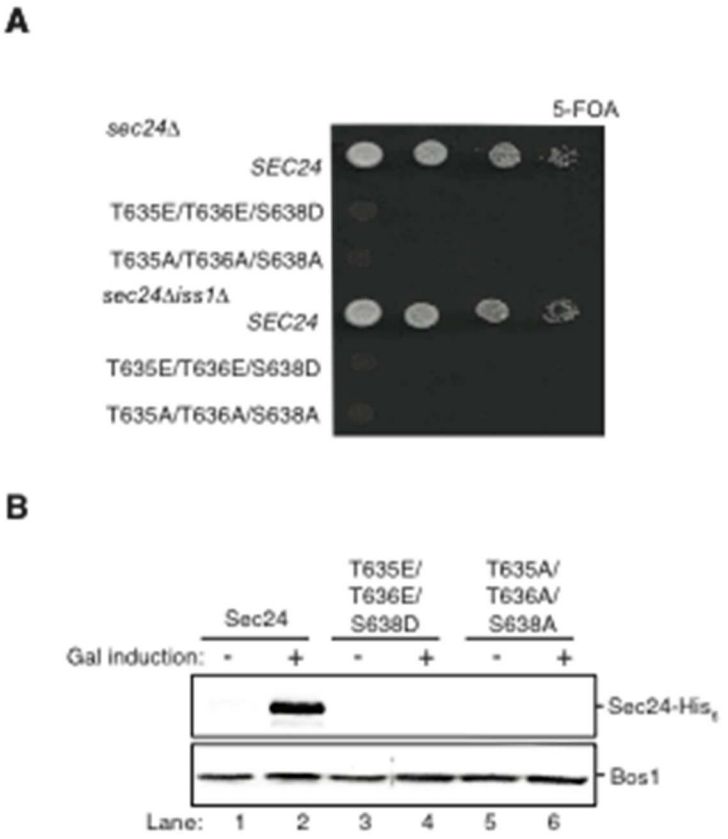

Figure 2.2. Mutations in Sec24 T635/T636/S638 affect growth and protein stability.
A WT *SEC24* or *sec24* mutants were introduced into *sec24*Δ (top) or *sec24*Δ*iss1*Δ (bottom) deletion strains and grown on 5-FOA to select against the WT balancing plasmid at 25ºC. **B** WT Sec23/Sec24-His_6 or mutant Sec23/Sec24-His_6 behind a galactose inducible promotor was induced with 0.2% galactose for 5 h and blotted for Sec24-His_6 (top). The SNARE Bos1 (bottom) was used as a loading control.

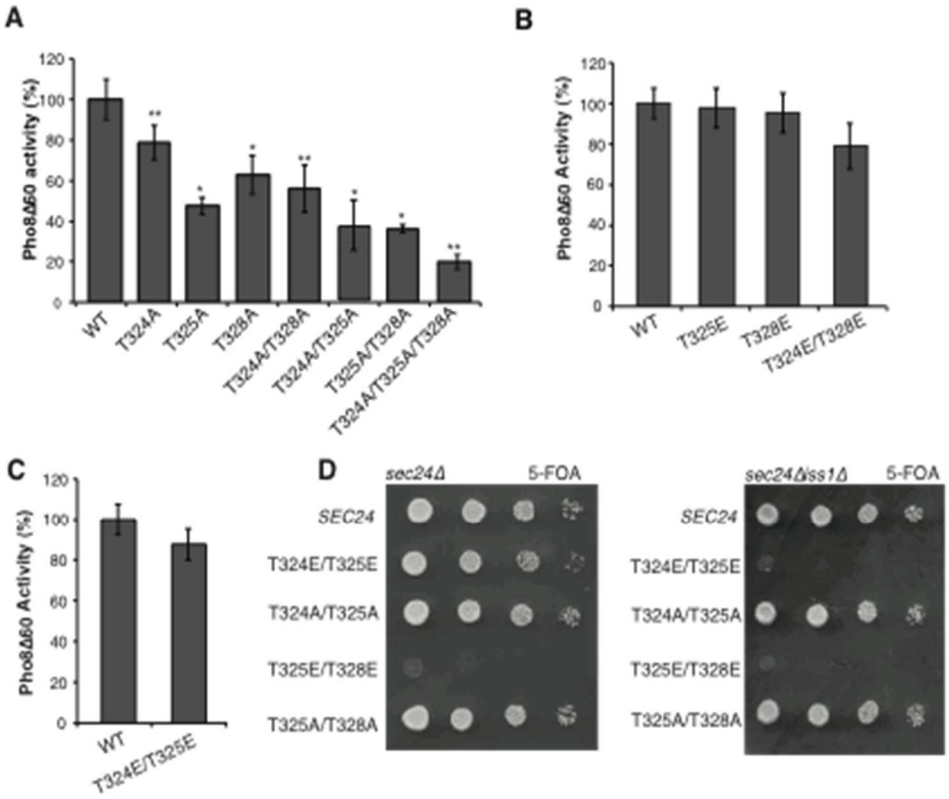

Figure 2.3. Phosphorylation of Sec24 T324/T325/T328 is required for autophagy. **A** Vacuolar alkaline phosphatase activity was assayed in lysates prepared from a *sec24*Δ*iss1*Δ deletion strain harboring *sec24* alanine mutations. The activity of wild-type (WT) 2 h after starvation was set as 100% and 0 time-point values were subtracted. **B, C** As in (A) except activity was assayed in extracts from phosphomimetic mutations in *sec24*Δ*iss1*Δ (B) or *sec24*Δ (C) deletion strains. Averages and s.e.m. are shown for 3 biological replicates. **D** Plasmids encoding *SEC24* (WT) or mutant *sec24* were expressed in *sec24*Δ (left) or *sec24*Δ*iss1*Δ (right) and grown on 5-FOA at 25°C to select against the WT balancing plasmid. *P < 0.05; **P < 0.01; Student's paired t-test.

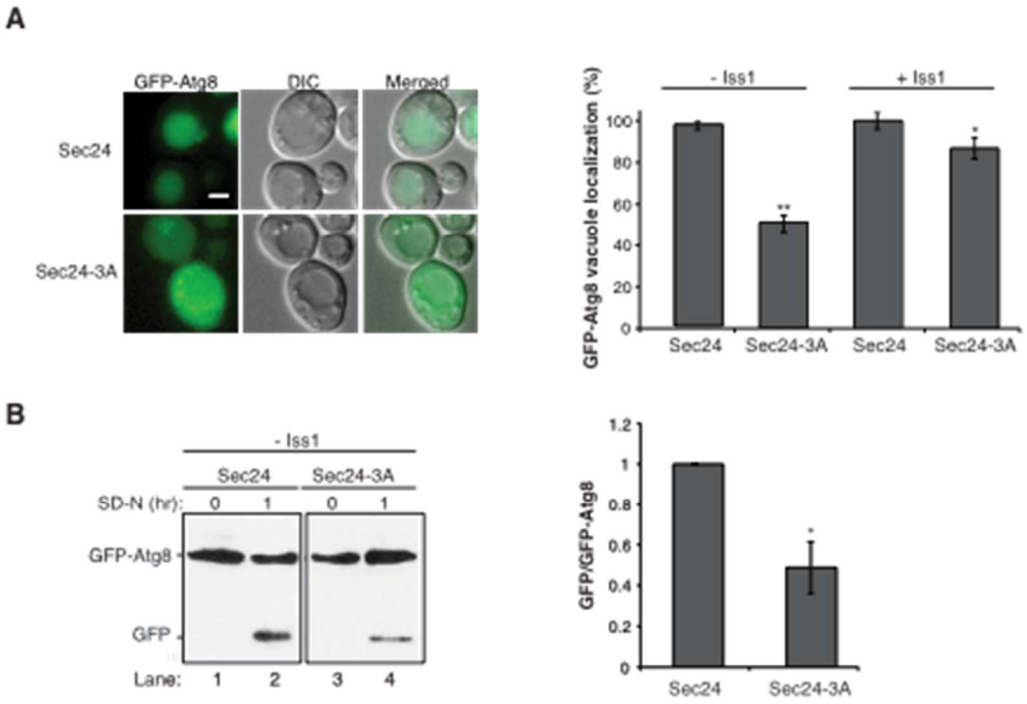

Figure 2.4. Iss1 can compensate for autophagy defects in Sec24-3A.
A The translocation of GFP-Atg8 to the vacuole was examined 1 h after nitrogen starvation at 25°C in *sec24*Δ*iss1*Δ and *sec24*Δ deletion strains in either the presence of WT Sec24 or Sec24-3A. Representative images (left) and quantification from 300 cells (right) are shown. Scale bar 2 μm. WT was set to 100% for each experiment and had an average vacuolar localization of 76% (*sec24*Δ*iss1*Δ*)* and 86% (*sec24*Δ). Averages and s.e.m. are shown for 3 biological replicates. **B** Cleavage of GFP-Atg8 was examined in *sec24*Δ*iss1*Δ cells expressing Sec24 or Sec24-3A after 1 h starvation at 25°C (left). The ratio of free GFP to GFP-Atg8 was quantitated (right). WT was set as 1 for each experiment. Averages and s.e.m. are shown for 3 biological replicates. *P < 0.05; **P < 0.01; Student's unpaired t-test.

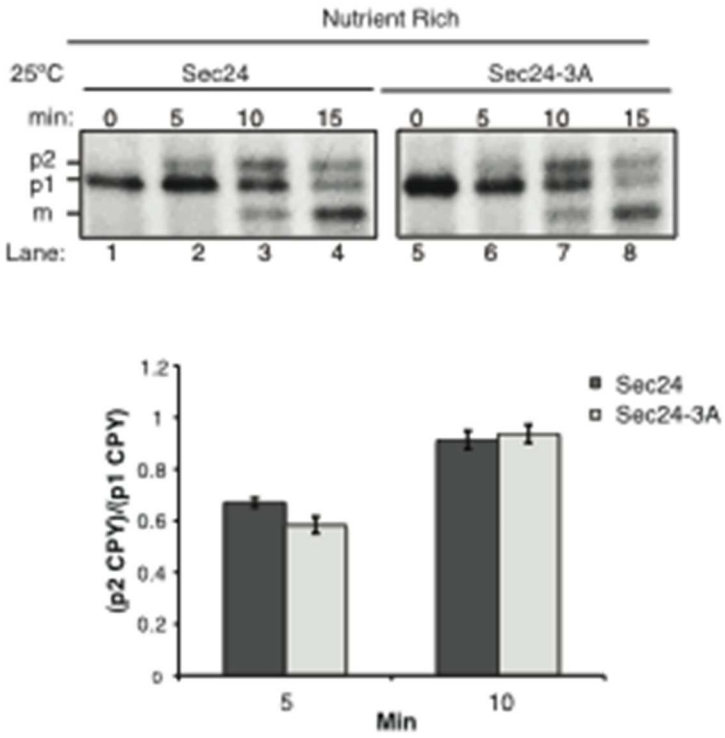

Figure 2.5. ER-Golgi transport is not affected by Sec24-3A.
*sec24*Δ*iss1*Δ cells expressing Sec24 (lanes 1-4) or Sec24-3A (lanes 5-8) were pulse-labeled for 4 min and chased for the indicated times (top). The p1 (ER), p2 (Golgi) and m (vacuolar) forms of CPY are labeled. Quantitation of the ratio of p2/p1 CPY for the 5 and 10 min time points are shown (bottom). Averages and s.e.m. are shown for 3 biological replicates.

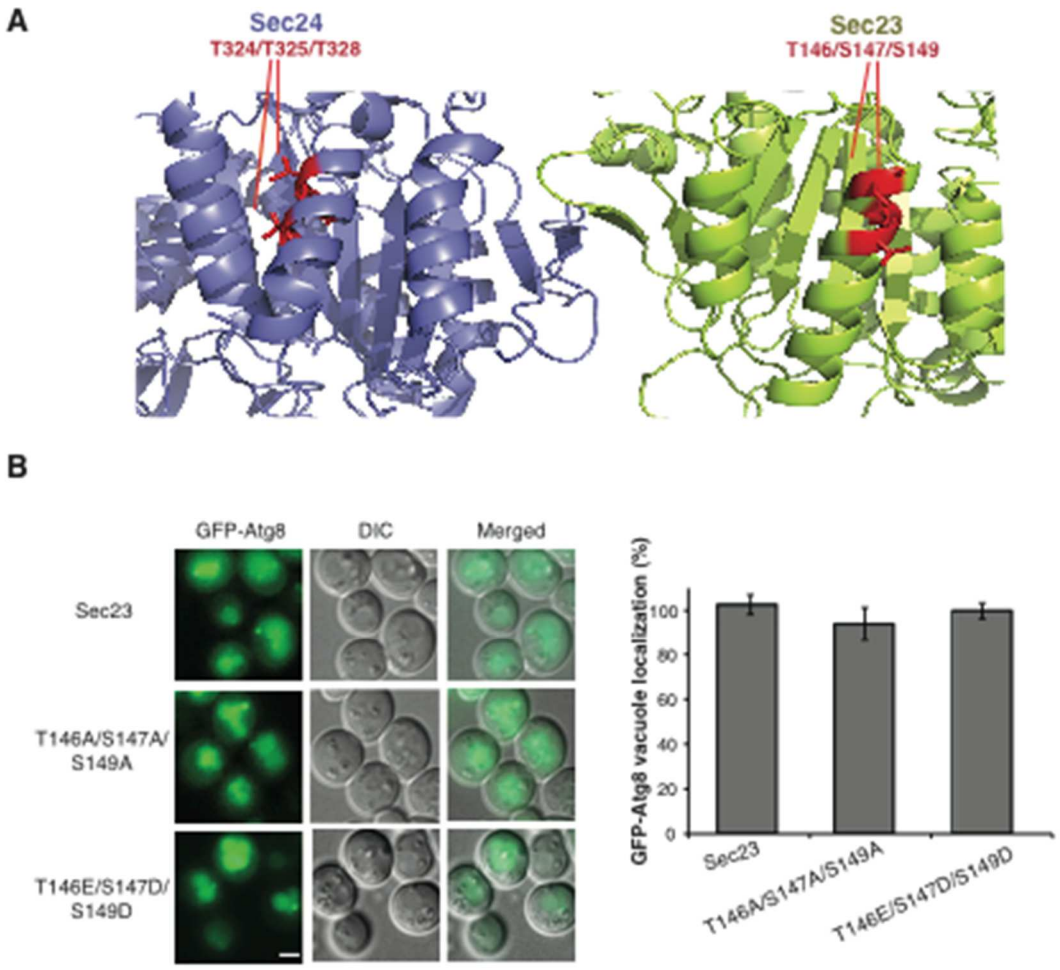

Figure 2.6. Phosphorylation of Sec23 membrane distal sites is not required for autophagy.
A Ribbon diagram of Sec23 (lime) and Sec24 (lavender). **B** Translocation of GFP-Atg8 to the vacuole was examined in WT and the *sec23* mutants 1 h after nitrogen starvation at 25°C (left). Scale bar 2 µm. 300 cells were quantitated (right). WT was set to 100% for each experiment and had an average of 75% vacuolar localization. Averages and s.e.m are shown for 3 biological replicates.

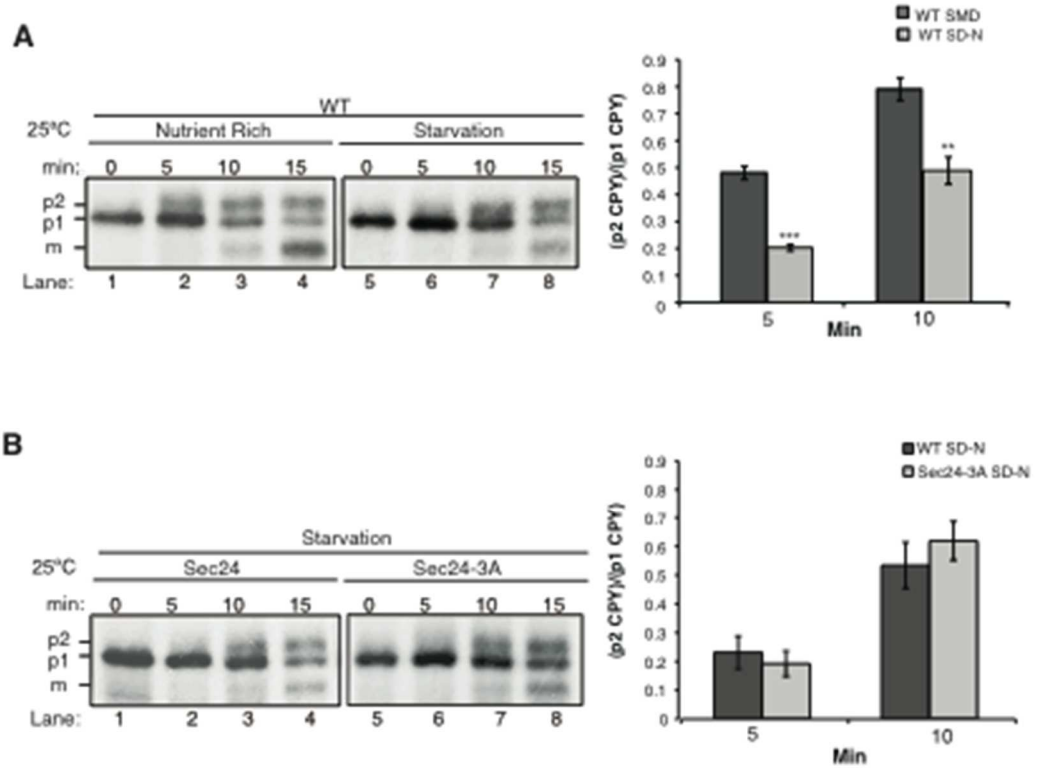

Figure 2.7. ER-Golgi traffic is delayed during autophagy.
A WT cells were grown in nutrient rich media (SMD) (lanes 1-4) or starved for nitrogen (SD-N) for 1 h at 25°C (lanes 5-8). Cells were pulse-labeled for 4 min and chased at the indicated times before CPY was immunoprecipitated. ER (p1), Golgi (p2) and vacuolar (m) forms of CPY are labeled (left). Ratio of p2 to p1 CPY was determined (right). Averages and s.e.m. are shown for 3 biological replicates. **B** As in (A) except *sec24*Δ*iss1*Δ cells expressing Sec24 (lanes 1-4) or Sec24-3A (lanes 5-8) were starved for nitrogen for 1 h at 25°C (left). Ratio of p2 to p1 CPY was determined (right). Averages and s.e.m. are shown for 3 biological replicates. **P < 0.01; ***P < 0.001; Student's unpaired t-test.

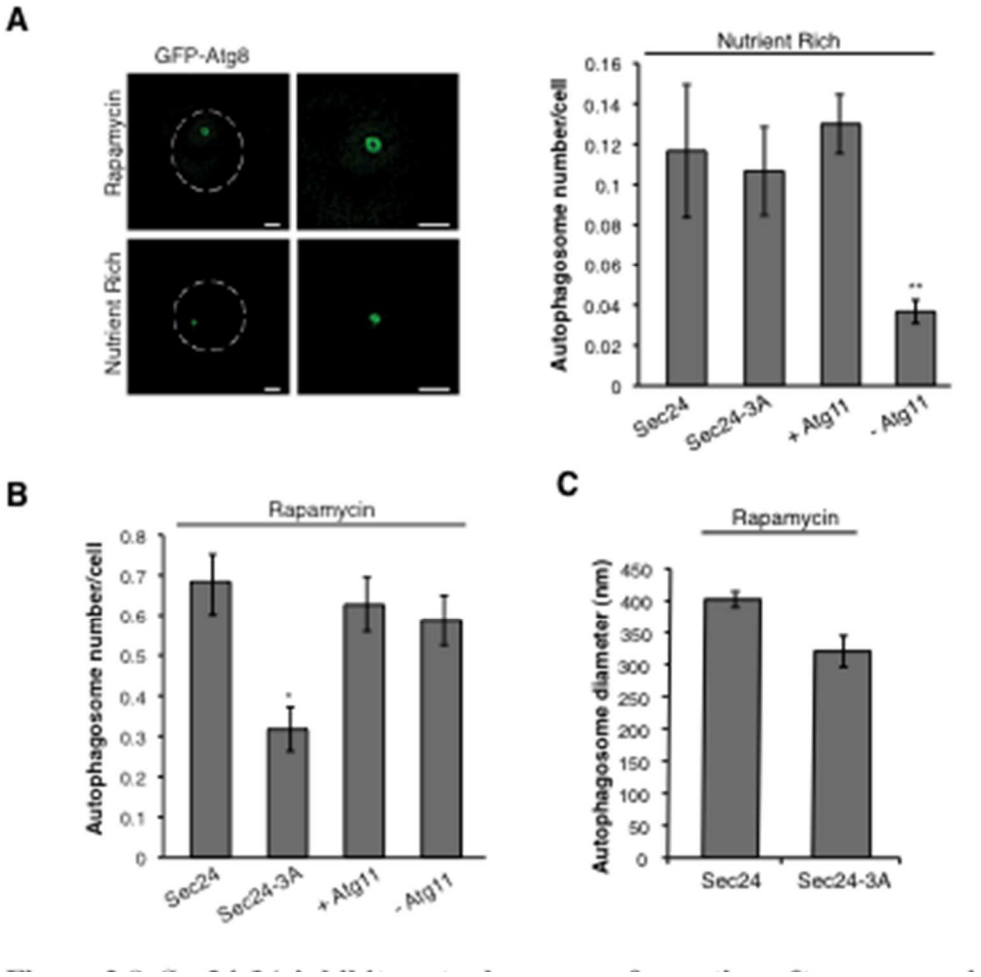

Figure 2.8. Autophagosome formation is reduced after rapamycin treatment in Sec24-3A.

A Representative images from WT cells expressing GFP-Atg8 treated with 400 ng/ml rapamycin for 1 h at 25°C (left top) or untreated (left bottom). Deconvolved images are shown. Scale bar, 1 µm. WT Sec24 and Sec24-3A expressed in the *sec24Δiss1Δ* deletion strain and WT (+Atg11) and *atg11Δ* cells (-Atg11) expressing GFP-Atg8 were imaged and the number of autophagosomes per cell was quantitated from 300 cells. Averages and s.e.m. are shown for 3 biological replicates. **B** As in (A) except cells were treated with 400 ng/ml rapamycin for 1 h at 25°C. Averages and s.e.m. are shown for 3 biological replicates. **C** As in (B) only the diameter of 100 autophagosomes was measured from cells expressing WT Sec24 and Sec24-3A in *sec24Δiss1Δ* deletion strains treated with 400 ng/ml rapamycin for 1 h at 25°C. Averages and s.e.m. are shown for 4 biological replicates.* $P < 0.05$; ** $P < 0.01$; Student's unpaired t-test.

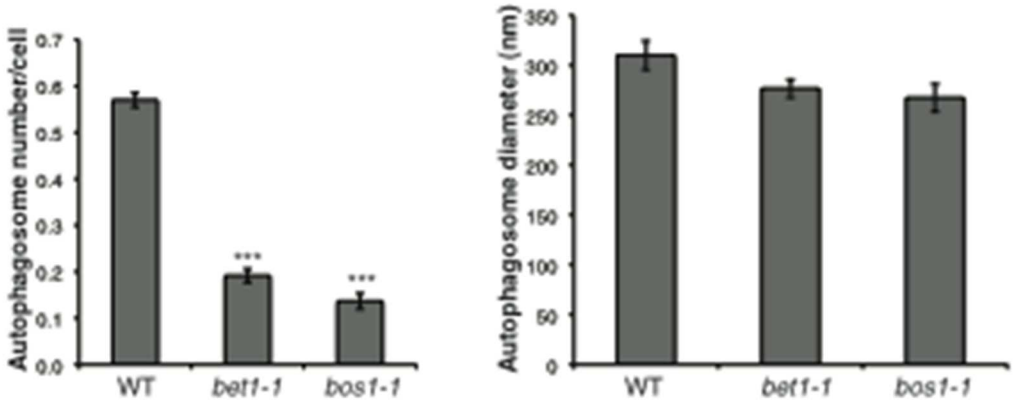

Figure 2.9. ER-Golgi SNAREs regulate autophagosome number.
WT, *bet1-1,* and *bos1-1* cells expressing GFP-Atg8 were treated with 400 ng/mL rapamycin for 1 h at 37°C and were imaged using SIM. The number of autophagosomes per cell was quantitated from 300 cells (left). The diameter of autophagosomes was measured (right). Averages and s.e.m. are shown for 3 biological replicates. ***P < 0.001; Student's unpaired t-test.

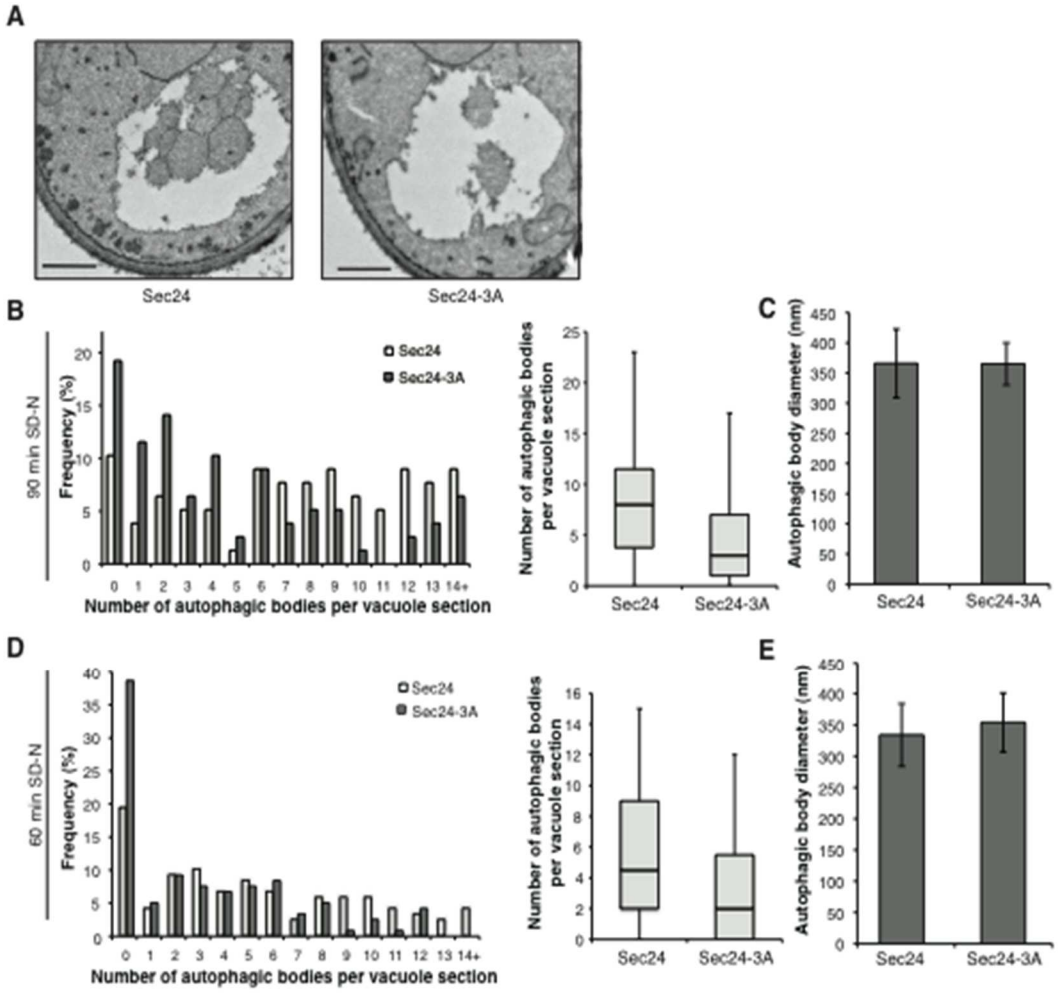

Figure 2.10. Autophagic body number is reduced in Sec24-3A.
A Representative images of autophagic bodies in cells expressing Sec24 (left) and Sec24-3A (right) in *sec24Δiss1Δpep4Δ* deletion strains after 1.5 h of nitrogen starvation at 30°C. Scale bar represents 500 nm. **B** Histogram showing the distribution of the number of autophagic bodies per vacuole section in Sec24 and Sec24-3A. The number of autophagic bodies was quantitated for 78 vacuole sections for each strain (left). p-value = 0.00012; Mann-Whitney Test. Box plot of the number of autophagic bodies per vacuole section. Bars show data between the lower and upper quartiles, the median is a horizontal line within the box. Whiskers indicate the smallest and largest observations (right). **C** The diameter of autophagic bodies was determined. N > 300. Averages with error bars as s.d. are shown. **D** Same as in (B) except after 60 min of nigtrogen starvation. The number of autophaghic bodies was quantitated for 100 vacuole sections for each strain. **E** Same as in (D) except after 60 min nitrogen starvation. Averages with error bars as s.d. are shown. N > 300.

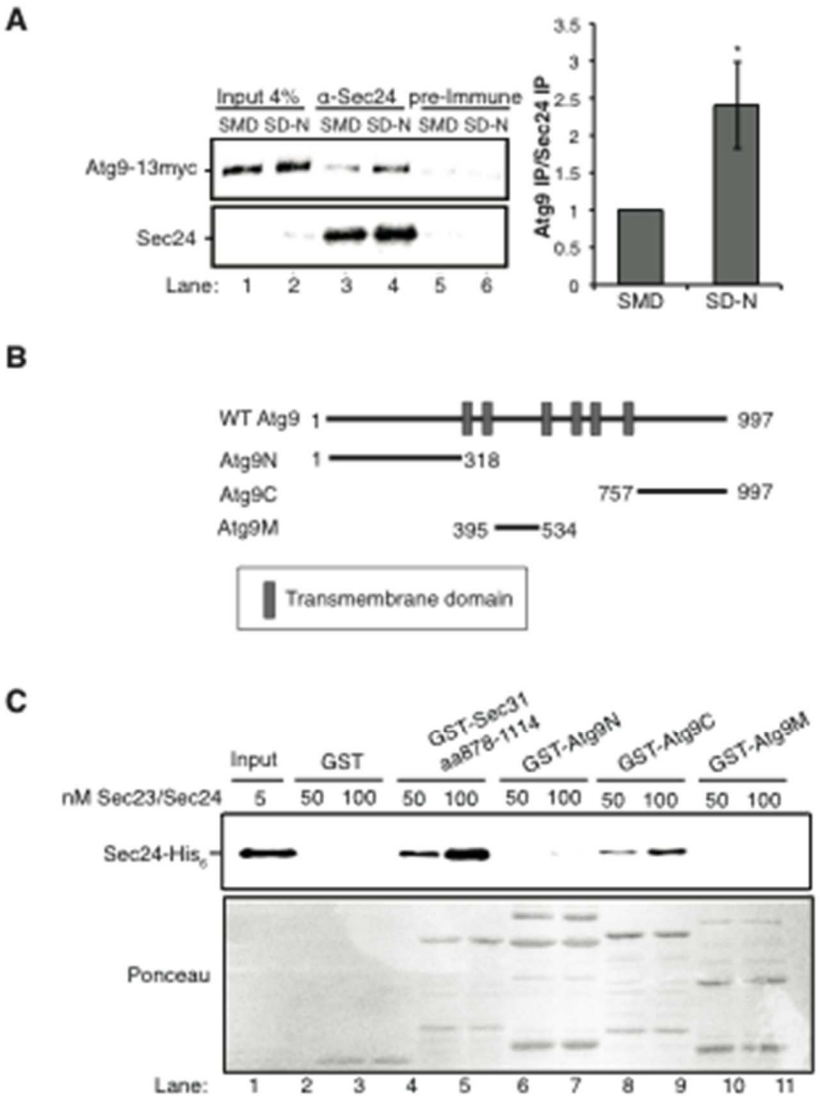

Figure 2.11. Sec24 interacts with the C-terminus of Atg9.
A *ypt7*Δ cells expressing Atg9-13myc were grown in nutrient rich (SMD) or starvation (SD-N) media for 4 h and Sec24 was immunoprecipitated and blotted for Atg9-13myc. Precipitated Atg9-13myc was quantitated and normalized to the amount of Sec24 in the precipitate. SMD was set as 1 for each experiment. Averages and s.e.m. are shown for 4 biological replicates. **B** Schematic showing cytosolic domains of Atg9. **C** Equimolar amounts (200 nM) of purified GST, GST-Sec31 (aa878-1114) or GST-Atg9 fragments were incubated with 50 or 100 nM of Sec23/Sec24-His_6. *$P < 0.05$; Student's unpaired t-test.

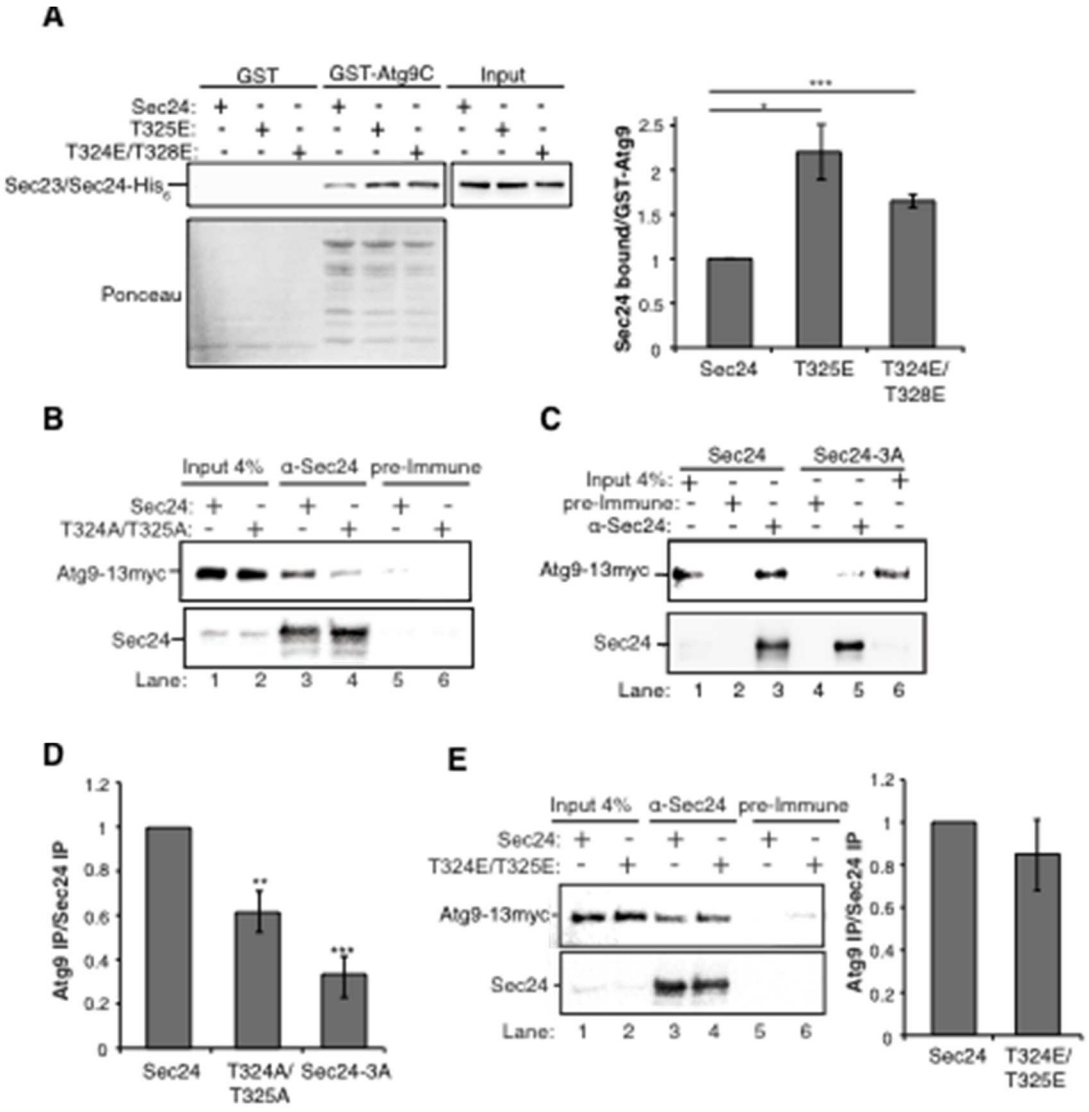

Figure 2.12. Sec24 phosphorylation regulates the Sec24-Atg9 interaction.
A Equimolar amounts (200 nM) of GST-Atg9C or GST was incubated with 37.5 nM of WT Sec23/Sec24-His_6, Sec23/Sec24-T325E-His_6 or Sec23/Sec24-T324E/T328E-His_6 (left). Ratio of Sec24 bound to GST-Atg9C was quantified from 3 biological replicates (right). Binding to WT Sec23/Sec24-His_6 was set as 1 for each experiment. Averages and s.e.m are shown. **B** Sec24 (WT) and Sec24-T324A/T325A or **C** Sec24-T324A/T325A/T325A were immunoprecipitated from lysates expressing Atg9-13myc as described in the Methods. **D** Precipitated Atg9-13myc was quantitated and normalized to the amount of Sec24 in the precipitate. WT Sec24 was set as 1 for each experiment. Averages and s.e.m. are shown for 4 (T324A/T325A) or 5 (Sec24-3A) biological replicates. **E** Same as B except Sec24-T324E/T325E was immunoprecipitated. Averages and s.e.m. are shown for 5 biological replicates. *P < 0.05; **P < 0.01; ***P < 0.001; Student's unpaired t-test.

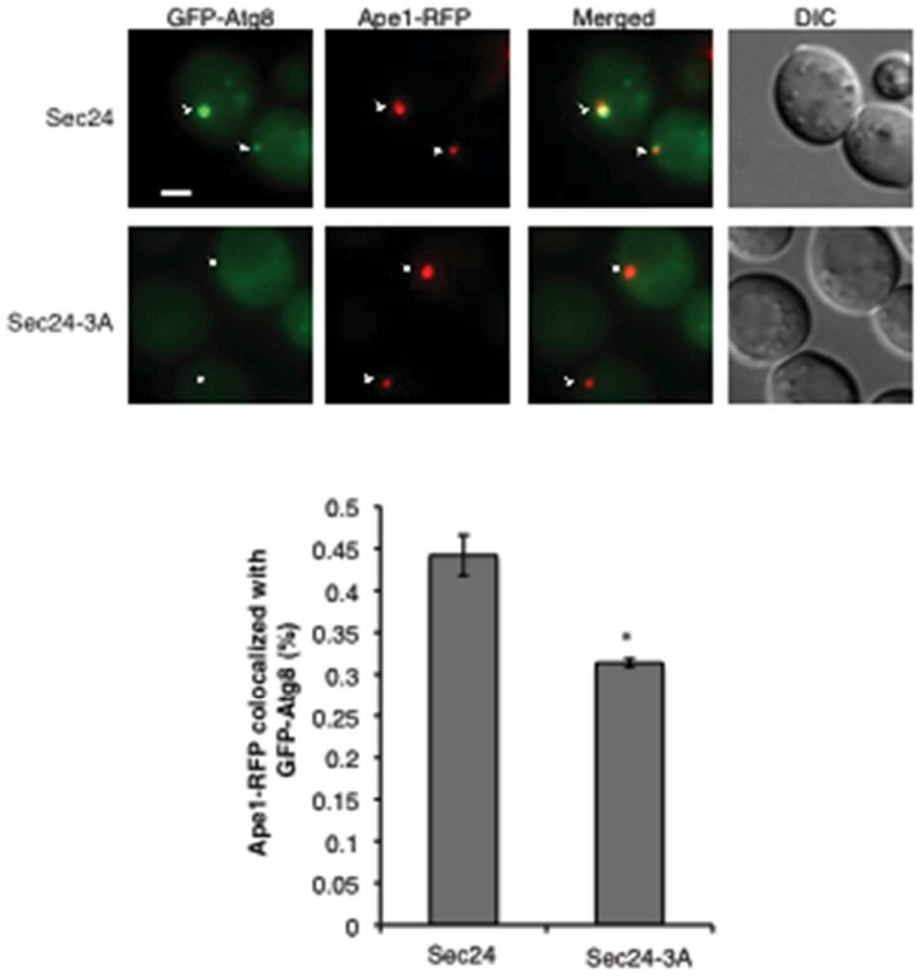

Figure 2.13. Sec24-3A modestly affects Atg8 recruitment to the PAS.
Sec24 or Sec24-3A cells expressing GFP-Atg8 and Ape1-RFP were treated with 400 ng/mL rapamycin for 30 min at 30°C and the percent of Ape1-RFP that colocalized with GFP-Atg8 was determined for 300 cells in 3 biological replicates. Scale bar 2 μM. Arrowheads point to the PAS. Averages and s.e.m are shown. *P < 0.05; Student's unpaired t-test.

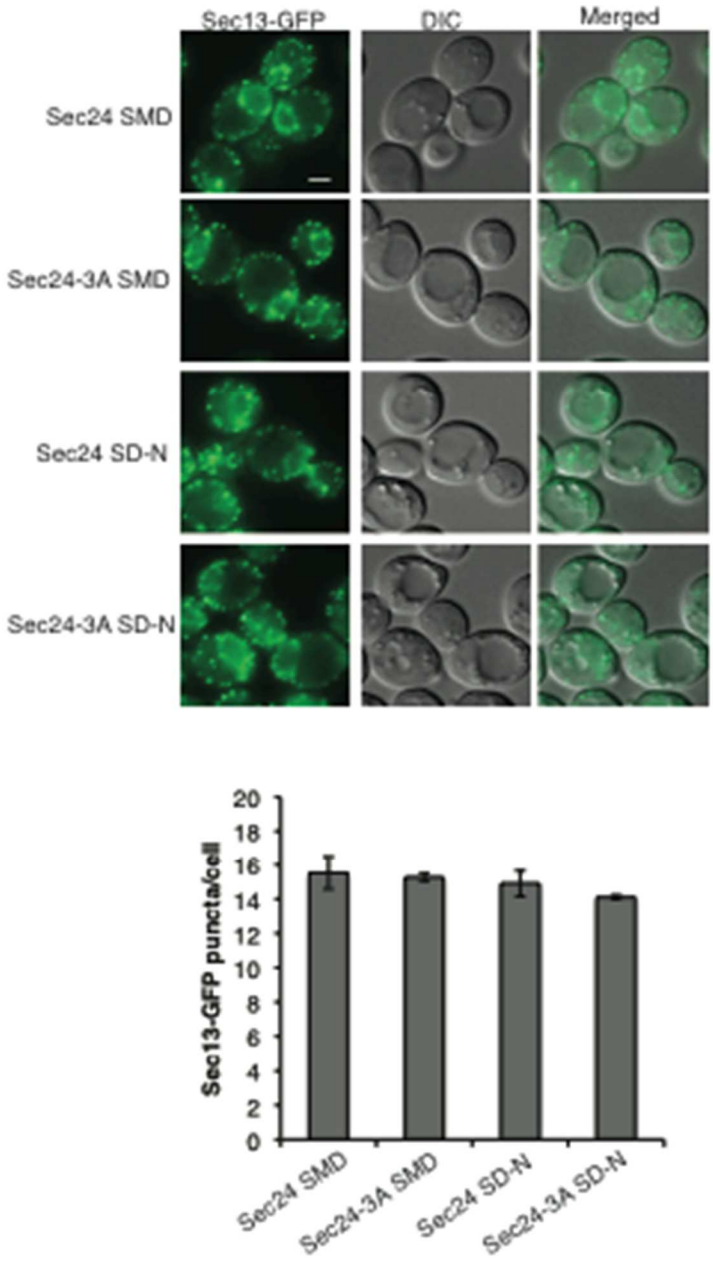

Figure 2.14. Sec24-3A does not affect ERES assembly.
Sec24 and Sec24-3A cells expressing Sec13-GFP were grown in nutrient rich (SMD) or starved for nitrogen (SD-N) for 2 h at 25°C (Top). Scale bar 2 μm. The number of Sec13-GFP puncta per cell was quantitated (bottom). Over 300 cells were quantitated form 3 biological replicates. Averages and s.e.m. are shown.

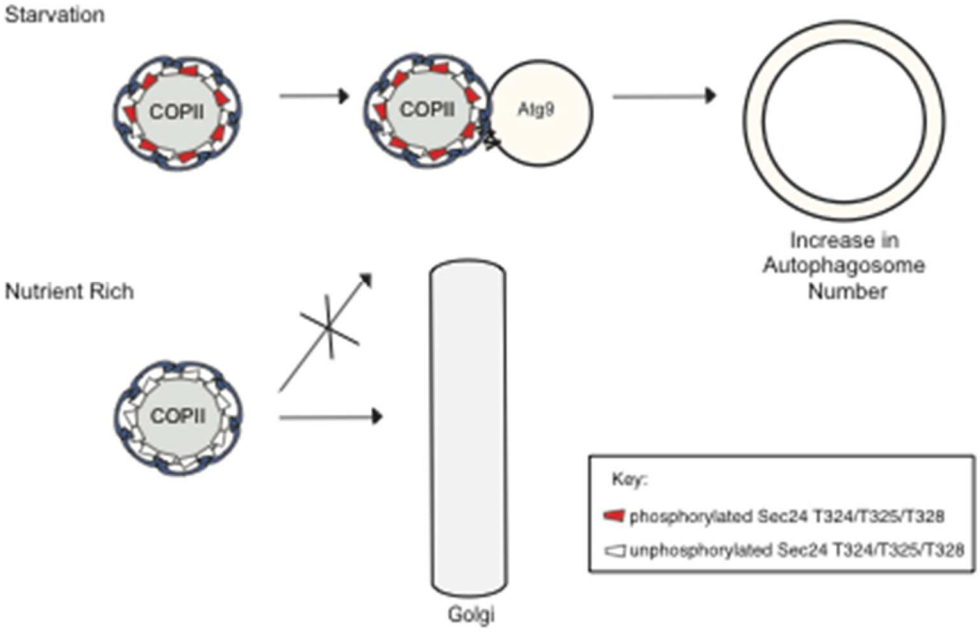

Figure 2.15. Sec24 phosphorylation regulates the Sec24-Atg9 interaction for autophagosome formation.
Phosphorylation of a conserved regulatory surface of Sec24 enhances the ability of the COPII coat to recognize the autophagy machinery. Phosphorylation of the Sec24 membrane distal sites regulates the interaction of Sec24 with the C-terminus of Atg9. During starvation, the Sec24-Atg9 interaction is needed to increase autophagosome number. If Sec24 is not phosphorylated, it is unable to efficiently interact with Atg9 and COPII vesicles traffic to the Golgi.

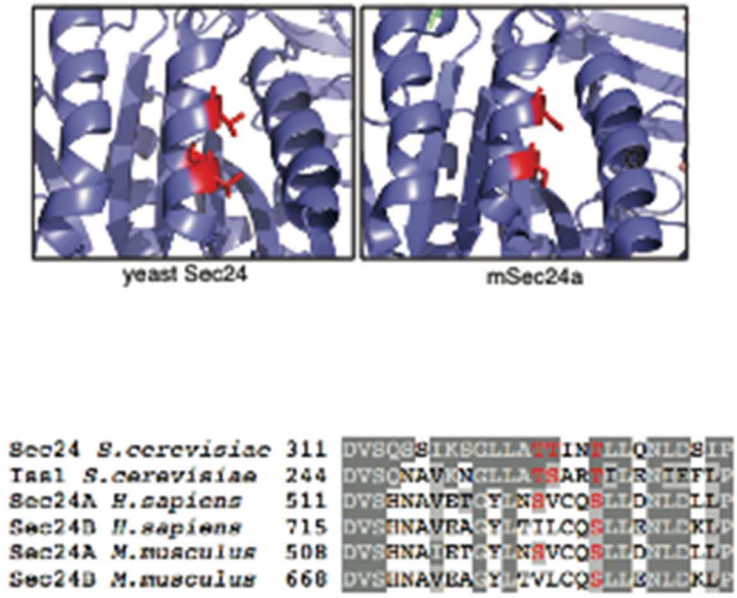

Figure 2.16. The Sec24 membrane distal patch is conserved.
Top, Structure of yeast Sec24 and mSec24a with conserved residues in membrane distal sites (red). Bottom, Alignment of the region surrounding T324/T325/T328 (shown in red) with Sec24 orthologues. Conserved residues shown in gray, similar residues shown in light gray.

Table 2.1. Identification of Sec24 phosphorylation sites.

Phosphosites in Sec24	Confidence (%)	Phosphomimetic Growth Phenotype		Conserved in Iss1
		sec24Δ	*sec24Δ/iss1Δ*	
T152/T155	99, 99	None	None	-, +
S172	46	None	None	+
T305	99	None	None	-
S316/S319	99, 97.8	None	None	-, -
T324/T325	99, 99	None	Not Viable	+, +
T324/T328	99, 99	None	None	+, +
T325/T328	99, 99	Not Viable	Not Viable	+, +
S363/S369/S395	99, 99, 99	None	None	-, -, -
S463	82.7	None	None	-
S469	99	None	None	-
T472	99	None	None	+
S549	97	None	None	+
T635	40	Not Viable	Not Viable	+
T636/S638	99, 99	None	Not Viable	+, +
S645/S678	99, 99	None	None	+, +
S693	99	None	None	+
S725	99	None	None	-
S730/S735	99, 99	None	None	+, +
T778/T780	99, 99	None	None	-, -

Table 2.2. Identification of Sec24 phosphorylation sites required for autophagy.

Phosphosites in Sec24	Confidence (%)	Alanine mutant Growth Phenotype		Conserved in Iss1	Autophagy
		sec24Δ	*sec24Δiss1Δ*		
T152/T155	99, 99	None	None	-, +	+
S172	46	None	None	+	+
T324/T325	99, 99	None	None	+, +	-
T324/T328	99, 99	None	None	+, +	-
T325/T328	99, 99	None	None	+, +	-
T472	99	None	None	+	+
S549	97	None	None	+	+
T635	40	None	None	+	+
T636/S638	99, 99	None	None	+, +	+
S645/S678	99, 99	None	None	+, +	+
S693	99	None	None	+	+
S730/S735	99, 99	None	None	+, +	+

2.4 Discussion

Although significant progress has been made in defining the upstream events leading to the assembly of Atg proteins at the PAS (Nakatogawa et al., 2009), the membrane rearrangements that occur during autophagy remain poorly understood. Here we show that phosphorylation of a conserved regulatory domain of the major COPII cargo adaptor Sec24 reprograms the function of COPII vesicles by modulating its interaction with the C-terminus of Atg9, a key component of the autophagy machinery (Figure 2.15). The C-terminus of Atg9 is present in vertebrates and is essential for autophagy (He et al., 2008; Young et al., 2006). Previous studies have shown that Atg9 functions early in autophagosome initiation (Suzuki et al., 2007; Yamamoto et al., 2012) and affects autophagosome number, but not size (Jin et al., 2014). Similarly, mutating the Sec24 regulatory sites specifically affects autophagosome number. Collectively these results imply that Sec24 functions with Atg9 during autophagy to regulate autophagosome abundance.

Previous work has established that COPII vesicles are required for autophagy (Ge et al., 2014; Graef et al., 2013; Lemus et al., 2016; Suzuki et al., 2013; Tan et al., 2013; Wang et al., 2015). However, because it has been difficult to fully tease apart the function of COPII vesicles on the secretory pathway from their role in autophagy, their contribution to autophagy has been problematic to address. Our finding that phosphorylation of a novel regulatory surface of Sec24 is specifically required for autophagy and not ER-Golgi transport conclusively demonstrates that COPII vesicles play a direct role in autophagy, rather than an indirect role in maintaining the trafficking of autophagy machinery through the secretory pathway. Additionally, we

can now ascribe an autophagy-specific role to COPII vesicles in enhancing autophagosome number during nutrient deprivation. This role of Sec24 in autophagy is likely to be conserved in mammalian cells as T324 and T328 are conserved in mSec24a (Figure 2.16).

Interestingly, membrane fractionation identified the mammalian ER-Golgi intermediate compartment (ERGIC) as the site of lipidation of LC3, Atg8 in mammals (Ge et al., 2014). During starvation, the ERES were found to translocate to the ERGIC fraction, and although the ERGIC is typically a location of COPI vesicle budding, COPII vesicle budding from this ERGIC fraction was shown to be required for LC3 lipidation (Ge et al. 2014). These observations suggested that, in higher eukaryotes, the COPII vesicles used in autophagy are spatially separated from those that traffic to the Golgi. The findings were report here could explain how these spatially segregated COPII vesicles engage the Atg machinery.

Here we have begun to unravel the stage at which COPII vesicles act during autophagosome formation. Current data strongly points to COPII vesicles fusing with Atg9 vesicles or an isolation membrane containing Atg9. This model is based on the interaction between the COPII coat and Atg9, the localization of Atg9 to the growing tip of the phagophore adjacent to the ERES (Graef et al., 2013; Suzuki et al., 2013) and the similar defect in autophagosome frequency in Sec24 and Atg9 mutants (Jin et al., 2014). Although a mechanism for COPII and Atg9 vesicle fusion is unknown, current evidence points to the ER-Golgi SNAREs as candidates to mediate these fusion events. The ER-Golgi SNAREs are required for autophagy (Tan et al., 2013)

and autophagosome formation (Figure 2.9). Furthermore, disrupting the packaging of the SNARE Sed5 into COPII vesicles inhibits autophagy (data not shown). Future work to further examine the roles of ER-Golgi SNAREs in autophagy will be discussed in Chapter 5.

In conclusion, our findings highlight an unexpected role for phosphorylation in regulating the reorganization of membrane trafficking pathways during starvation and demonstrate that the COPII coat is a key target of this regulation. Identification of a cellular mechanism that redirects the flow of membrane during autophagy makes it possible to now study how these complex membrane rearrangement events culminate in the formation of a distinct organelle, the autophagosome.

2.5 Methods

2.5.1 Mass spectrometry

Sec24-His_6 was purified from SFNY2181 as described previously (Kurihara et al., 2000) with the following modifications. Cells were grown overnight to log phase in SC-Ura-Leu medium with 10% glycerol as the carbon source, and induced at a starting OD_{600} of 0.6-0.8 with 0.2% galactose for 5 h at 30°C. These growth conditions were found to induce autophagy in the absence of rapamycin. Cells were lysed in approximately 20 ml HSLB (0.75 M potassium acetate, 50 mM HEPES pH 7.0, 0.1 mM EGTA, 20% glycerol) with protease and phosphatase inhibitor cocktails (Sigma). The cleared lysate was incubated with Ni-NTA beads for 1 h at 4°C and washed with 20 ml B-II and 20 ml B-III (Kurihara et al., 2000). Sample preparation for mass-spectrometry was carried out as described before (Guttman et al., 2009), then

liquid chromatography coupled tandem mass spectrometry analysis (LC-MS/MS) was performed as described previously (Meyer et al., 2014).

2.5.2 Generation of *sec24* mutants

Mutations in pSFN1915 (*SEC24*, *HIS3*, *CEN)* were made using the QuikChange Site-directed mutagenesis kit (Agilent technologies) and all mutations were confirmed by DNA sequencing. Plasmids were then introduced into SFNY2201 and SFNY2202 and grown on two round of 5-fluoroorotic acid (5-FOA) plates at 25°C to select against *pLM22* (*SEC24, URA3, CEN)*. To observe growth defects, *sec24* mutants were compared to WT *SEC24* at 25°C after two rounds of 5-FOA. For purification of mutant coat proteins, the mutations were made on *pSFNB1895 (GAL1-SEC24-His, LEU2, CEN)* and co-transformed with *pSFNB1894 (GAL1-SEC23, URA3, CEN)* into SFNY2367.

2.5.3 In vitro vesicle budding and fusion assays

COPII proteins (Sar1, Sec23/Sec24 and Sec13/Sec31) were purified (Miller et al., 2003) and used to generate vesicles from microsomal membranes prepared as described (Barlowe et al., 1994). Vesicle budding assays were performed as described previously (Miller et al., 2002). Vesicle fusion was monitored by measuring α-1,6-mannose modification of ^{35}S-labeled pro-α-factor as described previously (Barlowe et al., 1994).

2.5.4 Pho8Δ60 assay

Alkaline phosphatase assays were performed as previously described (Klionsky, 2007). Cells were grown overnight at 25°C to log phase, OD_{600} between

0.7 and 1.0, washed with 10 ml SD-N medium and incubated in SD-N medium for 2 to 4 h at 25°C or 37°C to induce autophagy. 2.5 OD_{600} units of cells were collected and washed, and lysed in 250 µl of lysis buffer (20 mM PIPES pH 7.2, 0.5% TritonX-100, 50 mM KCl, 100 mM potassium acetate, 10 mM $MgS0_4$, 10 µM $ZnSO_4$, and 1 mM PMSF) using glass beads. Lysates, with a protein concentration around 0.5 mg/ml, were spun for 5 min at 13,000 rpm, and 100 µl of lysate was assayed at 37°C in 400 µl reaction buffer (1.25 mM p-nitrophenyl phosphate, 250 mM Tris-HCl pH 8.5, 0.4% Triton X-100, 10 mM $MgSO_4$, and 10 µM $ZnSO_4$). The reaction was stopped with 500 µl of stop buffer (1 M glycine/KOH pH 11.0), and the OD_{400} value was determined. The data were normalized to protein concentration using the Bradford method and IgG as a standard.

2.5.5 Fluorescence Microscopy

For GFP-Atg8 vacuole localization, cells were grown at 25°C overnight in SC-Ura to early log phase, OD_{600} between 0.6 and 1.0. Cells were washed and resuspended in SD-N and incubated for 1 h at 25°C or 30 min at 37°C. For Sec13-GFP localization cells were grown overnight to early log phase at 30°C to early log phase, OD_{600} between 0.6 and 1.0. Cells were washed and resuspended in SD-N and incubated for 2 h at 30°C. For co-localization of Ape1-RFP with Atgs, cells were grown to an OD_{600} between 0.6 and 1.0 and treated with 400 ng/mL rapamycin for 30min to 1 h at 25°C. Cells were then visualized at 25°C with a Zeiss Axio Imager Z1 fluorescence microscope using a 100 x 1.3 NA oil-immersion objective. Images were

captured with a Zeiss AxioCam MRm digital camera and analyzed with AxioVision software.

To examine autophagosome formation by structured illumination (SIM) microscopy, cells were grown overnight at 25°C in SC-Ura to early log phase, OD_{600} between 0.6 and 1.0. For autophagy induction, cells were treated with 400 ng/ml rapamycin for 1 h at 25°C or for 1 h at 37°C for temperature-sensitive mutants. Cells were pelleted and incubated in 3.7% formaldehyde for 30 min at 25˚C and visualized on an Applied Precision DeltaVision OMX Super Resolution System using an Evolve 512 EMCCD camera. The data was acquired and processed using Delta Vision OMX Master Control software and SoftWoRx reconstruction and analysis software. To determine autophagosome size, deconvolved images were analyzed with Image J software.

2.5.6 GFP-Atg8 cleavage

Cells were grown overnight in SC media to early log phase and washed and shifted to SD-N for 1 h at 25°C. 2.5 OD_{600} units of cells were pelleted in 100 µl ddH_2O and 100 µl of 0.2 M NaOH was added. Cells were mixed and incubated at room temperature for 5 min. Cells were pelleted and boiled in sample buffer for 5 min at 95°C.

2.5.7 CPY Pulse Chase

Cells were grown overnight in minimal media at 25°C to early log phase and 16 OD_{600} units of cells were pelleted and resuspended in 3.6 ml of fresh minimal media. For starved samples, cells were washed and shifted to SD-N for 1 h at 25°C.

16 OD_{600} units of cells were then pelleted and resuspended in 3.6 ml of fresh SD-N. Cells were pulse labeled with 400 µCi of S^{35}-methionine for 4 min at 25°C, and 700 µl of the cell suspension was removed and added to 700 µl of ice-cold 20 mM sodium fluoride/sodium azide (0 min time-point). 250 µl of chase mix (250 mM methionine, 250mM cysteine) was added to the remaining sample, and then 700 µl of cells were removed at 5, 10 and 15 min. Cells were pelleted and washed with 1 ml of cold 10 mM sodium fluoride/sodium azide, resuspended in 150 µl spheroplasting buffer (1.4 M sorbitol, 100 mM sodium phosphate pH 7.5, 0.35% b-mercaptoethanol and 0.2 mg/ml zymolyase) and incubated at 37°C for 45 min. Spheroplasts were spun for 3 min at 6500 rpm and heated for 5 min at 95°C in 100 µl 1% SDS. 900 µl of PBS plus 2% Triton X-100 was added to the lysates before they were spun for 15 min at 14,000 rpm. CPY antibody (3 µl of anti-Rabbit serum prepared against CPY) was added to 920 µl of cleared lysate and incubated for 1 h at 4°C with rotation. 50 µl of 50% Protein-A sepharose was added and incubated for 1 h. The protein-A beads were washed twice with 1 ml of PBS, followed by two washes with 1 ml of 1% b-mercaptoethanol and heated in 70 µl of 1x sample buffer for 5 min at 95°C. Samples were normalized to cpm in the cell lysate, then loaded onto an 8% SDS-PAGE gel and processed for autoradiography. Protein bands were quantified using Image J software.

2.5.8 Electron Microscopy

Cells were grown overnight in YPD to an OD_{600} of 1.0 and shifted to SD-N for 1 or 1.5 h at 30°C. 30 OD_{600} units of cells were pelleted, resuspended in 1 mL of 1.5% $KMnO_4$ and incubated for 30 min at 4°C with nutation. Cells were then pelleted

and resuspended in 1 mL of 1.5% $KMnO_4$ and incubated overnight at 4°C with nutation. Samples were dehydrated in ethanol, embedded in Durcupan epoxy resin (Sigma-Aldrich) and sectioned at 60 nm on a Leica UCT ultramicrotome. Sections were picked up on Formvar and carbon-coated copper grids and stained with 2% uranyl acetate for 5 min and Sato's lead stain for 1 min. Grids were viewed using a Tecnai G2 Spirit BioTWIN transmission electron microscope equipped with an Eagle 4k HS digital camera (FEI, Hilsboro, OR). Autophagic body number and size were determined with Adobe Photoshop and Image J software as described previously (Backues et al., 2013).

2.5.9 Co-immunoprecipitation of Sec24 and Atg9

Cells were grown overnight to early log phase. For starvation, cells were shifted to SD-N for 4 h at 30°C. 100 OD_{600} units of cells were pelleted, resuspended in 2 ml of spheroplasting buffer (1.4 M sorbitol, 100 mM sodium phosphate pH 7.5, 0.35% b-mercaptoethanol and 0.5 mg/ml zymolyase) and incubated for 30 min at 37°C. Spheroplasts were loaded on top of a 5 ml sorbitol cushion (1.7 M sorbitol, 100 mM HEPES pH 7.2) and spun for 5 min at 3,000 rpm. Cells were lysed in 1 ml of lysis buffer II (20 mM Hepes pH 7.4, 150 mM NaCl, excess protease inhibitors – combination of Roche and Sigma inhibitors, phosphatase inhibitors (Sigma)) with a dounce homogenizer on ice. Cell debris was cleared by a 10 min spin at 500 xg. When cross-linking was performed, lysates were incubated on ice with 100 mM dithiobis (succinimidyl propionate) for 30 min. To quench excess crosslinker, 100 mM Tris pH 7.6 was added and incubated for 15 min on ice. Triton X-100 was added

to a final concentration of 1% and incubated on ice for 30 min followed by a 15 min spin at 15,000xg. The lysates were incubated with 50 µl of 50% protein A-sepharose for 20 min at 4°C with rotation to pre-clear the lysates and reduce background. To immunoprecipitate Sec24, 2 mg of lysate was incubated with 10 µl of Sec24 antibody (rabbit polyclonal prepared against GST-Sec24) or 10 µl of pre-immune serum for 2 h at 4°C with rotation. 50 µl of 50% protein A-sepharose was added and incubated for 45 min at 4°C with rotation. The beads were then washed 5 times with 1 ml of lysis buffer with 1% Triton X-100 and heated in 40 µl of 3x sample buffer for 5 min at 95°C.

2.5.10 Purification of fusion proteins from bacteria.

For purification of GST fusion proteins, bacterial cells were incubated at 18°C overnight with 0.5 mM isopropyl β-D-1-thiogalactopyranoside to induce protein expression. Cells were collected and resuspended in 1x phosphate-buffered saline (PBS) with 1 mM DTT and protease inhibitors. Cells were sonicated for 2 min total with 15 sec on/off bursts on ice. Triton X-100 was added to a final concentration of 1% and lysates were incubated on ice for 15 min. Lysates were cleared through a 15 min centrifugation at 15,000 rpm. The supernatant was incubated with 1 mL of 50% glutathione sepharose beads (GE Healthcare) that had been prewashed with PBS for 1 h at 4°C with rotation. The beads were washed extensively with PBS and stored at 4°C.

His_6-Sec23 was purified as described above for GST-fusion proteins except cells were lysed in 50 mM Hepes pH 7.2, 150 mM NaCl, 15 mM Imidazole, 1mM

DTT with protease inhibitors and incubated with Ni^{2+}-NTA resin (Qiagen). Protein was eluted from the resin with 50 mM Hepes pH 7.2, 150 mM NaCl, 250 mM Imidazole.

2.5.11 In vitro bindings with GST-Atg9 fragments

Equimolar amounts (0.2 μM) of immobilized GST fusions were incubated with increasing amounts of bacterially purified His_6-Sec23 or Sec23/Sec24-His_6 from yeast in binding buffer (50 mM HEPES pH 7.2, 150 mM NaCl, 1% Triton X-100, 1 mM $MgCl_2$, 1 mM EDTA, 1 mM DTT, protease inhibitors) for 4 h at 4°C with rotation. Beads were washed 3-4 times with binding buffer and eluted in 50 μL of sample buffer by heating for 5 min at 95°C.

2.6 Acknowledgements

Most of the work in Chapter 2 is taken from "Sec24 phosphorylation regulates autophagosome abundance during nutrient deprivation" which has been submitted for publication and is currently under review at Elife. Juan Wang, Ming Zhu, Kyle Stahmer, Ramya Lakshminarayan, Majid Ghassemian, Yu Jiang, Elizabeth Miller and Susan-Ferro-Novick are co-authors. The dissertation author is the primary researcher of this paper. Other non-published work in this section was performed by the dissertation author unless otherwise noted.

Juan Wang performed the Pho8Δ60 assays in Figure 2.3 and some of the Pho8Δ60 assays in Table 2.2. Juan Wang also performed the SIM in Figure 2.8 and the recruitment of additional Atg proteins to the PAS discussed in section 2.3.6. Elizabeth Miller and Kyle Stahmer performed the in vitro fusion and cargo-packaging

assays respectively with the Sec24-S730/S735 mutants discussed in section 2.3.2. Ramaya Lakshinmarayan performed the cargo-packaging assay with Sec24-S645/S678 mentioned in section 2.3.2. Ming Zhu helped with protein purification for in vitro bindings and performed some of the in vitro bindings in section 2.3.6. Wenyun Zhou assisted with the mutagenesis of Sec24 in Table 2.1. Deepali Bhandari purified Sec24 for mass spectrometry and Majid Ghassemian performed the mass spectrometry in section 2.3.1. Ying Jones prepared the samples for electron microscopy in section 2.3.4. The GST-Atg9C construct used in these studies is from Claudine Kraft and the pFA6a-3xyEGFP-CaURA3 construct is from Jodi Nunnari.

CHAPTER 3

Hrr25 functions in autophagosome formation through Sec24 phosphorylation

3.1 Summary

Phosphorylation of Sec24 is required for the COPII coat to recognize the autophagy machinery, which is critical for autophagosome formation. The kinase involved in phosphorylating Sec24 to regulate this novel role during autophagy is unknown. The casein kinase, Hrr25, has previously been shown to phosphorylate Sec24 and was recently implicated as a positive regulator of autophagy. However, the precise function of Hrr25 in autophagy was unclear. To determine if Hrr25 phosphorylates the Sec24 membrane distal patch, we identified in vitro phosphorylation sites on Sec24 by mass spectrometry and picked up Sec24-T328 at lower confidence. We next confirmed that Hrr25 regulates autophagic body number, but not size through electron microscopy. Consistent with Hrr25 phosphorylating the Sec24 membrane distal patch, Hrr25 is required for the Sec24-Atg9 interaction in vivo. Ectopic expression of Sec24 T325E/T328E partially rescued the Sec24-Atg9 interaction and autophagy defect in an *hrr25* mutant, whereas Sec24 T325A/T328A did not. Additionally, we looked at another COPII coat subunit Lst1, whose phosphorylation can be monitored by a gel shift and found that Lst1 was more phosphorylated during starvation in a manner dependent on Hrr25. Collectively these

results strongly implicate Hrr25 as a key kinase involved in phosphorylating the Sec24 membrane distal surface during autophagy.

Although we found that Hrr25 is not directly regulated during autophagy, it could work with additional kinases that phosphorylate the COPII coat during autophagy. Here we examined the two most obvious candidates: Atg1 and Nnk1. Atg1 is an essential kinase required for autophagosome formation. However, we found that Atg1 does not directly interact with Sec23/Sec24 and is not required for Lst1 phosphorylation during starvation suggesting it likely does not phosphorylate the COPII coat. Although Nnk1 does directly interact with the COPII coat and was previously linked to TOR, a key autophagy regulator, we found that Nnk1 is not required for autophagy.

3.2 Introduction

Autophagy requires significant membrane rearrangements in order to rapidly upregulate autophagosome formation during starvation. COPII coated vesicles, which act on the secretory pathway to transport cargo from the ER to the Golgi, are also required for autophagosome formation during nutrient deprivation (Ge et al., 2014; Ishihara et al., 2001; Tan et al., 2013). Our previous analysis showed that phosphorylation is a mechanism through which the function of COPII vesicles is regulated during autophagy. Specifically, we showed that phosphorylation of the membrane distal surface of the COPII coat subunit Sec24 allows it to recognize Atg9, a critical component of the autophagy machinery (Yamamoto et al., 2012). Consequently, we next sought to identify the kinase(s) responsible for this

phosphorylation event. The serine/threonine kinase, Hrr25, is the only kinase in yeast known to phosphorylate Sec24 and it was recently shown that Hrr25 is required for non-selective autophagy (Lord et al., 2011; Wang et al., 2015). Accordingly, we hypothesized that Hrr25 may be required for phosphorylation of the Sec24 membrane distal surface, which is needed to regulate COPII vesicles during starvation.

Hrr25 phosphorylates multiple COPII coat subunits including Sec24, Sec23, Sec31 and Lst1 (Bhandari et al., 2013; Lord et al., 2011). Hrr25 phosphorylation of Sec23 helps drive sequential interactions that mediate the forward flow of COPII vesicle traffic, preventing inappropriate vesicle fusion with the ER. These sequential interactions are required for both ER-Golgi transport and autophagy (Lord et al., 2011; Wang et al., 2015). However, epistasis studies suggested Hrr25 may have an additional role in autophagy, upstream of COPII vesicle delivery to the PAS (Wang et al., 2015). Specifically, it was shown that while COPII coated structures accumulate at the PAS when autophagy is blocked in cells deleted for the key autophagy kinase Atg1, they failed to accumulate in the *hrr25-5* mutant or in an *hrr25-5atg1*Δ double mutant (Wang et al., 2015). Moreover, Sec24 T328 fits the CK1 consensus motif (pS/pT-X-X-S/T) (Knippschild et al., 2005) (Figure 3.2; A) making Hrr25 a likely kinase for phosphorylating this residue.

We also examined two additional kinases as potential candidates for Sec24 phosphorylation: Atg1 and Nnk1. Atg1 is a serine/threonine kinase that is part of the initiating complex that helps assemble the PAS and recruits downstream Atg proteins (Nakatogawa et al., 2009). Atg1 is the central kinase involved in autophagosome formation and its kinase activity is activated upon autophagy induction (Kamada et al.,

2000). Although Atg1 displays a strong preference for serines over threonines, it also prefers hydrophobic residues at the N-3 position, which fits Sec24 T325 (Papinski et al., 2014) (Figure 3.2; A). Additionally, the mammalian homologue of Atg1, Ulk1, was recently shown to phosphorylate Sec16, which regulates COPII vesicle assembly at ER exit sites (Joo et al., 2016), indicating there could be a connection between Atg1 and the COPII coat.

Nnk1 is a poorly characterized kinase, which was initially identified in a high throughput screen as interacting with the TOR network, an upstream negative regulator of autophagy (Breitkreutz et al., 2010). Additionally, mass spectrometry screens identified Nnk1 as physically interacting with COPII coat subunits (Breitkreutz et al., 2010). Direct interaction of Nnk1 with Sec23 and Sec24 was verified in our lab through in vitro bindings (data not shown). Thus we sought to determine whether Nnk1 works with Hrr25 to regulate autophagy.

3.3 Results

3.3.1 Hrr25 regulates autophagy in part through the Sec24-Atg9 interaction

To begin to address whether Hrr25 is involved in phosphorylating the Sec24 membrane distal sites we began by identifying Hrr25 in vitro phosphorylation sites on Sec24. GST-Sec24 was purified from bacteria and phosphorylated in vitro with His_6-Hrr25 (aa1-394). A truncated Hrr25 construct was used as it removes a c-terminal inhibitory domain increasing Hrr25 kinase activity. We performed two independent rounds of mass spectrometry with different digestion enzymes in order to increase the sequence coverage of Sec24. This analysis identified 11 high confidence Hrr25

phosphorylation sites on Sec24, four of which were also picked up with high confidence in vivo (Table 3.1). Interestingly, Sec24 T328 was identified as a lower confidence in vitro site.

If Hrr25 phosphorylates the Sec24 membrane distal sites in vivo, we predicted that an *hrr25* mutant would have a similar autophagy phenotype as Sec24-3A. Autophagosome formation was previously analyzed by SIM in *hrr25-5* and *hrr25-5* showed a defect in autophagosome number (Wang et al., 2015). To confirm these findings transmission electron microscopy was performed on *hrr25-5* in a *pep4*Δ background after 90 min of starvation at 37°C. Similar to Sec24-3A, *hrr25-5* caused a reduction in autophagic body number but not size (Figure 3.1; A, B, C).

We previously showed that phosphorylation of the Sec24 membrane distal surface modulates the interaction of Sec24 with Atg9, a key regulator of autophagosome formation. Therefore, we next sought to determine if Hrr25 is required for the Sec24-Atg9 interaction. Consistent with a role for Hrr25 in phosphorylating the Sec24 membrane distal patch, less Atg9 co-immunoprecipitated with Sec24 from an *hrr25-5* mutant lysate (Figure 3.2; B). To determine if Hrr25 regulates the Sec24-Atg9 interaction via Sec24 phosphorylation, we asked whether the Sec24 phosphomimetic mutations could rescue the Sec24-Atg9 interaction defect in *hrr25*-5. Sec24 T325/T328 was chosen for this analysis as it contained T328, which is phosphorylated by Hrr25. WT Sec24, Sec24 T325A/T328A or Sec24 T325E/T328E was ectopically expressed in *hrr25-5* containing Atg9-13myc and Sec24 was immunoprecipitated. Sec24 T325E/T328E partially rescued the Sec24-Atg9 interaction in *hrr25-5*, whereas Sec24 T325A/T328A did not (Figure 3.2; C). To

determine if this improved Sec24-Atg9 interaction alleviates the autophagy defect in *hrr25-5,* GFP-Atg8 vacuolar localization was examined after 2 h starvation at 37°C in *hrr25-5* cells expressing WT Sec24*,* Sec24 T325A/T328A or Sec24 T325E/T328E. Consistent with Hrr25 phosphorylating the Sec24 membrane distal sites, Sec24 T325E/T328E partially rescued the GFP-Atg8 translocation defect in *hrr25-5* while Sec24 T325A/T328A did not (Figure 3.3; A). To confirm the fluorescence results, GFP-Atg8 cleavage was also examined. Sec24 T325E/T328E almost fully rescued the GFP cleavage defect in *hrr25-5*, while Sec24 T325A/T328A had no effect (Figure 3.3; B). Therefore, even though Hrr25 may have additional roles in autophagy, phosphorylation of Sec24 is a primary function of this kinase during starvation.

3.3.2 Hrr25 regulates Lst1 phosphorylation during starvation

We next wanted to determine if Hrr25 phosphorylates the COPII coat during starvation. For technical reasons, we have been unable to address if the Sec24 membrane distal sites are phosphorylated as a consequence of inducing autophagy. As a result we looked at another cargo adaptor of the COPII coat, Lst1, that is a known Hrr25 substrate whose phosphorylation can be monitored by a gel mobility shift (Bhandari et al., 2013). This gel shift assay enabled us to ask if Hrr25 phosphorylates a COPII coat subunit during starvation. For this analysis we used W303 strains, since the shift in Lst1 is most dramatic in this strain background. Furthermore, while Hrr25 is essential in most strain backgrounds, it is not essential in W303 strains, allowing us to test a null mutant (DeMaggio et al., 1992). After nitrogen starvation, the mobility of Lst1 decreased (Figure 3.4; A). The higher molecular weight form (lane 3) was abolished when immunoprecipitated Lst1 was treatment with calf intestinal

phosphatase (CIP), in the absence (lane 4) but not presence (lane 5) of EDTA, demonstrating this mobility shift is a consequence of phosphorylation. The starvation-dependent Lst1 mobility shift was not seen in the *hrr25*Δ mutant (Figure 3.4; B), indicating that Hrr25 is required for phosphorylation of Lst1 during starvation. Although Lst1 is not essential for autophagy (data not shown), these findings demonstrate that Hrr25 substrates can be more phosphorylated as a consequence of autophagy induction.

We next asked whether Hrr25 is regulated during starvation. Hrr25 expression levels were assayed after a time course of nitrogen starvation and were found to be unaffected (Figure 3.5; A). Next, Hrr25 kinase activity was assayed by immunoprecipitating Hrr25-HA from cells grown in nutrient rich media or starved for nitrogen and myelin basic protein (MBP) was phosphorylated in vitro. The kinase activity of Hrr25 was also unaffected by starvation (Figure 3.5; B). These findings indicate that Hrr25 is not directly regulated during autophagy. Alternatively, Hrr25 may act with one or more kinases that are regulated during starvation. Given that CK1 kinases prefer prephosporylated substrates at the N-3 position (Knippschild et al., 2005) (Figure 3.2; A), it is likely another kinase phosphorylates the coat in response to autophagy induction, making COPII cargo adaptors more effective substrates for Hrr25.

3.3.2 Atg1 does not interact with Sec23/Sec24

Atg1 is an essential kinase for autophagosome formation, whose substrates are only recently being identified. To test if Atg1 directly regulates the COPII coat we

first tested whether Atg1 interacts with Sec23/Sec24 in vitro. Sec23/Sec24-His_6 was purified from yeast and tested for binding in vitro with bacterially purified GST-Atg1 (aa1-500) and GST-Atg1 (aa501-end). GST-Sec31 (aa878-1114), a fragment of the outer coat that interacts with Sec23/Sec24, was used as a positive control and GST as a negative control (Bi et al., 2007). Neither the N-terminal kinase domain nor the C-terminal domain of Atg1 bound to Sec23/Sec24, suggesting Atg1 does not directly interact with Sec23/Sec24 (Figure 3.6; A).

We next looked to see if Atg1 regulates COPII coat phosphorylation in vivo. The phosphorylation of Lst1 was monitored in an Atg1 kinase dead mutant, *atg1 D211A,* after nutrient rich or starvation conditions. Lst1 phosphorylation was not reduced in *atg1 D211A* and actually tended to be more phosphorylated in this mutant (Figure 3.6; B). These findings support the idea that Atg1 is not required for phosphorylation of the COPII coat during starvation.

3.3.3 Nnk1 is not required for autophagy

Because Nnk1 is connected to the TOR network (Breitkreutz et al., 2010) and it directly interacts with the COPII coat we asked whether Nnk1 works with Hrr25 during autophagy. To test this hypothesis we monitored autophagy in an *nnk1*Δ mutant. The translocation of GFP-Atg8 to the vacuole during starvation was not affected by *nnk1*Δ (Figure 3.7; B) nor was pho8Δ60 activity (data not shown). To determine whether Nnk1 has a synthetic interaction with Hrr25, Nnk1 was deleted in the *hrr25-5* mutant. Deletion of Nnk1 in *hrr25*-5 did not affect the growth of *hrr25*-5

or the translocation of GFP-Atg8 to the vacuole (Figure 3.7; A, B). These results demonstrate that Nnk1 does not work with Hrr25 during autophagy.

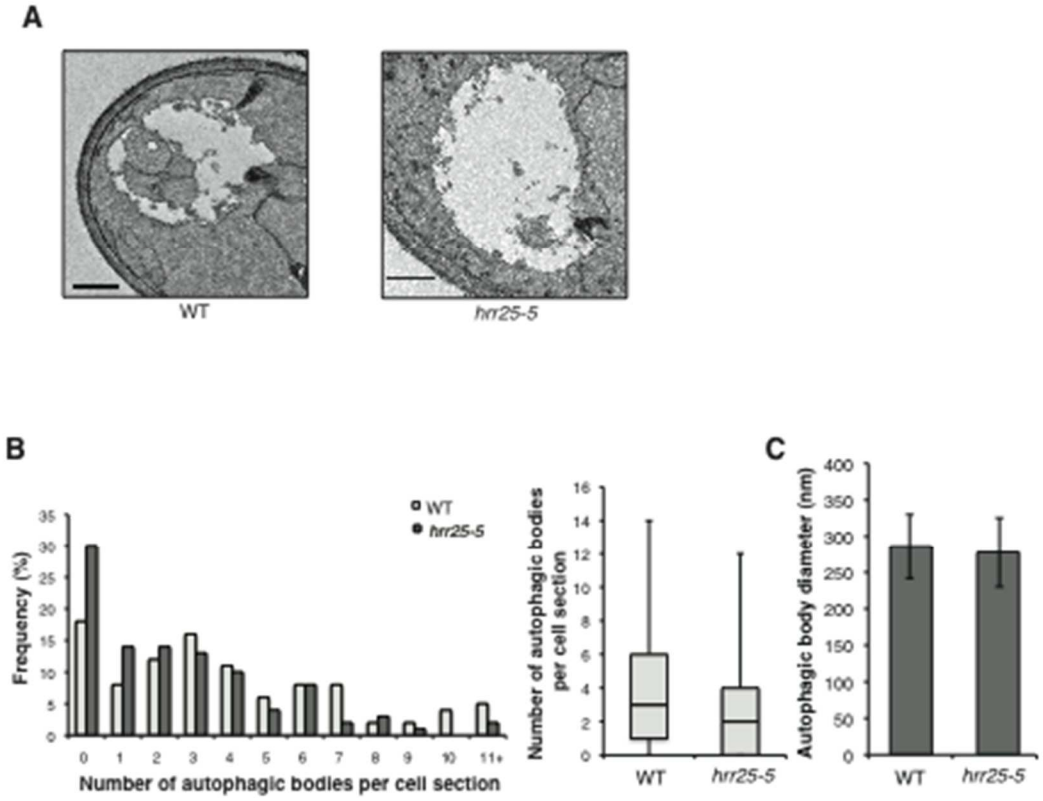

Figure 3.1. Autophagic body number is reduced in *hrr25-5.*
A Representative images of autophagic bodies in *pep4*Δ (left) or *hrr25-5pep4*Δ (right) after 1.5 h of nitrogen starvation at 37°C. Scale bar represents 500 nm. **B** Histogram showing the distribution of the number of autophagic bodies per cell section in WT and *hrr25-5*. The number of autophagic bodies was quantitated for 100 cell sections for each strain (left). p-value = 0.0016; Mann-Whitney Test. Box plot of the number of autophagic bodies per cell section. Bars show data between the lower and upper quartiles, the median is a horizontal line within the box. Whiskers indicate the smallest and largest observations (right). **C** The diameter of autophagic bodies was determined. For WT N = 396, for *hrr25-5* N = 254. Averages with error bars as s.d. are shown.

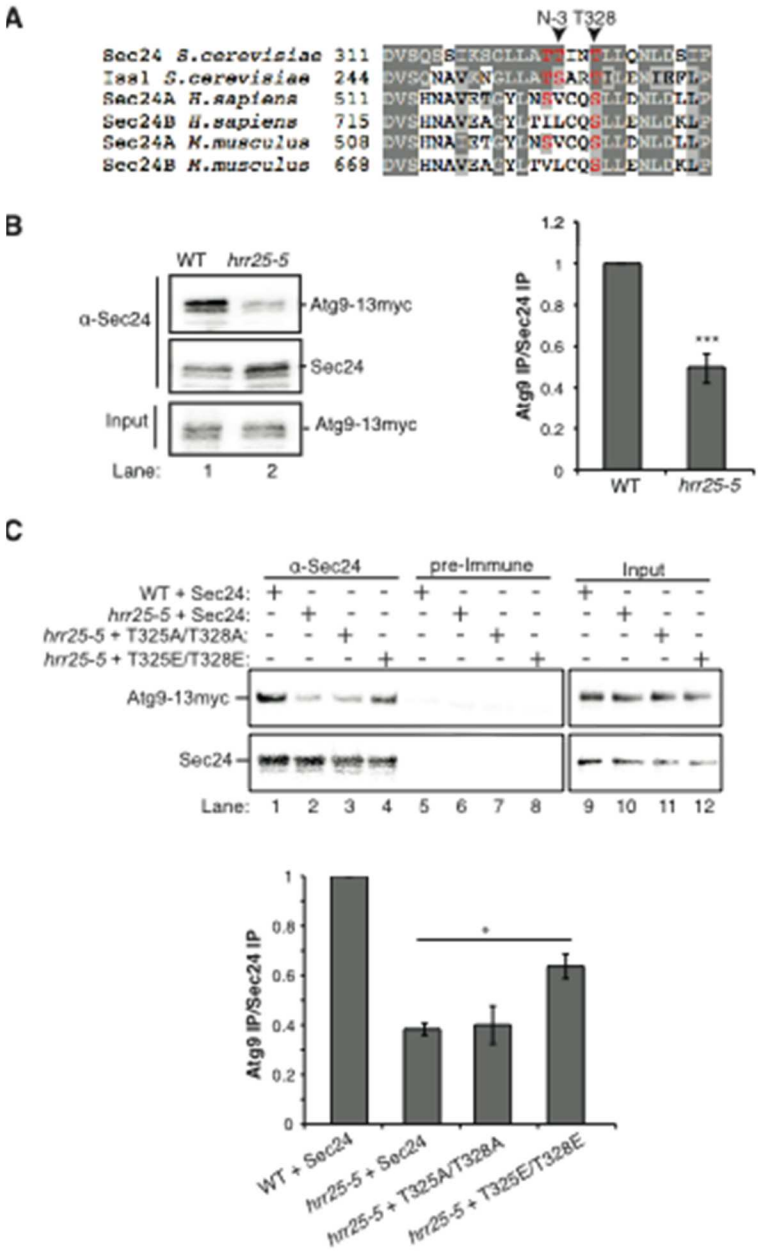

Figure 3.2. Hrr25 is required for the Sec24-Atg9 interaction.
A Alignment of the region surrounding T324/T325/T328 (shown in red) with Sec24 homologues. **B** Sec24 was immunoprecipitated from WT or *hrr25-5* lysates expressing Atg9-13myc (left). Precipitated Atg9-13myc was quantitated and normalized to the amount of Sec24 in the precipitate (right). WT was set as 1 for each experiment. Averages and s.e.m. are shown for 5 biological replicates. **C** Same as B except Sec24 was immunoprecipitated from WT or *hrr25-5* cells expressing WT Sec24 or Sec24 T325/T328 mutants. Averages and s.e.m. are shown for 3 biological replicates. *P < 0.05; ***P < 0.001, Student's unpaired t-test.

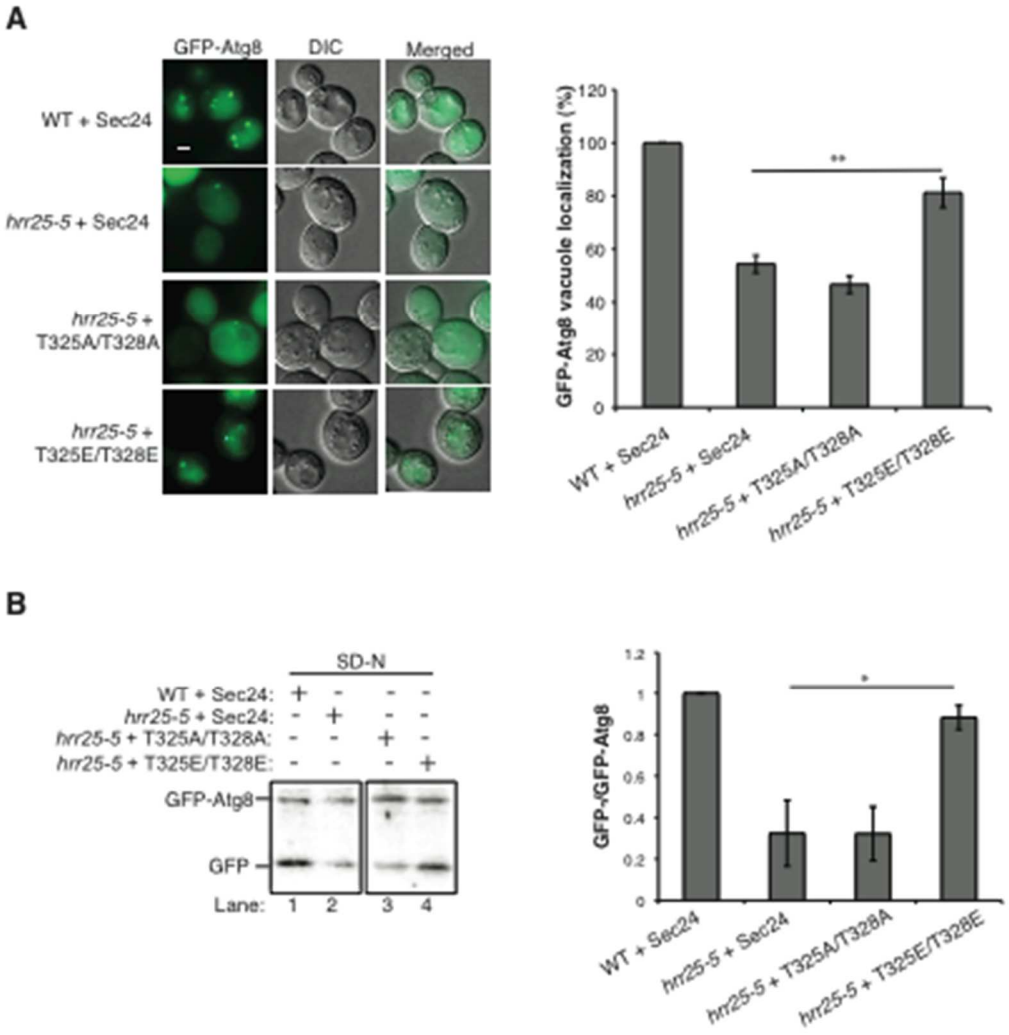

Figure 3.3. Sec24 T325E/T328E partially rescues the autophagy defect in *hrr25-5*.

A Vacuolar localization of GFP-Atg8 was examined 2 h after nitrogen starvation at 37°C in WT or *hrr25-5* cells expressing either WT Sec24 or Sec24 T325/T328 mutants. Scale bar, 2 μm (left). Over 300 cells were quantitated from 3 biological replicates. WT was set as 100%. Averages and s.e.m. are shown. **B** Cleavage of GFP-Atg8 in *hrr25-5* cells expressing WT Sec24 or Sec24 T325/T328 mutants was examined after 2 h nitrogen starvation at 37°C. The ratio of GFP to GFP-Atg8 was quantitated from 3 biological replicates. Cleavage in WT was set to 1 for each experiment. Averages and s.e.m. are shown. *P < 0.05; **P < 0.01; Student's unpaired t-test.

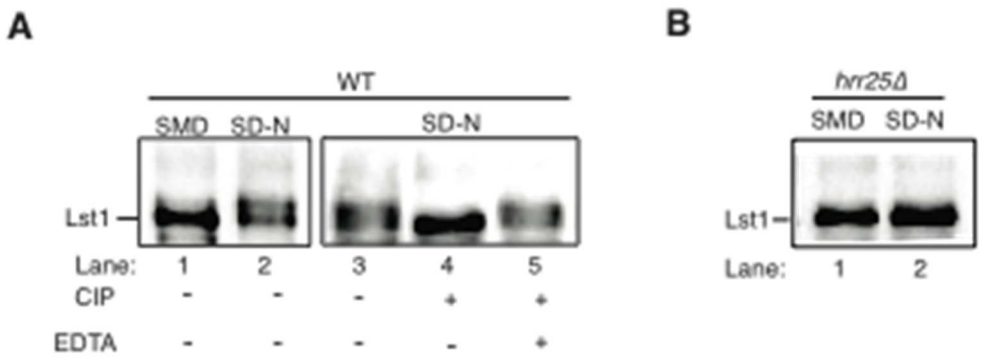

Figure 3.4. Hrr25 is required for phosphorylation of Lst1 during starvation. **A** Lst1 was immunoprecipitated from lysates prepared from WT cells grown in nutrient rich media (SMD) (lane 1) or starved for nitrogen (SD-N) for 4 h (lanes 2-5). The precipitates were untreated (lanes 1-3), treated with CIP (lane 4) or CIP and EDTA (lane 5). **B** Lst1 was immunoprecipitated from lysates prepared from *hrr25Δ* cells grown in nutrient rich (lane 1) or starved for nitrogen for 4 h (lane 2).

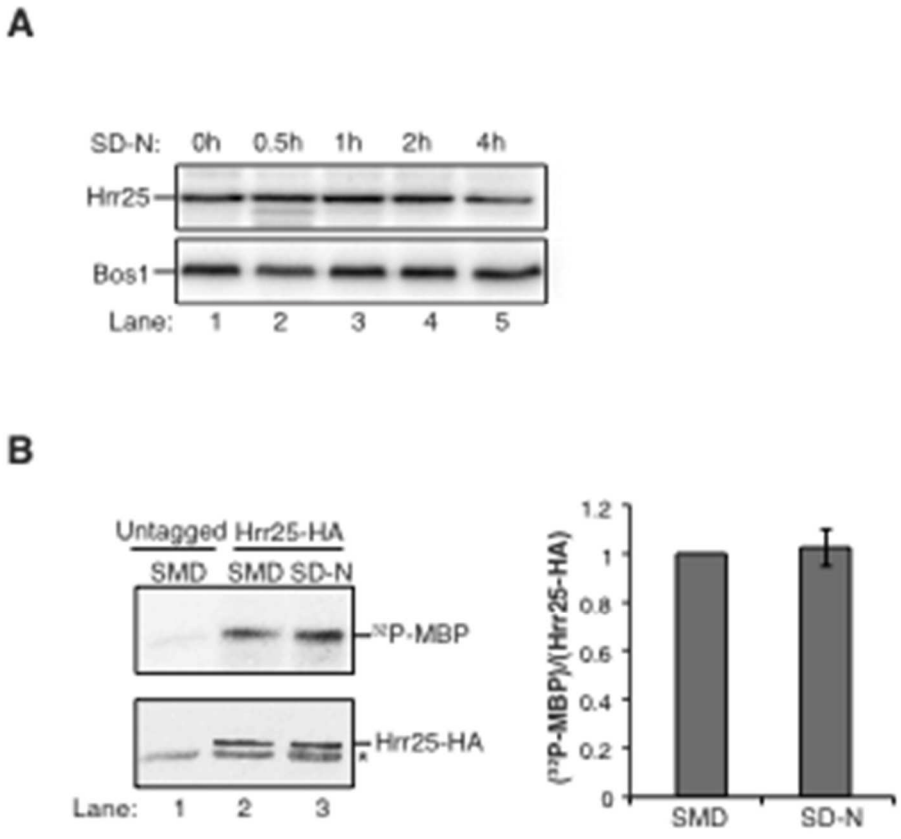

Figure 3.5. Hrr25 is not regulated during starvation.
A Lysates were prepared from WT cells starved for nitrogen for the indicated time periods by incubating 2.5 OD_{600} units of cells with 200 µl 0.1 M NaOH for 5 min at room temperature. The precipitate was pelleted and heated in sample buffer for 5 min at 95°C. Lysates were immunoblotted with anti-Hrr25 (top) and anti-Bos1 (bottom) antibodies. The SNARE Bos1 was used as a loading control. **B** Hrr25-HA was immunoprecipitated from cells grown in nutrient rich media (SMD) or starved for nitrogen (SD-N) for 1 h at 25°C. The kinase activity of Hrr25 was assayed in vitro using myelin basic protein (MBP) as a substrate as described in the Materials and Methods. Asterisk denotes contaminate band from HA resin. Hrr25 activity was quantitated and normalized to amount of Hrr25-HA in the precipitate (right). SMD was set to 1 for each experiment. Averages and s.e.m. are shown for 4 biological replicates.

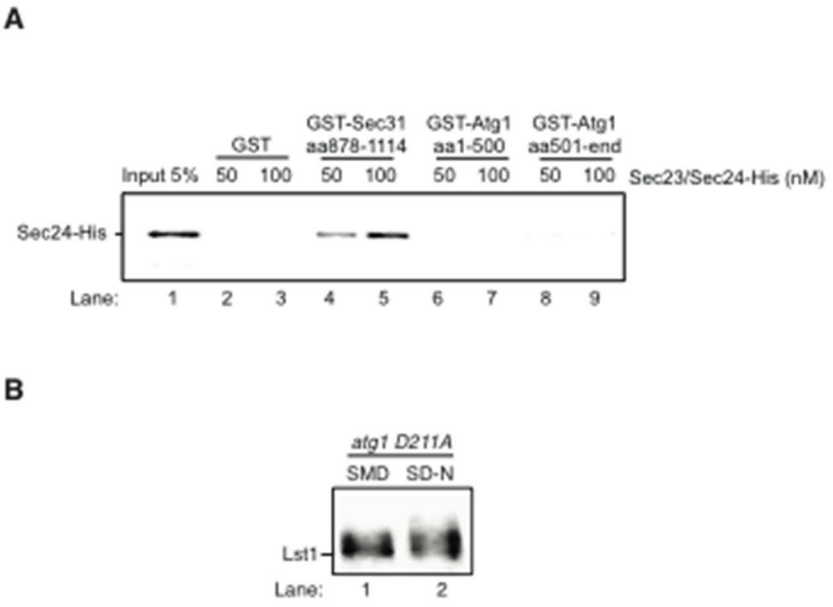

Figure 3.6. Atg1 does not interact with the COPII coat.
A Equimolar amounts (200nM) of GST, GST-Sec31 (aa878-1114) or GST-Atg1 fragments were incubated with 50 or 100 nM Sec23/Sec24-His_6. **B** Lst1 was immunoprecipitated from lysates prepared from *atg1 d211a* cells grown in nutrient rich media (SMD) (lane 1) or starved for nitrogen (SD-N) for 4 h (lanes 2).

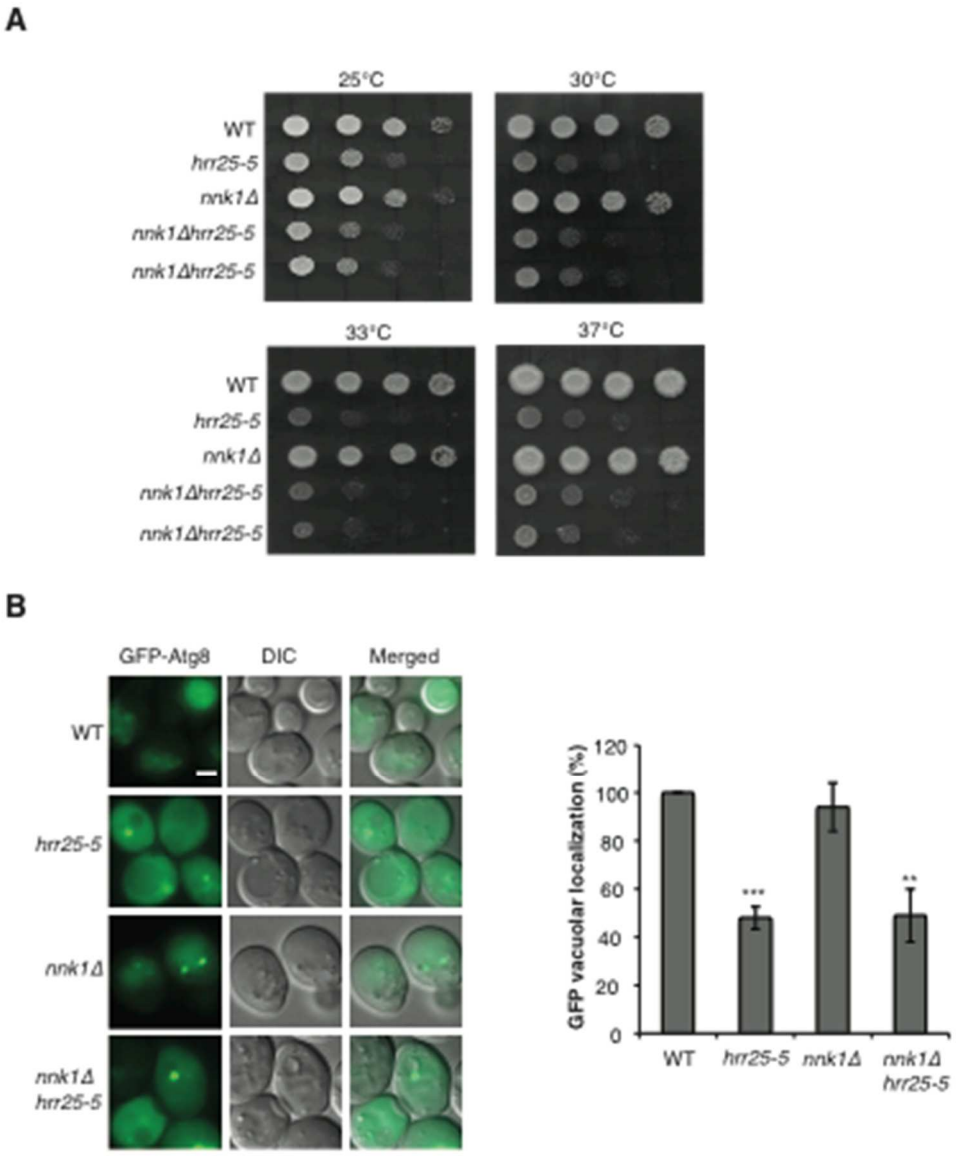

Figure 3.7. Nnk1 is not required for autophagy.
A Nnk1 was deleted in the *hrr25-5* mutant and growth was tested on a YPD plate at the indicated temperatures. Two *nnk1Δhrr25-5* transformants are shown. **B** The translocation of GFP-Atg8 to the vacuole was examined after 1 h nitrogen starvation at 37°C (left). Scale bar 2μM. The vacuolar localization of GFP-Atg8 was quantitated in over 300 cells from 3-4 biological replicates (right). WT was set as 100% for each experiment. Averages and s.e.m. are shown. **P < 0.01, ***P < 0.001; Student's unpaired t-test.

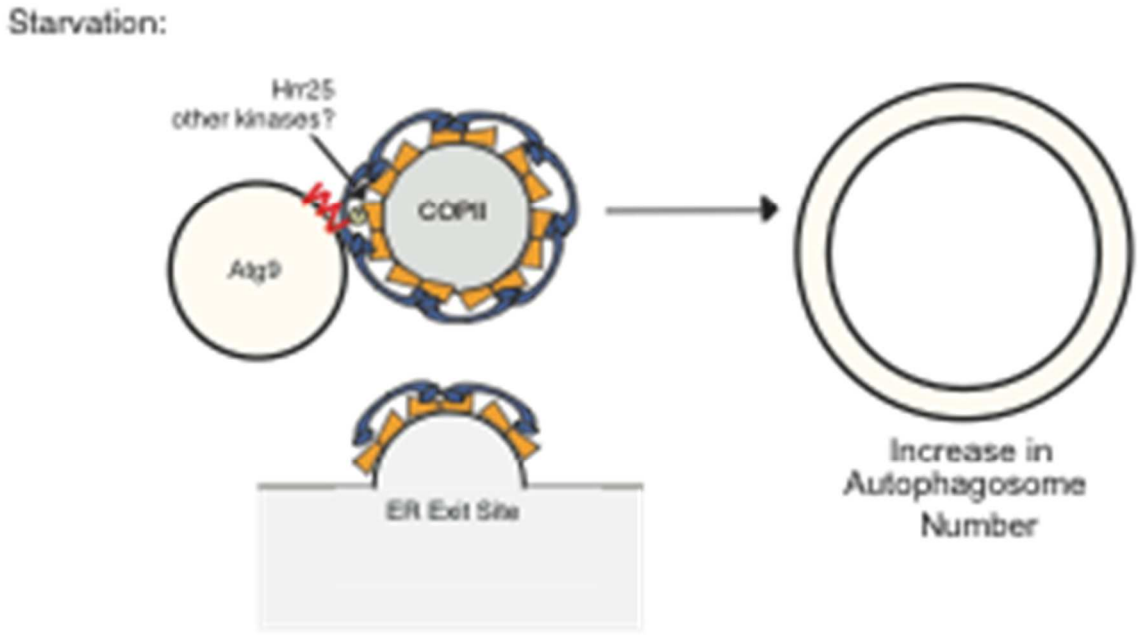

Figure 3.8. A model for Hrr25 during autophagy.
During autophagy Hrr25 regulates autophagosome number through phosphorylation of the Sec24 membrane distal sites. This phosphorylation event promotes the interaction between Sec24 and Atg9 and is required for autophagy.

Table 3.1. In vitro Hrr25 phosphorylation sites on Sec24.

Sec24 Residue	Confidence*	In vivo site	Round†
T77	High	No	2
T78	High	No	2
S79	High	No	2
S125	High	No	2
T145	High	Yes	2
T155	Low	Yes	2
S172	Medium	Yes	2
S175	Medium	No	2
S193	High	No	2
S184	High	No	1
S319	Low	Yes	1
T328	Low	Yes	1
S463	Low	Yes	1
S469	High	Yes	1
S549	High	Yes	1
S563	High	No	1
S678	High	Yes	2
S693	Low	Yes	1

*High confidence > 75%, Medium 30-75%, Low < 30%

†First round trypsin digest, second round pepsin digest

3.4 Discussion

Phosphorylation of the Sec24 membrane distal surface is regulated at least in part by Hrr25. Previous studies suggested Hrr25 may function upstream of COPII vesicle delivery to the PAS (Wang et al., 2015), but how Hrr25 acts as a positive regulator of autophagy was unclear. Here we have shown that Hrr25 functions in autophagy largely by enhancing the Sec24-Atg9 interaction through the Sec24 membrane distal patch. A model depicting the role of Hrr25 in regulating COPII vesicle traffic during autophagy is in Figure 3.8.

For technical reasons, we have been unable to address if the Sec24 membrane distal sites are phosphorylated as a consequence of inducing autophagy. However, given that the membrane distal Sec24 phosphosites are only required for autophagosome formation during starvation-induced autophagy and that the Sec24-Atg9 interaction is enhanced during autophagy (see Chapter 2), it seems likely that these sites are more phosphorylated when autophagy is induced. Additionally, another Hrr25 substrate that is part of the COPII coat, Lst1, is more phosphorylated during starvation and Hrr25 is required for this starvation specific phosphorylation. This result is consistent with recent findings that two other Hrr25 substrates that are receptors for different types of selective autophagy, Atg19 and Atg34, are also more phosphorylated during starvation in an Hrr25 dependent manner (Mochida et al., 2014; Tanaka et al., 2014). Together these findings highlight the growing importance of an Hrr25 mediated signaling pathway that is upregulated during starvation. However, given that Hrr25 is not directly regulated during starvation the mechanism through

which this pathway is regulated is not clear. One likely possibility is that Hrr25 may be acting with another kinase, which is activated during autophagy. This second kinase could phosphorylate the COPII coat during starvation, creating new phosphorylation sites for Hrr25.

Hrr25 is part of the casein kinase 1 (CK1) family. In yeast there are three other members of this family, Yck1, Yck2 and Yck3 (Wang et al., 1996). Yck1/2 is a pair of essential kinases that are involved in glucose sensing, endocytosis and secretion (Reddi and Culotta, 2013; Stalder and Novick, 2016; Wang et al., 1996). Yck3 may share some redundancy with Hrr25 and functions in both vacuole fusion and vesicle trafficking of AP-3 vesicles (Anand et al., 2009; LaGrassa and Ungermann, 2005; Wang et al., 1996). It is currently unknown whether these other CK1 kinases are involved in autophagy. Given the general role of this kinase family in membrane trafficking and that multiple mass-spectrometry screens have picked up interactions between these kinases with various Atgs (Breitkreutz et al., 2010; Graef et al., 2013; Ptacek et al., 2005) it is likely that these other family members also act in autophagy. Experiments to dissect the role of this kinase family in autophagy are discussed in Chapter 5.

Atg1 does not appear to be required for COPII coat phosphorylation as it does not directly interact with Sec23/Sec24 in vitro and it did not affect the phosphorylation of Lst1 in vivo. Interestingly, Atg9 is phosphorylated by Atg1 and potentially other kinases (Feng et al., 2016; Papinski et al., 2014). Atg1 was reported to predominately phosphorylate the C-terminus of Atg9 and this phosphorylation regulates the

recruitment of Atg18, which helps recycle Atg9 from the PAS (Papinski et al., 2014). Whether Atg9 phosphorylation regulates its interaction with the COPII coat remains to be determined. Additionally, a recent report has linked Ulk1 (Atg1 in mammals) to ER-to-Golgi trafficking in mammalian cells. Specifically, Ulk1/2 was found to phosphorylate Sec16, which affected ERES assembly and trafficking of a subset of cargo through regulating the interaction of Sec16 with mSec24C (Joo et al., 2016). Future work will be needed to determine if this is a conserved function of the Ulk family.

These findings begin to unravel the signal that regulates the function of COPII vesicles during autophagy. Hrr25 plays a central role in phosphorylating the Sec24 membrane distal surface, which enhances the interaction of the COPII coat with Atg9. This interaction between Sec24 and Atg9 is required for autophagy. These results raise the possibility that a novel Hrr25 mediated signaling pathway coordinates membrane trafficking machinery during starvation. Future studies will be needed to understand the upstream signaling factors and whether other CK1 family members are involved.

3.5 Materials and Methods

3.5.1 Purification of GST fusion proteins

For purification of GST fusions, BL21(DE3) cells were grown overnight to stationary phase in LB-Amp. 50-100 OD_{600} units of stationary cells were diluted in 500mL to 1L of LB-Amp and grown for 2 h at 37 °C. The temperature was then shifted to 18°C for 30 min before adding isopropyl β-D-1-thiogalactopyranoside to a final concentration of 0.5 mM to induce protein expression overnight. Cells were

subsequently spun down and resuspended in 25 mL of cold PBS with 1mM DTT and protease inhibitors. Cells were sonicated for 2 min total at 50% amplitude with 15 sec on/off pulses. Triton X-100 was added to a final concentration of 1% and incubated on ice for 15 min. Lysates were cleared by a 15 min centrifugation at 15,000 rpm in a Sorvell SS-34 rotor at 4°C. The cleared lysate was incubated with 1 mL of 50% glutathione sepharose beads (GE) for 1 h at 4°C with rotation. The beads were washed with 25 mL PBS, transferred to a fresh tube and washed 3x with 5 mL PBS. The beads were run on an SDS-PAGE gel and stained with coomassie along with a BSA standard to estimate protein concentration. The beads were stored at 4°C for up to 5 days.

3.5.2 Purification of His_6-Hrr25 (aa1-394)

Rosetta(DE3) cells were transformed with a vector expressing a 1-394 amino acid truncated form of His_6-tagged Hrr25 (gift from Kevin Corbett, UCSD). Transformed cells were grown overnight in 50 mL LB-Amp at 37 °C to a stationary phase. 100 OD_{600} units of stationary cells were diluted in 1 L of LB-Amp and grown for 2 hr at 37 °C. The temperature was then shifted to 18 °C for 30 min before adding isopropyl β-D-1-thiogalactopyranoside to a final concentration of 0.5 mM to induce protein expression overnight. The cells were collected by centrifugation of 10 min at 5000 rpm at 4°C and re-suspended in cold 25 ml sonication buffer (20 mM Tris pH 8.0, 300 mM NaCl, 10 mM imidazole, 10% glycerol, 0.1% 2-mercaptoethanol) along with 2 mM phenylmethylsulfonyl fluoride and 1x protease inhibitors (Roche). The cells were then sonicated a total of 2 min with a 15 sec on/off cycle on ice and

centrifuged at 34500 rcf in a Sorvall SS-34 rotor for 30 min at 4°C. The supernatant was moved to a new tube and incubated with 1 ml of Ni-NTA agarose for 1 hr at 4°C with rotation. The lysate-agarose mixture was loaded onto an econo column and washed with 50 ml of sonication buffer. The Ni-NTA agarose was then washed with 25 ml of wash buffer (20 mM Tris pH 8.0, 300 mM NaCl, 45 mM imidazole, 10% glycerol, 0.1% 2-mercaptoethanol). The agarose was washed 5x with 1 ml elution buffer (20 mM Tris pH 8.0, 80 mM NaCl, 300 mM imidazole, 10% glycerol, 0.1% 2-mercaptoethanol) to elute protein from the Ni-NTA agarose. The elute was buffer exchanged 3 times with 20 mM HEPES pH 7.4 and 30% glycerol and concentrated to a final volume of 150 µl.

3.5.3 In vitro kinase reaction

For pepsin digestion, GST-Sec24 was purified as described in Section 3.5.1 from bacteria. GST-Sec24 was then eluted from the glutathione sepharose prior to the in vitro kinase reaction, by incubating the glutathione sepharose with 50 mM Tris pH 8.0, 10 mM glutathione. GST-Sec24 was then buffer exchanged into 1x PBS. 5 ug of GST-Sec24 was incubated with 125 ng of His_6-Hrr25 (aa1-394) for 1 h at 30°C in kinase buffer (20 mM Tris pH 7.4, 8 mM EDTA, 10 mM $MgCl_2$).

3.5.4 Electron Microscopy

Cells were grown overnight in YPD to an OD_{600} of 1.0 and shifted to SD-N for 1.5 h at 37°C. 30 OD_{600} units of cells were pelleted, resuspended in 1 mL of 1.5% $KMnO_4$ and incubated for 30 min at 4°C with nutation. Cells were then pelleted and resuspended in 1 mL of 1.5% $KMnO_4$ and incubated overnight at 4°C with nutation.

Samples were dehydrated in ethanol, embedded in Durcupan epoxy resin (Sigma-Aldrich) and sectioned at 60 nm on a Leica UCT ultramicrotome. Sections were picked up on Formvar and carbon-coated copper grids and stained with 2% uranyl acetate for 5 min and Sato's lead stain for 1 min. Grids were viewed using a Tecnai G2 Spirit BioTWIN transmission electron microscope equipped with an Eagle 4k HS digital camera (FEI, Hilsboro, OR). Autophagic body number and size were determined with Adobe Photoshop and Image J software as described previously (Backues et al., 2013).

3.5.5 Sec24-Atg9 Co-immunoprecipitation in *hrr25-5*

Cells were grown overnight to early log phase. For the *hrr25-5* mutant, cells were shifted to SD-N for 2 h at 37°C. 100 OD_{600} units of cells were pelleted, resuspended in 2 ml of spheroplasting buffer (1.4 M sorbitol, 100 mM sodium phosphate pH 7.5, 0.35% b-mercaptoethanol and 0.5 mg/ml zymolyase) and incubated for 30 min at 37°C. Spheroplasts were loaded on top of a 5 ml sorbitol cushion (1.7 M sorbitol, 100 mM HEPES pH 7.2) and spun for 5 min at 3,000 rpm. Cells were lysed in 1 ml of lysis buffer II (20 mM Hepes pH 7.4, 150 mM NaCl, excess protease inhibitors – combination of Roche and Sigma inhibitors, phosphatase inhibitors (Sigma)) with a dounce homogenizer on ice. Cell debris was cleared by a 10 min spin at 500 xg. When cross-linking was performed, lysates were incubated on ice with 100 mM dithiobis (succinimidyl propionate) for 30 min. To quench excess crosslinker, 100 mM Tris pH 7.6 was added and incubated for 15 min on ice. Triton X-100 was added to a final concentration of 1% and incubated on ice for 30 min followed by a 15

min spin at 15,000xg. The lysates were incubated with 50 µl of 50% protein A-sepharose for 20 min at 4°C with rotation to pre-clear the lysates and reduce background. To immunoprecipitate Sec24, 2 mg of lysate was incubated with 10 µl of Sec24 antibody (rabbit polyclonal prepared against GST-Sec24) or 10 µl of pre-immune serum for 2 h at 4°C with rotation. 40 µl of 50% protein A-sepharose was added and incubated for 45 min at 4°C with rotation. The beads were then washed 5 times with 1 ml of lysis buffer with 1% Triton X-100 and heated in 40 µl of 3x sample buffer for 5 min at 95°C.

3.5.6 Fluorescence Microscopy

For GFP-Atg8 vacuole localization, cells were grown at 25°C overnight in SC media to early log phase, OD_{600} between 0.6 and 1.0. Cells were washed and resuspended in SD-N and incubated for 1-2 h at 37°C. Cells were then visualized at 25°C with a Zeiss Axio Imager Z1 fluorescence microscope using a 100 x 1.3 NA oil-immersion objective. Images were captured with a Zeiss AxioCam MRm digital camera and analyzed with AxioVision software.

3.5.7 Immunoprecipitation and CIP treatment of Lst1

Cells grown overnight in YPD to early log phase were collected by centrifugation, washed and resuspended in either SD-N or SC media for 4 h at 30°C. Subsequent to this incubation, the cells were collected by centrifugation, washed with 20 mM Tris pH 7.4, resuspended in 2 ml of spheroplasting buffer and incubated for 30 min at 37°C. Spheroplasts were pelleted through a 5 ml sorbitol cushion, resuspended in 1 ml of IP buffer (50 mM Tris pH 8.0, 100 mM NaCl, 10 mM $MgCl_2$, 0.5% Triton

X-100, 1 mM DTT, 1 mM PMSF, 2x phosphatase (Sigma) and 10x protease inhibitors (Roche)) and lysed with a dounce homogenizer on ice using 70-80 strokes. Insoluble material was removed by centrifugation at 13,000 rpm for 15 min. 4 mg of cleared lysate was incubated with 10 µl of anti-Lst1 antibody (rabbit antiserum prepared against GST-Lst1) for 1 h at 4°C with rotation. 40 µl of 50 % Protein-A beads were added and incubated for 1 h at 4°C before the samples were washed 3 times with IP buffer. For the CIP assays, the Protein-A beads were washed three times with CIP buffer (New England BioLabs) that contained excess protease inhibitor cocktail (Roche and Sigma cocktails) before the beads were resuspended in 100 µl of CIP buffer with CIP (0.5 U/µl), or with CIP plus 50 mM EDTA and incubated at 37°C for 20 min. The samples were heated in 3x sample buffer at 100°C for 5 min and analyzed on a 6% SDS-PAGE gel by Western blotting.

3.5.8 NaOH lysis

For detecting Hrr25 levels after starvation, cells were grown overnight in YPD to early log phase, OD_{600} 0.6-0.8, then washed and shifted to SD-N medium and grown for the indicated time at 25°C. At the time point 2.5 OD_{600} units of cells were removed, spun down and resuspended in 100 µl of ddH20. 100 µl of 0.2 M NaOH was added and samples were mixed by tapping. Samples were incubated for 5 min at room temperature, spun down and the pellet was resuspended in 50 µl of 3x sample buffer and boiled at 95°C for 5 min.

For GFP-Atg8 cleavage cells were grown overnight in SC media to early log phase, OD_{600} 0.6-0.8, then washed and shifted to SD-N medium for 2 h at 37°C. Cells

were then lysed as described above.

3.5.9 Hrr25 kinase assay

Cells expressing Hrr25-HA were grown overnight in SC-Ura to early log phase, OD_{600} 0.6-0.8, then washed and shifted to SD-N medium for 1 h at 25°C to induce autophagy. The cells were harvested by centrifugation, washed with 20 mM Tris pH 7.4, resuspended in 5 ml of spheroplasting buffer and incubated at 37°C for 30 min. Spheroplasts were pelleted through a 10 ml sorbitol cushion, resuspended in 5 ml of lysis buffer (50 mM Tris-HCl pH 7.4, 100 mM NaCl, 5 mM EDTA, 1 mM PMSF, 1% Triton X-100, 2X protease inhibitor mixture (Roche)) and lysed with a dounce homogenizer on ice. Lysates were then cleared by a 15 min centrifugation at 14,000 rpm. To immunoprecipitate Hrr25-HA, lysates were incubated with 20 µl anti-HA resin (Sigma) for 2 h at 4°C with rotation. The beads were washed 3 times with lysis buffer and 2 times with kinase buffer (50 mM HEPES pH 7.4, 5 mM $MgCl_2$, 0.2% NP-40 and 1 mM DTT). The kinase activity of immunopurified Hrr25-HA was assayed in a 50 µl reaction volume using 1 µg of myelin basic protein (MBP) as substrate as described before (Wang et al., 2013).

3.5.10 Purification of Sec23/Sec24-His_6 from yeast

For purification of the inner COPII coat, yeast cells were transformed with GAL1-Sec23 and GAL1-Sec24-His_6 constructs. Cells were grown to stationary phase in SC-Leu-Ura media with 0.1% glucose and 5% glycerol (SGG media). 6 L of SGG media was inoculated at a starting OD_{600} of 0.008 and incubated overnight at 30°C.

Cells were induced at an OD_{600} of 0.6-0.9 with 0.2% galactose and grown for 5 h at 30°C. Cells were pelleted, washed with ddH_2O and the pellet was frozen at -80°C.

The pellet was thawed on ice and stock solutions were added to give the following final concentrations 0.75 M KOAc, 50 mM HEPES pH 7.0, 10% glycerol, 0.1 mM EGTA, 2 mM DTT, 2 mM PMSF, 2x PIC cocktail (Roche). Cells were lysed in a chilled bead beater with 6 x 1 min bursts with 2 min rest on ice in between each burst. The lysate was cleared with a 20,000 rpm spin in a SS-34 rotor for 30 min at 4°C. The supernatant was then incubated with 1 mL packed Ni-NTA resin for 1 h at 4°C. The resin was spun down and loaded onto an econo-column. The resin was washed with 25 mL of B-II buffer (50 mM HEPES pH 6.8, 0.75 M KOAc, 0.1 mM EGTA, 50 mM Imidazole, 10% glycerol) and 25 mL B-III buffer (50 mM HEPES pH 7.0, 0.1 mM EGTA, 0.25M sorbitol, 50 mM Imidazole, 10% glycerol). Sec23/Sec24-His_6 was eluted off the resin with 3 mL of B-III buffer with 200 mM Imidazole.

The Ni-NTA elute was diluted with 6 mL dilution buffer (50 mM HEPES pH 7.0, 0.1 mM EGTA, 10% glycerol) then loaded onto a 1 mL DEAE column (GE Healthcare). The column was washed with 5 mL of dilution buffer and 10 mL of wash buffer (50 mM HEPES pH 7.0, 0.25 M KOAc, 0.1 mM EGTA, 50 mM Imidazole, 10% glycerol). Sec23/Sec24-His_6 was eluted off the column with increasing amounts of KOAc in wash buffer (0.5 M, 0.6 M, 0.7 M, 0.8 M). 0.5 ml fractions were collected. The column was cleared with 1 M NaCl in wash buffer. The protein concentration of Sec23/Sec24-His_6 in the eluted fractions was determined on a coomassie gel with a BSA standard.

3.5.11 In vitro bindings with Sec23/Sec24-His_6

Equimolar amounts (0.2 μM) of immobilized GST fusion proteins were incubated with increasing amounts of purified Sec23/Sec24-His_6 from yeast in binding buffer (25 mM HEPES pH 7.2, 150 mM NaCl, 1% Triton X-100, 1 mM $MgCl_2$, 1 mM DTT, protease inhibitors) for 4 h at 4°C with rotation. Beads were washed 4x with 1 mL binding buffer and eluted in 50 μL of sample buffer by heating for 5 min at 100°C.

3.6 Acknowledgements

Some of the work in Chapter 3 is taken from "Sec24 phosphorylation regulates autophagosome abundance during nutrient deprivation" which has been submitted for publication and is currently under review at Elife. Juan Wang, Ming Zhu, Kyle Stahmer, Ramya Lakshminarayan, Majid Ghassemian, Yu Jiang, Elizabeth Miller and Susan-Ferro-Novick are co-authors. The dissertation author is the primary researcher of this paper. Other non-published work in this section was performed by the dissertation author unless otherwise noted.

Christopher Lord performed the in vitro bindings with Nnk1 and COPII coat subunits mentioned in Section 3.1. Majid Ghassemian performed the mass spectrometry in Section 3.3.1. Deepali Bhandari performed the in vitro kinase reaction for the first round of mass spectrometry in Section 3.3.1. Ying Jones prepared the samples for electron microscopy in Section 3.3.1. Juan Wang performed the pho8Δ60 assay in *nnk1*Δ discussed in Section 3.3.3. Yu Jiang offered essential advice and protocols for the Hrr25-HA kinase assays.

CHAPTER 4

Identification of Uso1 interacting domains

4.1 Summary

Uso1 is a long coiled-coil tether previously shown to be an effector of the GTPase Ypt1 and is required for COPII vesicle tethering at the Golgi. Which domain of Uso1 interacts with Ypt1 was unknown. Additionally, what factors connect Uso1 to the cis-Golgi in order to link COPII vesicles to their acceptor compartment was unclear. In this Chapter we used an in vitro binding approach to identify the regions of Uso1 that interact with Ypt1 and ER-Golgi SNAREs. This approach demonstrated that a conserved region in the N-terminal globular head of Uso1 interacts with Ypt1. Additionally, Uso1 contains a region in its second coiled-coil domain (CC2), which interacts with the t-SNARE Sed5. CC2 is essential for Uso1 function as truncating this region affected growth and Uso1 localization. These findings shed light on the mechanism of Uso1 tethering, which is well conserved in mammalian cells.

4.2 Introduction

On the secretory pathway, COPII coated vesicles transport cargo from the ER to the Golgi (Lord et al., 2013). After vesicle budding a multimeric guanine nucleotide exchange factor (GEF), TRAPPI, binds the Sec23 subunit of the COPII coat and activates the GTPase Ypt1 (Cai et al., 2007). GTPases function as molecular switches that cycle between an active GTP-bound state and an inactive GDP-bound state (Hutagalung and Novick, 2011). Activated Ypt1 recruits effector proteins,

which regulate COPII vesicle tethering and fusion. One of these effectors is the long coiled-coil tether Uso1, which was previously shown to be required for COPII vesicle tethering at the cis-Golgi (Cao et al., 1998), but the precise mechanism of Uso1 tethering and how it is regulated is less clear. After the vesicle has been tethered to the Golgi, pairing of a v-SNARE on the vesicle with a t-SNARE complex at the target membrane catalyzes membrane fusion (Jahn and Scheller, 2006).

Uso1 has a homologue in mammalian cells, p115, which has been studied more extensively. p115 is an effector of the mammalian homologue of Ypt1, Rab1 (Allan et al., 2000), and it regulates trafficking from the ER to the ER Golgi intermediate compartment (ERGIC) as well as intra-Golgi transport (Alvarez et al., 1999; Nakamura et al., 1997). Separate groups have reported different Rab1 binding domains in p115, in the N-terminal globular head and the first coiled-coil domain (An et al., 2009; Beard et al., 2005). Additionally, p115 interacts with the t-SNARE syntaxin-5 and v-SNARE Gos28, potentially catalyzing SNARE complex formation (Shorter et al., 2002). Whether these interactions are conserved in other eukaryotes is unknown.

Rabs contain two switch regions, which undergo conformational changes depending upon the nucleotide binding state (Hutagalung and Novick, 2011). A chimera protein that replaces the switch 1 (SW1) domain of Ypt1 with the SW1 domain of Sec4, involved in the delivery of secretory vesicles to the plasma membrane, has been used to study the activation mechanism of these two Rabs (Brennwald and Novick, 1993). This chimera, Ypt1-SW1^{Sec4} can be activated by the

GEF of Sec4, Sec2 (Dong et al., 2007) and is recruited to Golgi derived secretory vesicles (data not shown). Interestingly, it was recently determined that Ypt1-SW1^{Sec4} causes the inappropriate recruitment of Uso1 to sites of polarized cell growth, leading to some trafficking defects and toxicity upon overexpression (data not shown). Therefore, a more detailed analysis of the interacting domains of Uso1 would provide insights into the mechanism of Ypt1-SW1^{Sec4} as well as a better understanding of COPII vesicle tethering.

4.3 Results

4.3.1 Uso1 interacts with Ypt1 through its head domain

In order to better understand the mechanism of Uso1 tethering and the trafficking defects associated with Ypt1-SW1^{Sec4}, we aimed to identify the Ypt1 binding site on Uso1. Uso1 contains a conserved N-terminal globular head domain, four coiled-coil domains, followed by a short C-terminal acidic domain (Figure 4.1; A). The N-terminus of Uso1 (aa1-726) was fused to GST, purified from bacteria and tested for binding in vitro with Ypt1-His_6. Uso1 (aa1-726) bound to Ypt1-His_6, as did a smaller N-terminal fragment (aa1-246), which contains only the Uso1 globular head domain (Figure 4.1; B, C). A fragment of Uso1 containing the first and second coiled-coil domains (CC1 and CC2) did not bind (Figure 4.1; C). These findings demonstrate that Uso1 is able to directly interact with Ypt1 through a conserved binding site in the N-terminal globular head domain.

4.3.2 Uso1 CC2 interacts with the SNARE Sed5

SNARE complex assembly is achieved through short 60-70 amino acid domains, called SNARE-motifs (Weimbs et al., 1997). p115 has been shown to interact with SNAREs, through a SNARE-like motif (Shorter et al., 2002; Weimbs et al., 1997). This interaction helps link the vesicle with fusion machinery at the target membrane and potentially catalyzes SNARE complex assembly (Shorter et al., 2002). However, as the coiled-coil domains of p115 and Uso1 are not well conserved, it is unknown whether Uso1 also contains a SNARE interacting domain. To find a potential SNARE binding domain, we aligned Uso1 CC1-CC4 with SNARE motifs from members of the t-SNARE family and found a region in CC2, aa1019-1076, that possesses weak sequence homology (37% similarity) to a t-SNARE motif (Figure 4.2; A). Similar to the domain identified in p115, this SNARE-like motif lacks the highly conserved arginine or glutamine residue required to be a bonafide member of the SNARE family. To determine whether this region is required to interact with SNAREs, a fragment containing Uso1 CC1-CC2 was used in in vitro bindings with the ER-Golgi SNARES. The t-SNARE Sed5 bound to Uso1 CC1-CC2, but not to a fragment containing the head domain and CC1 (Figure 4.2; B, C). This finding is consistent with Sed5 interacting with Uso1 through its SNARE-like motif in CC2. The other ER-Golgi SNAREs, Bet1, Bos1 and Sec22 did not interact with Uso1 CC1-CC2 in vitro (Figure 4.3; A, B, C).

4.3.3 Uso1 SNARE-like motif is required for Uso1 localization

We next wanted to determine if the Uso1 SNARE-like motif is required for Uso1 function. As Uso1 is an essential gene a significant disruption in Uso1 function will result in a growth defect. A Uso1 truncation deleting the C-terminal acidic domain and Uso1 CC3-CC4 did not disrupt growth. However, further truncating of the Uso1 SNARE-like motif in CC2, led to a severe growth defect at 37°C (Figure 4.4; B). This growth defect corresponded with a defect in the trafficking of carboxypeptidase Y (CPY) from the ER to the Golgi at the non-permissive temperature (data not shown). The above findings indicate that this region in CC2 regulates a critical function of Uso1.

The t-SNARE Sed5 is predominantly localized to the Golgi (Weinberger et al., 2005) and consequently may help target Uso1 to this organelle. In order to determine whether CC2 is required for Uso1 localization, GFP was tagged at the C-terminus of both WT Uso1 and the Uso1 truncations. WT Uso1-GFP localizes to puncta structures at the cis-Golgi (Cao et al., 1998; Gillingham et al., 2004). Uso1 (aa1-1123)-GFP, which contains the SNARE-like motif, displayed a WT puncta localization (Figure 4.4; C). However, even at the permissive temperature of 25°C, fewer cells containing Uso1 (aa1-950)-GFP displayed a puncta localization (Figure 4.4; C). Frequently, Uso1 (aa1-950)-GFP had a "bar" localization, suggesting that the SNARE binding region of Uso1 is important for the proper localization of Uso1.

Ypt1-SW1^{Sec4} causes the inappropriate recruitment of Uso1 to Golgi derived secretory vesicles. Interestingly, toxicity induced by Ypt1-SW1^{Sec4} can be rescued by

both Uso1 (aa1-950) and Uso1 (aa1-1123) truncations (data not shown). These Uso1 truncations contain the Ypt1 binding site in the N-terminal head domain, indicating they can still be recruited by Ypt1-SW1^{Sec4} to sites of polarized cell growth. Additionally, the presence or absence of the SNARE-like motif had no effect on the ability of the Uso1 truncations to rescue Ypt1-SW1^{Sec4} defects. Therefore, it seems likely that the bulky coiled-coil domain of Uso1 may physically interfere with secretory vesicle trafficking and shortening this domain seems to relieve this interference.

Uso1 is a phosphoprotein with phosphorylation sites identified near the SNARE-like motif in CC2 (Figure 4.5; A) (Swaney et al., 2013). To determine whether these phosphorylation sites in CC2 are essential for Uso1 function, these phosphorylation sites were mutated to a non-phosphorylatable alanine or to a phosphomimetic residue and tested for their ability to complement Uso1 (aa1-950). Even when mutations in all four of the phosphorylated residues in CC2 were combined, there was no effect on growth (Figure 4.5; B). Although we cannot rule out that these mutations have a subtler defect in Uso1 localization or Uso1-Sed5 binding, these phosphorylation sites do not significantly regulate Uso1 function in vivo.

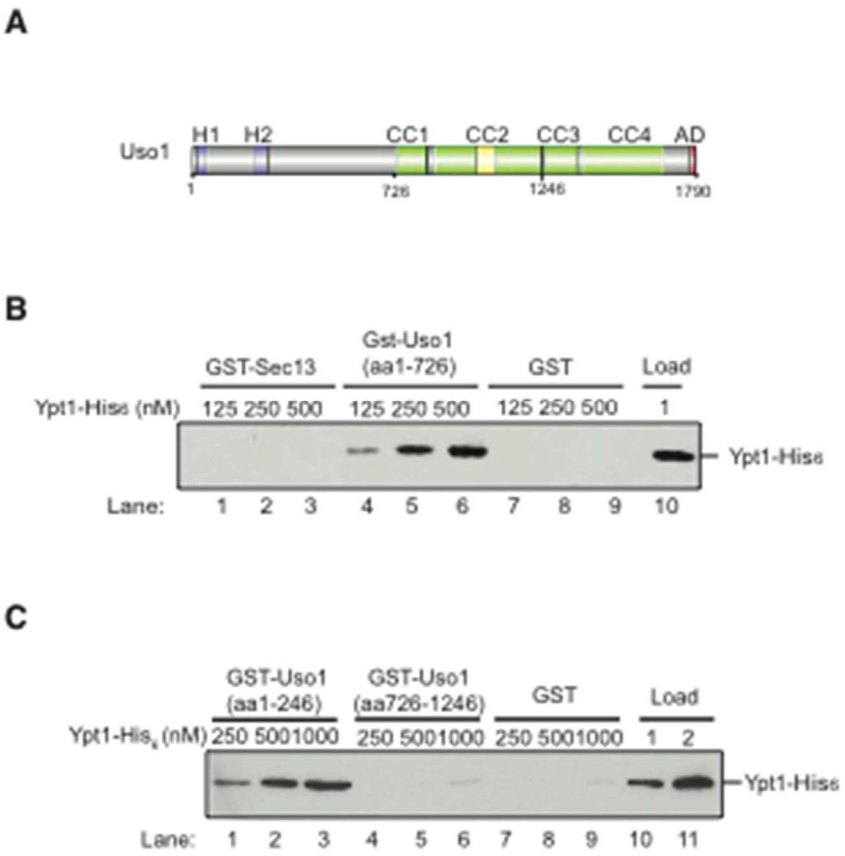

Figure 4.1. Ypt1 binds to the N-terminus of Uso1.
A Schematic of Uso1 with head domains (H) coiled-coil domains (CC) and acidic domain (AD) labeled. **B** Equimolar amounts of GST (lanes 7-9), GST-Sec13 (lanes 1-3) or GST-Uso1 (aa1-726) was incubated with increasing amounts of Ypt1-His_6. **C** Equimolar amounts of GST (lanes 7-9), GST-Uso1 (aa1-246) (lanes 1-3) or GST-Uso1 (aa726-1246) was incubated with increasing amounts of Ypt1-His_6.

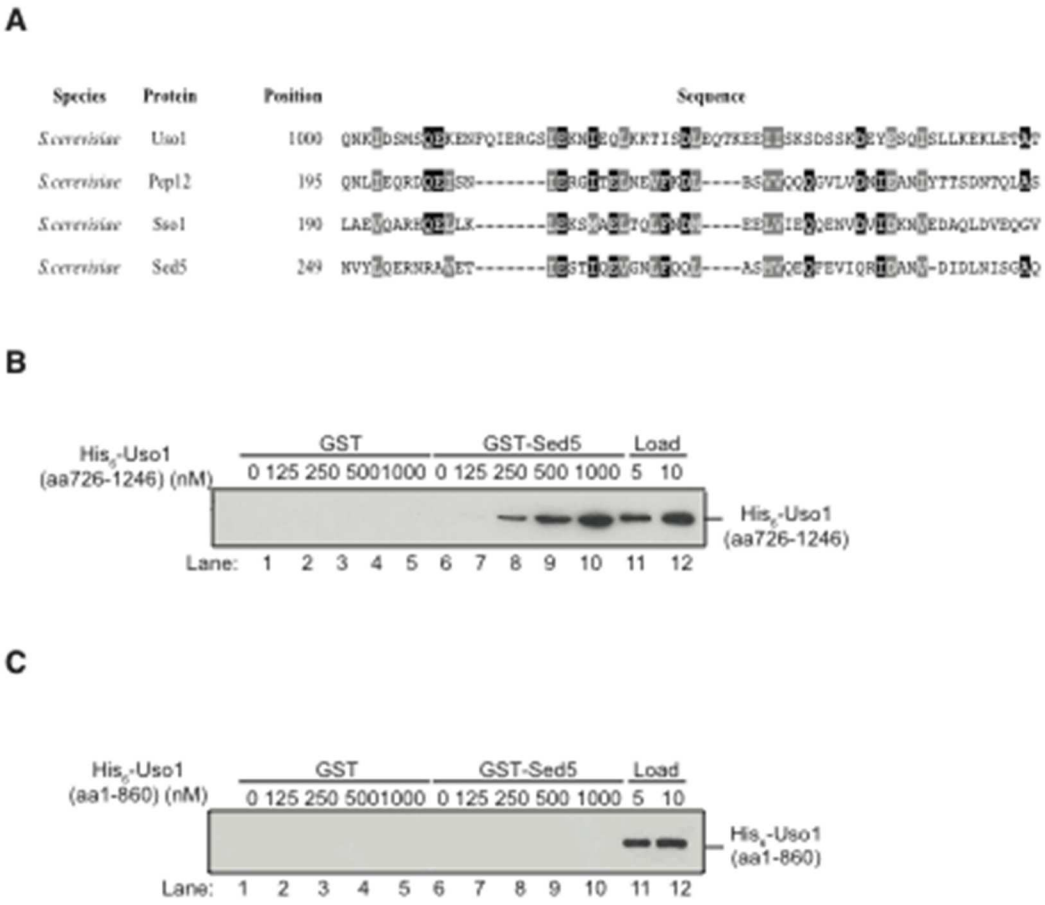

Figure 4.2. Uso1 CC2 binds the SNARE Sed5.
A Alignment of Uso1 with SNARE motifs. Conserved residues highlighted in black, similar residues highlighted in gray. **B** Equimolar amounts of GST (lanes 1-5) or GST-Sed5 (lanes 6-10) was incubated with increasing amounts of His_6-Uso1 (aa726-1246). **C** Same as in (B) except His_6-Uso1 (aa726-1246) was used.

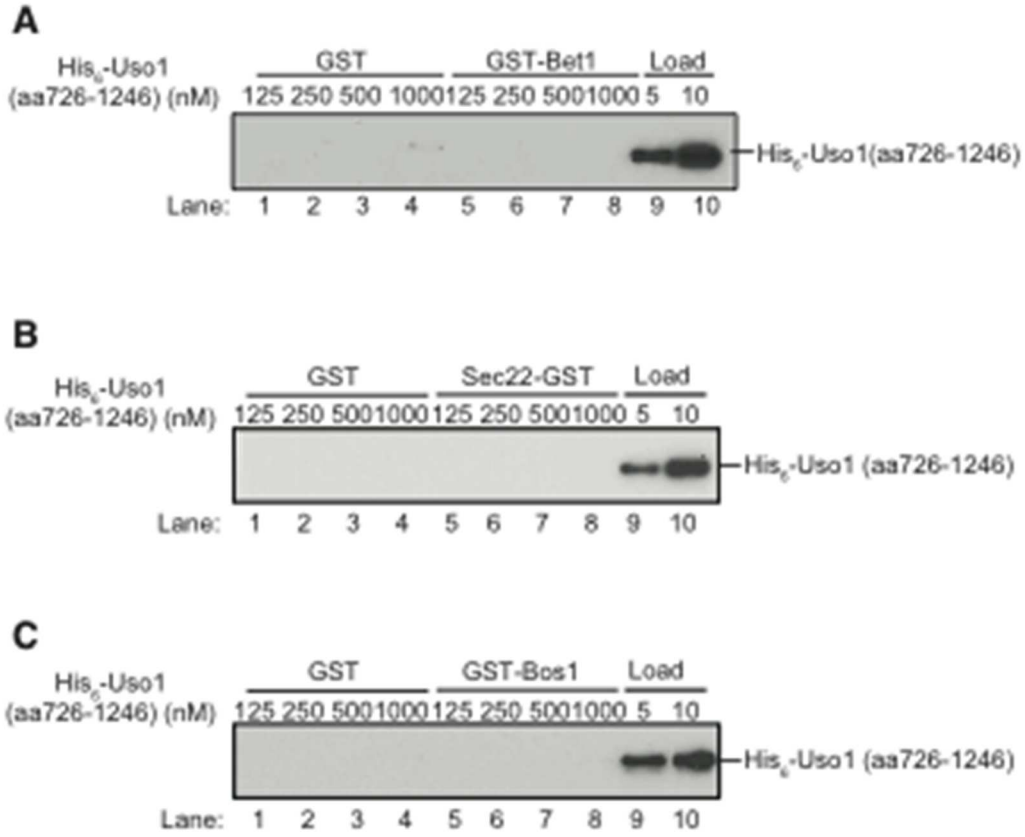

Figure 4.3. Uso1 does not bind Bet1, Bos1 or Sec22.
A Equimolar amounts of GST (lanes 1-4) or GST-Bet1 (lanes 5-8) was incubated with increasing amounts of His_6-Uso1 (aa726-1246). **B** Same as in (A) except Sec22-GST was used. **C** Same as in (A) except GST-Bos1 was used.

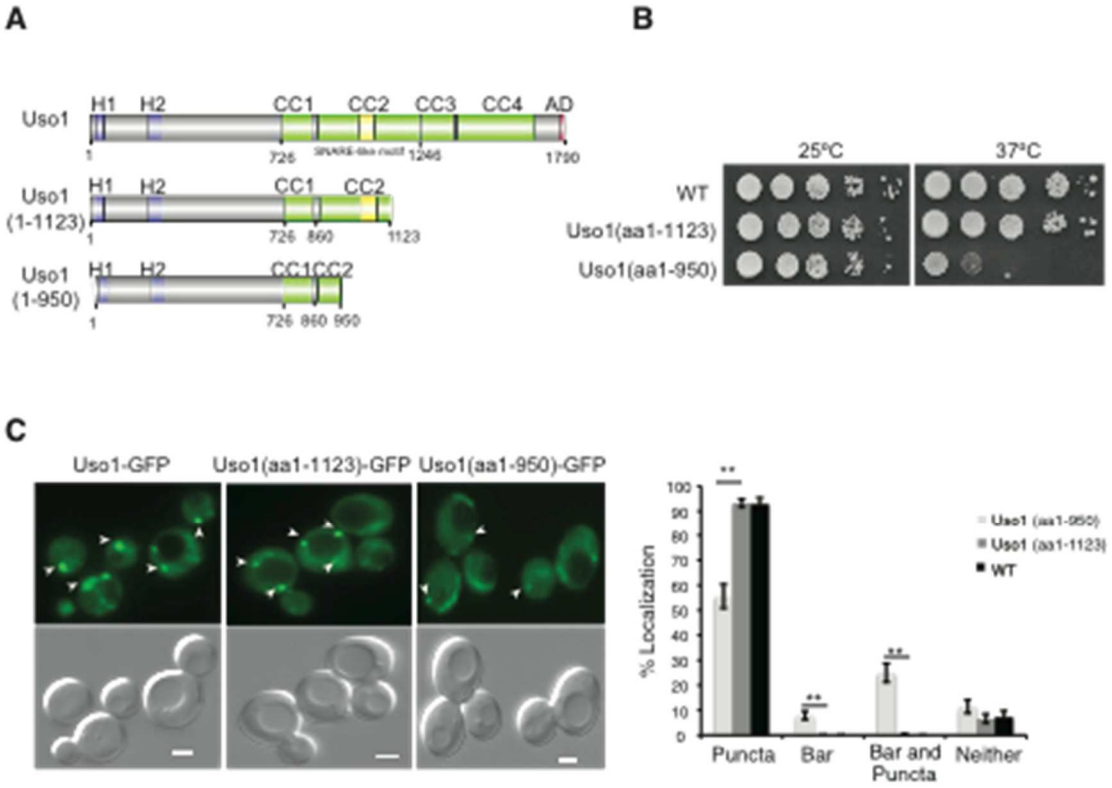

Figure 4.4. Uso1 CC2 is essential for Uso1 function.
A Schematic showing Uso1 truncations. SNARE-like motif shown in yellow. **B** Growth of WT and Uso1 truncations at 25°C (left) and 37°C (right) on a YPD plate. **C** The localization of WT Uso1-GFP and Uso1-GFP truncations was determined in over 300 cells. Scale bar 2 µM. Averages and s.e.m. are shown. **P < 0.01, Student's unpaired t-test.

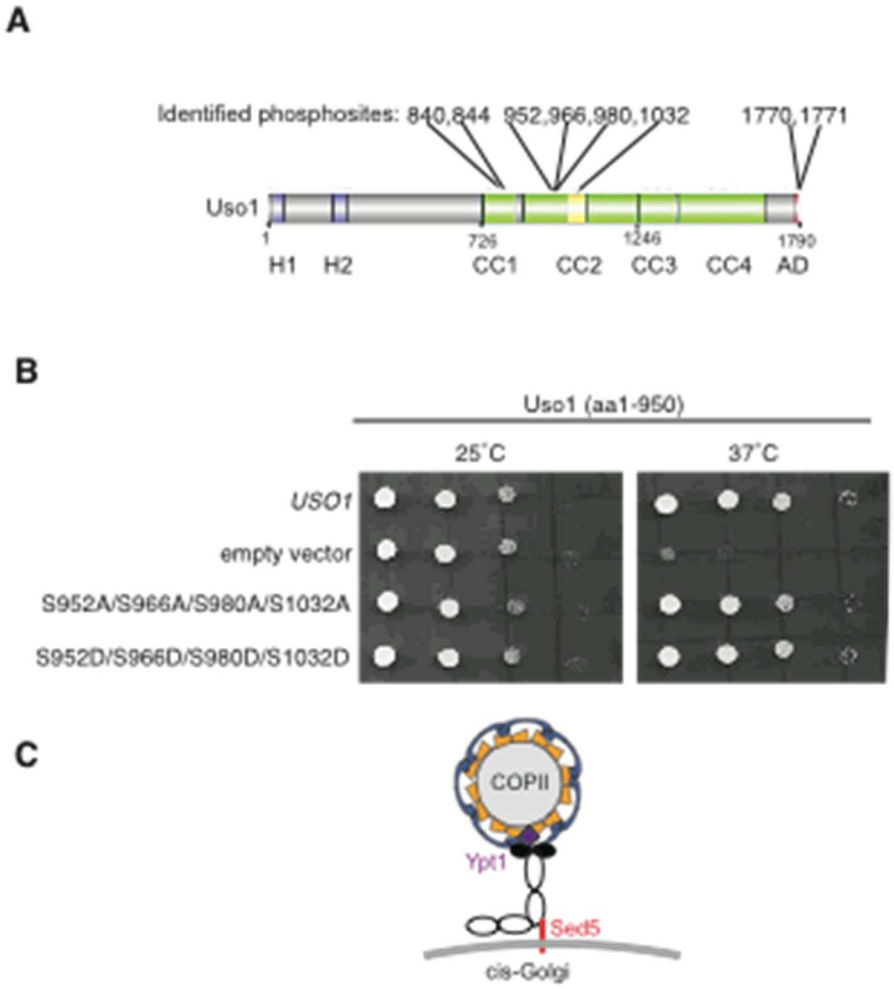

Figure 4.5. Model for Uso1 tethering.
A Location of identified phosphorylation sites on Uso1 schematic. **B** WT *USO1*, empty vector, or *uso1* mutants were transformed into Uso1 (aa1-950) and grown at 25ºC (left) or 37ºC (right). **C** Uso1 head domain interacts with activated Ypt1 on COPII vesicles, while Uso1 CC2 binds to the t-SNARE Sed5 at the target membrane.

4.4 Discussion

Here we have identified both a Ypt1 and Sed5 binding domain in the essential tether Uso1. Although previous work had identified Uso1 as a Ypt1 effector (Cao et al., 1998), how Uso1 interacted with Ypt1 was unknown. Identification of these interactions leads to a model in which Uso1 localizes to the Golgi through interacting with the t-SNARE Sed5 and tethers COPII vesicles by interacting with Ypt1 through its head domain (Figure 4.5; C). Truncating the domain of Uso1 that interacts with Sed5 disrupted growth and Uso1 localization. These findings highlight the conservation in COPII vesicle tethering in yeast and mammalian cells. In mammalian cells, p115 has been reported to bind Rab1 through both its globular head domain and a domain in CC1 (An et al., 2009; Beard et al., 2005). Our findings indicate the Rab binding domain in the head group is conserved and may be the primary Rab binding site. Additionally, although the coiled-coil region of Uso1 is significantly longer and not well conserved, the coiled-coil regions of both Uso1 and p115 contain a SNARE binding domain. Uso1 interacts with the t-SNARE Sed5, while p115 interacts with its mammalian homologue syntaxin-5 and another v-SNARE Gos28 (Shorter et al., 2002).

It is unknown whether Uso1 interacts with other factors on COPII vesicles in addition to Ypt1, in order to enhance its tethering specificity. We were unable to detect a direct interaction between the inner COPII coat, Sec23/Sec24, and Uso1 in vitro (data not shown). Alternatively, Uso1 may indirectly interact with the COPII coat through the nonessential tethers Grh1 and Bug1. Grh1 and Bug1 are thought to

be similar to the Golgins, GRASP65 and GM130, in mammalian cells (Behnia et al., 2007). Interestingly, Grh1 was shown to interact with Sec23/Sec24 and displayed some genetic interactions with Uso1 and Ypt1 (Behnia et al., 2007). Therefore, these non-essential tethers may function with Uso1 to facilitate COPII vesicle tethering, although additional experiments would be required to test this model.

Interestingly, Uso1 is the only essential COPII trafficking component not required for autophagy (Hamasaki et al., 2003; Ishihara et al., 2001; Tan et al., 2013). This finding suggests that COPII vesicle tethering to the Golgi is not required for autophagosome formation. In Chapter 2, we showed that ER-Golgi traffic is disrupted during starvation. Whether this disruption is solely due to COPII vesicles being actively diverted away from the secretory pathway or whether ER-Golgi transport is negatively regulated is unclear. Uso1 could be a potential target for negative regulation during starvation given its critical and specific role in ER-Golgi transport.

The above findings have identified domains of Uso1 that are essential for its tethering function. The globular head domain interacts with Ypt1, while CC2 likely links the vesicle to the Golgi through binding the t-SNARE Sed5. In summary, these findings highlight the highly conserved mechanism of COPII vesicle tethering in yeast and mammalian cells.

4.5 Methods

4.5.1 Immobilization of GST fusion proteins

For purification of GST fusion proteins, BL21(DE3) cells were incubated at 18°C overnight with 0.5 mM isopropyl β-D-1-thiogalactopyranoside to induce protein expression. Cells were collected and resuspended in 1x phosphate-buffered saline (PBS) with 1 mM DTT and protease inhibitors. Cells were sonicated for 2 min total with 15 sec on/off bursts on ice. Triton X-100 was added to a final concentration of 1% and lysates were incubated on ice for 15 min. Lysates were cleared through a 15 min centrifugation at 15,000 rpm. The supernatant was incubated with 1 mL of 50% glutathione sepharose beads (GE Healthcare) that had been prewashed with PBS for 1 h at 4°C with rotation. The beads were washed extensively with PBS and stored at 4°C.

4.5.2 Purification of His_6 fusion proteins

For purification of His_6-tagged fusion proteins, cells were incubated overnight at 18°C with 0.5 mM isopropyl β-D-1-thiogalactopyranoside to induce protein expression. Cells were collected and resuspended in sonication buffer (25 mM Hepes pH 7.4, 150 mM NaCl, 1 mM DTT, 15 mM Imidazole and protease inhibitors). Cells were sonicated for 2 min total with 15 sec on/off bursts on ice. Lysates were cleared through a 15 min centrifugation at 15,000 rpm. The supernatant was incubated with 2 mL of 50% Ni-NTA resin (Qiagen) for 1 h at 4°C with rotation. The Ni-NTA resin was prewashed with sonication buffer. Following binding the resin was washed extensively with sonication buffer. Fusion proteins were eluted off the resin with

sonication buffer containing 250 mM Imidazole. Proteins were buffer exchanged with 20 mM Hepes pH 7.4, 150 mM NaCl. Glycerol was added to a final concentration of 30% and proteins were stored at -20°C.

4.5.3 In vitro bindings with recombinant proteins

Equimolar amounts (0.2 μM) of immobilized GST fusions were incubated with increasing amounts of bacterial purified His_6-Uso1 in binding buffer (25 mM HEPES pH 7.4, 150 mM NaCl, 2% Triton X-100, 1 mM $MgCl_2$, 1 mM EDTA, 1 mM DTT, protease inhibitors) for 4 h at 4°C with rotation. Beads were washed 3 times with binding buffer and eluted in 25 μL of sample buffer by heating for 5 min at 100°C.

Bindings with bacterially purified Ypt1-His_6 were performed as described above except with binding buffer II (25 mM HEPES pH 7.4, 150 mM NaCl, 0.5% Triton X-100, 1 mM $MgCl_2$, 1 mM EDTA, 1 mM DTT, protease inhibitors).

4.5.4 Fluorescence microscopy for Uso1-GFP

Cells were grown at 25°C overnight in YPD to an OD between 0.5-1.0. Cells were visualized with a Carl Zeiss Observer Z.1 spinning-disk confocal fluorescence microscope using DIC or GFP filters with a 100x oil-immersion objective. Images were captured with a Zeiss AxioCam MRm and analyzed using AxioVision Rel. 4.7 software. At least 300 cells were examined.

4.6 Acknowledgements

Some of the work in Chapter 4 was performed by other researchers. Hua Yuan is a co-author of this Chapter.

Hua Yuan, from the lab of Peter Novick, performed the studies with Ypt1-Sw1^{Sec4} that are discussed. Shuliang Chen constructed the Uso1 truncations and Wenyun Zhou constructed some of the Uso1 fusion proteins. Elizabeth Miller provided the Sec22-GST and GST-Bet1 constructs used in this study.

CHAPTER 5

Future Directions and Conclusions

5.1 Summary of past chapters

How intracellular membranes are rearranged to meet the increased demand for autophagosomes during nutrient deprivation is not well understood. A growing consensus in the field is that the ER is the dominant organelle required for autophagosome biogenesis. Recently, specialized subdomains of the ER have also been implicated, including ER exit sites (ERES), which produce COPII vesicles that mediate the forward flow of traffic from the ER to the Golgi (Graef et al., 2013; Suzuki et al., 2013). The COPII coat contains an inner layer composed of the Sec23/Sec24 heterodimer and an outer shell made up of the Sec13/Sec31 heterotetramer. Previous work has shown that mutations that inhibit COPII vesicle production block autophagosome formation (Hamasaki et al., 2003; Ishihara et al., 2001). However, it had previously been difficult to tease apart the function of COPII vesicles during autophagy, as inhibiting the secretory pathway likely has indirect downstream effects on other pathways.

My project was focused on identifying the role of phosphorylation of Sec24, the major cargo adaptor subunit of the COPII coat. We initially ruled out a central role for Sec24 phosphorylation in regulating ER-Golgi transport. Given growing

evidence supporting a role for COPII vesicles in autophagy, we next screened alanine mutations in the conserved Sec24 phosphorylation sites for autophagy defects using the Pho8Δ60 assay. This analysis identified a group of phosphorylation sites, Sec24-T324/T325/T328, which are required for autophagy, but not ER-Golgi transport. Autophagosome formation was analyzed in the Sec24-3A mutant through structured illumination microscopy (SIM) and electron microscopy. Both methods showed a decrease in autophagosome number, but not size, during starvation conditions in the Sec24-3A mutant. We next tested whether Sec24 phosphorylation was functioning in autophagy by regulating the interaction of the COPII coat with the Atg machinery. Through co-immunoprecipitation experiments we confirmed an interaction between Sec24 and Atg9, an essential Atg involved in autophagosome initiation. We next determined that the Sec23/Sec24 complex directly interacts with the C-terminal cytoplasmic domain of Atg9 and Sec24 phosphomimetic mutants enhance the Sec24-Atg9 interaction. Additionally, the co-immunoprecipitation of Atg9 with Sec24 was diminished in the Sec24-3A mutant, demonstrating that phosphorylation of the Sec24 membrane distal sites regulates the Sec24-Atg9 interaction both in vitro and in vivo. Additionally, Sec24-3A did not affect the formation of ERES or assembly of Atg proteins at the PAS.

In Chapter 3 we examined the role of various kinases in regulating the COPII coat and autophagy. Hrr25, part of the casein kinase 1 family, is known to phosphorylate Sec24 (Lord et al., 2011) and was recently shown to be required for autophagy (Wang et al., 2015), but how it acts as a positive regulator of autophagy was unclear. Here we identified Hrr25 in vitro phosphorylation sites on Sec24 and

identified Sec24 T328 as a low confidence site. We next determined that similar to the Sec24-3A mutant, Hrr25 is required for the Sec24-Atg9 interaction in vivo and regulates autophagic body number during starvation. The defective Sec24-Atg9 interaction and autophagy defect in an *hrr25* mutant could be partially rescued by expression of Sec24 T325E/T328E, indicating Hrr25 acts through phosphorylation of Sec24. Although we found that another COPII coat subunit, Lst1, was more phosphorylated during starvation in an Hrr25 dependent manner, Hrr25 expression levels or kinase activity was not affected by starvation. These observations indicate Hrr25 may work with another kinase during autophagy. Atg1, an essential kinase in autophagosome formation, does not directly interact with the COPII coat and does not regulate the phosphorylation of Lst1 during starvation in vivo. These findings suggest that Atg1 is not involved in COPII coat phosphorylation. Additionally, another kinase connected to the TOR network, Nnk1, was examined. Although Nnk1 directly interacts with the COPII coat, Nnk1 is not required for autophagy. Thus future work will be required to identify additional kinases that may work with Hrr25 to phosphorylate the COPII coat during autophagy.

In Chapter 4 we examined the interactions of the COPII vesicle tether Uso1. Interestingly, Uso1 is required for COPII vesicle tethering during secretion but not during autophagy (Tan et al., 2013). Uso1 is an effector of the GTPase Ypt1 (Cao et al., 1998). In vitro bindings revealed that Ypt1 directly interacts with the conserved head domain of Uso1, but not with its coiled-coil domain. The second coiled-coil domain (CC2) contains a SNARE-like motif and this region binds the t-SNARE Sed5, but not other ER-Golgi SNAREs. Uso1 truncations that disrupt the SNARE-like motif

result in a temperature-sensitive growth phenotype and disturb Uso1 localization. Together these results suggest Uso1 tethers COPII vesicles through interacting with Ypt1 on the vesicle through its N-terminal head domain and Sed5 at the target membrane through its CC2 domain.

5.2 Future Directions

5.2.1 SNAREs required for Atg9-COPII vesicle fusion

The precise membrane fusion events that occur during autophagosome formation have been difficult to uncover. Our findings support a model where Atg9 and COPII vesicles fuse at an early stage of autophagosome formation. Testing this model through in vitro reconstitution of COPII and Atg9 vesicles is not technically feasible at the moment. Although the core of Atg9 has been able to be expressed in liposomes (Rao et al., 2016), this portion does not contain the Atg9 C-terminal domain, which interacts with Sec24. Efforts are currently underway to express Atg9 with its C-terminus in liposomes. COPII vesicles can be generated in vitro from microsomal membranes with purified coat proteins (Miller et al., 2002). If full-length Atg9 can be expressed in liposomes, the interaction between Atg9 and COPII vesicles can be determined in vitro through co-immunoprecipitation experiments. This study would further support our model that COPII and Atg9 vesicles directly interact as Atg9 and the COPII coat would be in a more physiological state compared with purified proteins.

An additional limitation for examining fusion between Atg9 and COPII vesicles in vitro is that we do not know which SNAREs are present on Atg9 vesicles at

the PAS. Current candidates for regulating the fusion of COPII vesicles with Atg9 containing membranes are the ER-Golgi SNAREs (Sed5, Bet1, Bos1 and Sec22) and the ER-derived SNARE Ufe1, which are required for autophagy and are packaged into COPII vesicles (Lemus et al., 2016; Tan et al., 2013). It is thought that Atg9 vesicles are derived from the late-Golgi in yeast (Ohashi and Munro, 2010; Yamamoto et al., 2012), so these vesicles may contain Golgi SNAREs, although this has not been verified.

If a SNARE were required for Atg9 fusion at the PAS, we would expect that Atg9 could traffic to the PAS, but fusion at the PAS would be blocked. Therefore, the localization of Atg9 during starvation in temperature-sensitive SNARE mutants could be tested to determine if they affect Atg9 retrograde trafficking. Atg9 anterograde versus retrograde trafficking is commonly tested in an epistasis experiment that examines the localization of Atg9 in a WT and *atg1*Δ background. In an *atg1*Δ background Atg9 accumulates at the PAS (Sekito et al., 2009), therefore if a SNARE is required for Atg9 trafficking to the PAS, Atg9 will fail to accumulate in a SNARE *atg1*Δ double mutant. However, if the SNARE is required after Atg9 has been trafficked to the PAS, Atg9 will accumulate at the PAS in a SNARE mutant as well as in a SNARE *atg1*Δ double mutant. Similarly, it would be expected that COPII coated structures would accumulate at the PAS in temperature-sensitive SNARE mutants required for COPII fusion during autophagy. Although indirect, these findings would provide evidence that SNAREs block the fusion of COPII vesicles and Atg9 membranes at the PAS.

Recent work has indicated that the ER-localized SNARE Ufe1 is delivered to the vacuole during starvation in a manner dependent on the COPII coat (Lemus et al., 2016). It would be interesting to determine if the ER-Golgi SNAREs are also delivered to the vacuole during starvation, as this would suggest that these SNAREs reside on the autophagosome. To test this hypothesis the localization of GFP tagged SNAREs could be examined during starvation. Blocking autophagosome formation through an *atg* mutant should block their delivery to the vacuole. Similarly, it would be important to determine whether their delivery to the vacuole is dependent on COPII vesicle budding. However, some proteins involved in autophagosome formation are retrieved from the autophagosomal membrane before fusion with the vacuole by an unknown mechanism. Therefore, this experiment is limited, as a lack of SNARE delivery to the vacuole does not demonstrate these SNAREs are not temporarily localized to the isolation membrane. Consequently, the colocalization of GFP tagged SNAREs with the autophagosome marker Atg8 should also be examined during starvation. These colocalization experiments should be performed in an *ypt7*Δ background in order to enhance the number of autophagosomes in the cell. Additionally, it would be important to determine whether this colocalization is dependent on COPII or Atg9 vesicle formation.

5.2.2 Involvement of other CK1 family members in autophagy

Hrr25 is part of a larger family of casein kinases in yeast, consisting of Yck1/2 and Yck3 (Wang et al., 1996). These kinases have been implicated in a variety of membrane trafficking events and mass-spectrometry screens have identified

interactions between these kinases and the Atg machinery (Breitkreutz et al., 2010; Graef et al., 2013; Ptacek et al., 2005). Consequentially, it is tempting to speculate that these kinases function with Hrr25 in autophagy either through working with Hrr25 to regulate Sec24 phosphorylation or by acting at a different stage of autophagosome formation.

Pho8Δ60 activity and GFP-Atg8 cleavage could be assayed to determine whether these kinases are required for autophagy. As Yck1 and Yck2 are redundant (Wang et al., 1996) these assays should be performed in a *yck1Δ/yck2-ts* and *yck3Δ* background. If the kinases are required for autophagy, it will be critical to subsequently determine if they are required for autophagosome formation or autophagosome fusion with the vacuole. In particular, Yck3 localizes to the vacuole and regulates the HOPS tethering complex (LaGrassa and Ungermann, 2005), indicating it could act at the autophagosome-vacuole fusion step. To separate these stages, autophagosome formation should be visualized by structured illumination microscopy (SIM) in a WT and *ypt7Δ* background, which inhibits autophagosome-vacuole fusion (Kirisako et al., 1999). Alternatively electron microscopy can be performed to determine if autophagosomes accumulate in the cytoplasm in a kinase mutant during starvation. Additionally, as Yck1/2 are involved in glucose sensing (Reddi and Culotta, 2013), they may be required upstream of autophagosome initiation for nutrient sensing. To determine whether autophagy is induced normally, the phosphorylation state of Atg13 can be examined by western blot. Atg13 is commonly used to test for autophagy induction because during nutrient rich conditions Atg13 is

phosphorylated by TOR, but is rapidly dephosphorylated upon autophagy induction (Miller-Fleming et al., 2014).

If these kinases are directly required for autophagosome formation, it will be necessary to determine whether they also regulate the Sec24-Atg9 interaction through co-immunoprecipitation experiments in a kinase mutant. If they regulate the Sec24-Atg9 interaction, it would suggest Hrr25 is acting with CK1 family members to phosphorylate Sec24 during autophagy. In vitro kinase assays would need to be performed to determine whether Sec24 is a direct substrate of the kinase. Additionally, it would be important to determine whether the activity of the kinase is regulated during starvation through in vitro kinase assays comparing kinase immunoprecipitated from yeast in nutrient rich or starvation conditions. If these other CK1 kinases are required at a similar stage of autophagy as Hrr25, it will be interesting to determine if the CK1 family members can compensate for Hrr25 during autophagy. To test this idea, GFP-Atg8 cleavage or Pho8Δ60 activity could be assayed in an *hrr25* mutant, overexpressing the CK1 family member on a 2μM vector.

If these kinases are not regulating autophagosome formation through Sec24 phosphorylation, they may act by phosphorylating one of the Atgs identified as interacting by mass spectrometry screens. Examining the assembly of the Atg hierarchy at the PAS by fluorescence in a kinase mutant would be a helpful starting point to determine which Atg complexes are affected by these kinases.

5.2.3 Conserved role for Sec24-Atg9 in autophagy

ERES and COPII vesicles have been shown to play an important role in autophagy in mammalian cells (Ge et al., 2014; Graef et al., 2013; Zoppino et al., 2010), but it is unclear how the COPII coat interacts with the Atg machinery in higher eukaryotes. Given that the phosphorylation sites on Sec24 are conserved and the mammalian homologue of Hrr25, CK1∂, has many conserved roles, it is likely that the events described here are conserved. In order to determine whether the Sec24-Atg9 interaction is conserved in mammals, tagged mAtg9 could be immunoprecipitated from cell lysates with and without starvation and blotted for mSec24. Furthermore, the larger size of mammalian cells would permit a more detailed visualization of the relationship between the COPII coat, Atg9, and the growing isolation membrane during starvation. It has been reported that the COPII coat subunit Sec31 relocalizes to the ER-Golgi intermediate compartment (ERGIC) during autophagy (Ge et al., 2014). It will be important to determine whether Sec31 also colocalizes with Atg9 during starvation. If they colocalize, live-cell imaging could be used to examine possible fusion events between these two vesicle classes during starvation.

To determine whether CK1∂ is required for autophagy in mammalian cells, CK1∂ can be knockdown through siRNA and the formation of GFP-LC3 puncta can be quantitated during starvation. This experiment should be done in the presence and absence of bafilomycin, a H^+ ATPase inhibitor, which prevents autophagosome degradation (Klionsky et al. 2013). This would distinguish between a defect in autophagosome formation and a defect in autophagosomal flux. Other assays should

be used to confirm the role of CK1∂ in autophagy, including monitoring the degradation of long-lived proteins or p62, which are delivered to the lysosome after autophagy induction (Klionsky et al. 2013). In yeast, mutations in Hrr25 do not affect PAS assembly, but dramatically inhibit the PAS recruitment of Atg8, the most downstream Atg (Wang et al., 2015). Consequently, if CK1∂ were required for autophagosome formation, we would predict it might function after or independently of omegasome formation. To test this, formation of the omegasome can be visualized in CK1∂ knockdown cells through DFCP1 labeling. DFCP1 is a PI(3)P binding protein commonly used as an omegasome marker (Axe et al., 2008).

5.2.4 Role of COPII vesicles in selective autophagy

The events described here are for the non-selective autophagy pathway that is rapidly upregulated during starvation. Phosphorylation of Sec24 does not appear to be required for the cytoplasmic to vacuole targeting pathway (Cvt) (Figure 2.8), a type of selective autophagy that targets the cargo Ape1 to the vacuole for processing during nutrient rich conditions (Lynch-Day and Klionsky, 2010). Although the Cvt pathway is commonly used as a model for selective autophagy, other selective autophagy pathways degrade larger cargo and are induced under different types of cellular stress. As a result, it is conceivable that other selective autophagy pathways employ different mechanisms of autophagosome formation from the Cvt pathway. It is unknown whether COPII vesicles are required for other types of selective autophagy and more specifically whether phosphorylation of Sec24 is needed.

To determine whether phosphorylation of Sec24 is required for other forms of selective autophagy we can examine the degradation of specific cargo for autophagy of the ER (ER-phagy), mitochondria (mitophagy) or peroxisomes (pexophagy) in the Sec24-3A mutant. ER-phagy is induced in yeast through long-term rapamycin treatment and the cleavage of the ER proteins Sec63-GFP or Rtn1-GFP can be examined by fluorescence or western blot (Mochida et al., 2015). Mitophagy can be induced through extended growth in a non-fermentable carbon source such as glycerol and monitored through examining the cleavage of the mitochondrial matrix-targeted DHFR-mCherry or Idh1-GFP (Kondo-Okamoto et al., 2012). Pexophagy is initiated through inducing peroxisome proliferation by growth in oleate medium and then shifting to nitrogen starvation media. Alternatively long-term growth in oleate medium can be used (Motley et al., 2012). Cleavage of Pex11-GFP is typically examined to monitor pexophagy (Motley et al., 2012). These studies would clarify whether phosphorylation of Sec24 is involved in other types of selective autophagy.

Another possibility is that COPII vesicles are required on other selective autophagy pathways, but Sec24 does not need to be phosphorylated. To distinguish between these possibilities a more general COPII vesicle mutant should be tested for selective autophagy defects. However, most COPII trafficking components are essential and as a result temperature-sensitive mutants are used. As cells can only tolerate short shifts to the restrictive temperature, these temperature-sensitive mutants cannot be tested for the selective autophagy pathways described above, which require extended induction times. Therefore, nonessential COPII trafficking machinery must

be examined. These include Trs85, the TRAPPIII specific subunit, *ypt1*-2 a non temperature-sensitive allele that affects non-selective autophagy (Wang et al., 2013) or the ER-Golgi SNARE Sec22. Additionally, it was recently reported that *sec23-1* displays autophagy defects at the permissive temperature when secretion is normal (Lemus et al., 2016) and therefore could used to examine selective autophagy. These studies would help clarify the contribution of the early secretory pathway to selective autophagy as well as provide a better understanding of the underlying mechanisms of autophagosome formation in non-selective and selective autophagy.

5.3 Concluding Remarks

This dissertation shows that phosphorylation of the COPII coat subunit Sec24 is required for autophagy through regulating the interaction between the COPII coat and Atg9. Additionally, we find that the casein kinase, Hrr25, regulates the Sec24-Atg9 interaction through Sec24 phosphorylation and that these events are required for autophagy. These studies identify a novel role for the COPII coat in actively targeting the vesicle on the autophagy pathway and begin to dissect how COPII vesicles are trafficked during starvation. These results are likely to be conserved given the importance of COPII vesicles and Atg9 in mammalian autophagy. Although these findings represent an important step forward in our understanding of membrane trafficking events during autophagosome formation, many questions still remain. Future studies will be required to understand membrane fusion events during autophagosome formation as well as to identify additional kinases that may work with Hrr25 to regulate its function during starvation.

REFERENCES

Allan, B.B., B.D. Moyer, and W.E. Balch. 2000. Rab1 recruitment of p115 into a cis-SNARE complex: programming budding COPII vesicles for fusion. *Science*. 289:444-8.

Alvarez, C., H. Fujita, A. Hubbard, and E. Sztul. 1999. ER to Golgi transport: Requirement for p115 at a pre-Golgi VTC stage. *J Cell Biol*. 147:1205-22.

An, Y., C.Y. Chen, B. Moyer, P. Rotkiewicz, M.A. Elsliger, A. Godzik, I.A. Wilson, and W.E. Balch. 2009. Structural and functional analysis of the globular head domain of p115 provides insight into membrane tethering. *J Mol Biol*. 391:26-41.

Anand, V.C., L. Daboussi, T.C. Lorenz, and G.S. Payne. 2009. Genome-wide analysis of AP-3-dependent protein transport in yeast. *Mol Biol Cell*. 20:1592-604.

Axe, E.L., S.A. Walker, M. Manifava, P. Chandra, H.L. Roderick, A. Habermann, G. Griffiths, and N.T. Ktistakis. 2008. Autophagosome formation from membrane compartments enriched in phosphatidylinositol 3-phosphate and dynamically connected to the endoplasmic reticulum. *J Cell Biol*. 182:685-701.

Backues, S.K., D. Chen, J. Ruan, Z. Xie, and D.J. Klionsky. 2013. Estimating the size and number of autophagic bodies by electron microscopy. *Autophagy*. 10:155-64.

Backues, S.K., D.P. Orban, A. Bernard, K. Singh, Y. Cao, and D.J. Klionsky. 2015. Atg23 and Atg27 act at the early stages of Atg9 trafficking in S. cerevisiae. *Traffic*. 16:172-90.

Balderhaar, H.J., and C. Ungermann. 2013. CORVET and HOPS tethering complexes - coordinators of endosome and lysosome fusion. *J Cell Sci*. 126:1307-16.

Barlowe, C., L. Orci, T. Yeung, M. Hosobuchi, S. Hamamoto, N. Salama, M.F. Rexach, M. Ravazzola, M. Amherdt, and R. Schekman. 1994. COPII: a membrane coat formed by Sec proteins that drive vesicle budding from the endoplasmic reticulum. *Cell*. 77:895-907.

Barrowman, J., D. Bhandari, K. Reinisch, and S. Ferro-Novick. 2010. TRAPP complexes in membrane traffic: convergence through a common Rab. *Nat Rev Mol Cell Biol*. 11:759-63.

Bassik, M.C., M. Kampmann, R.J. Lebbink, S. Wang, M.Y. Hein, I. Poser, J. Weibezahn, M.A. Horlbeck, S. Chen, M. Mann, A.A. Hyman, E.M. Leproust, M.T. McManus, and J.S. Weissman. 2013. A systematic mammalian genetic interaction map reveals pathways underlying ricin susceptibility. *Cell*. 152:909-22.

Beard, M., A. Satoh, J. Shorter, and G. Warren. 2005. A cryptic Rab1-binding site in the p115 tethering protein. *J Biol Chem*. 280:25840-8.

Behnia, R., F.A. Barr, J.J. Flanagan, C. Barlowe, and S. Munro. 2007. The yeast orthologue of GRASP65 forms a complex with a coiled-coil protein that contributes to ER to Golgi traffic. *J Cell Biol*. 176:255-61.

Bhandari, D., J. Zhang, S. Menon, C. Lord, S. Chen, J.R. Helm, K. Thorsen, K.D. Corbett, J.C. Hay, and S. Ferro-Novick. 2013. Sit4p/PP6 regulates ER-to-Golgi traffic by controlling the dephosphorylation of COPII coat subunits. *Mol Biol Cell*. 24:2727-38.

Bi, X., J.D. Mancias, and J. Goldberg. 2007. Insights into COPII coat nucleation from the structure of Sec23.Sar1 complexed with the active fragment of Sec31. *Dev Cell*. 13:635-45.

Bockler, S., and B. Westermann. 2014. Mitochondrial ER contacts are crucial for mitophagy in yeast. *Dev Cell*. 28:450-8.

Bodemann, B.O., A. Orvedahl, T. Cheng, R.R. Ram, Y.H. Ou, E. Formstecher, M. Maiti, C.C. Hazelett, E.M. Wauson, M. Balakireva, J.H. Camonis, C. Yeaman, B. Levine, and M.A. White. 2011. RalB and the exocyst mediate the cellular starvation response by direct activation of autophagosome assembly. *Cell*. 144:253-67.

Breitkreutz, A., H. Choi, J.R. Sharom, L. Boucher, V. Neduva, B. Larsen, Z.Y. Lin, B.J. Breitkreutz, C. Stark, G. Liu, J. Ahn, D. Dewar-Darch, T. Reguly, X. Tang, R. Almeida, Z.S. Qin, T. Pawson, A.C. Gingras, A.I. Nesvizhskii, and M. Tyers. 2010. A global protein kinase and phosphatase interaction network in yeast. *Science*. 328:1043-6.

Brennwald, P., and P. Novick. 1993. Interactions of three domains distinguishing the Ras-related GTP-binding proteins Ypt1 and Sec4. *Nature*. 362:560-3.

Budnik, A., and D.J. Stephens. 2009. ER exit sites--localization and control of COPII vesicle formation. *FEBS Lett*. 583:3796-803.

Cai, H., S. Yu, S. Menon, Y. Cai, D. Lazarova, C. Fu, K. Reinisch, J.C. Hay, and S. Ferro-Novick. 2007. TRAPPI tethers COPII vesicles by binding the coat subunit Sec23. *Nature*. 445:941-4.

Cao, X., N. Ballew, and C. Barlowe. 1998. Initial docking of ER-derived vesicles requires Uso1p and Ypt1p but is independent of SNARE proteins. *EMBO J*. 17:2156-65.

Chen, Y., F. Zhou, S. Zou, S. Yu, S. Li, D. Li, J. Song, H. Li, Z. He, B. Hu, L.O. Bjorn, Z. Lipatova, Y. Liang, Z. Xie, and N. Segev. 2014. A Vps21 endocytic module regulates autophagy. *Mol Biol Cell*. 25:3166-77.

DeMaggio, A.J., R.A. Lindberg, T. Hunter, and M.F. Hoekstra. 1992. The budding yeast HRR25 gene product is a casein kinase I isoform. *Proc Natl Acad Sci U S A*. 89:7008-12.

Diao, J., R. Liu, Y. Rong, M. Zhao, J. Zhang, Y. Lai, Q. Zhou, L.M. Wilz, J. Li, S. Vivona, R.A. Pfuetzner, A.T. Brunger, and Q. Zhong. 2015. ATG14 promotes membrane tethering and fusion of autophagosomes to endolysosomes. *Nature*. 520:563-6.

Dong, G., M. Medkova, P. Novick, and K.M. Reinisch. 2007. A catalytic coiled coil: structural insights into the activation of the Rab GTPase Sec4p by Sec2p. *Mol Cell*. 25:455-62.

Dooley, H.C., M. Razi, H.E. Polson, S.E. Girardin, M.I. Wilson, and S.A. Tooze. 2014. WIPI2 links LC3 conjugation with PI3P, autophagosome formation, and pathogen clearance by recruiting Atg12-5-16L1. *Mol Cell*. 55:238-52.

Feng, Y., S.K. Backues, M. Baba, J.M. Heo, J.W. Harper, and D.J. Klionsky. 2016. Phosphorylation of Atg9 regulates movement to the phagophore assembly site and the rate of autophagosome formation. *Autophagy*. 12:648-58.

Fujita, N., T. Itoh, H. Omori, M. Fukuda, T. Noda, and T. Yoshimori. 2008. The Atg16L complex specifies the site of LC3 lipidation for membrane biogenesis in autophagy. *Mol Biol Cell*. 19:2092-100.

Ge, L., D. Melville, M. Zhang, and R. Schekman. 2013. The ER-Golgi intermediate compartment is a key membrane source for the LC3 lipidation step of autophagosome biogenesis. *Elife*. 2:e00947.

Ge, L., M. Zhang, and R. Schekman. 2014. Phosphatidylinositol 3-kinase and COPII generate LC3 lipidation vesicles from the ER-Golgi intermediate compartment. *Elife*. 3:e04135.

Geng, J., U. Nair, K. Yasumura-Yorimitsu, and D.J. Klionsky. 2010. Post-Golgi Sec proteins are required for autophagy in Saccharomyces cerevisiae. *Mol Biol Cell*. 21:2257-69.

Gillingham, A.K., A.H. Tong, C. Boone, and S. Munro. 2004. The GTPase Arf1p and the ER to Golgi cargo receptor Erv14p cooperate to recruit the golgin Rud3p to the cis-Golgi. *J Cell Biol*. 167:281-92.

Graef, M., J.R. Friedman, C. Graham, M. Babu, and J. Nunnari. 2013. ER exit sites are physical and functional core autophagosome biogenesis components. *Mol Biol Cell*. 24:2918-31.

Guttman, M., G.N. Betts, H. Barnes, M. Ghassemian, P. van der Geer, and E.A. Komives. 2009. Interactions of the NPXY microdomains of the low density lipoprotein receptor-related protein 1. *Proteomics*. 9:5016-28.

Hale, A.N., D.J. Ledbetter, T.R. Gawriluk, and E.B. Rucker, 3rd. 2013. Autophagy: regulation and role in development. *Autophagy*. 9:951-72.

Hamasaki, M., N. Furuta, A. Matsuda, A. Nezu, A. Yamamoto, N. Fujita, H. Oomori, T. Noda, T. Haraguchi, Y. Hiraoka, A. Amano, and T. Yoshimori. 2013. Autophagosomes form at ER-mitochondria contact sites. *Nature*. 495:389-93.

Hamasaki, M., T. Noda, and Y. Ohsumi. 2003. The early secretory pathway contributes to autophagy in yeast. *Cell Struct Funct*. 28:49-54.

Hanada, T., N.N. Noda, Y. Satomi, Y. Ichimura, Y. Fujioka, T. Takao, F. Inagaki, and Y. Ohsumi. 2007. The Atg12-Atg5 conjugate has a novel E3-like activity for protein lipidation in autophagy. *J Biol Chem*. 282:37298-302.

Hayashi-Nishino, M., N. Fujita, T. Noda, A. Yamaguchi, T. Yoshimori, and A. Yamamoto. 2009. A subdomain of the endoplasmic reticulum forms a cradle for autophagosome formation. *Nat Cell Biol*. 11:1433-7.

He, C., M. Baba, Y. Cao, and D.J. Klionsky. 2008. Self-interaction is critical for Atg9 transport and function at the phagophore assembly site during autophagy. *Mol Biol Cell*. 19:5506-16.

He, C., H. Song, T. Yorimitsu, I. Monastyrska, W.L. Yen, J.E. Legakis, and D.J. Klionsky. 2006. Recruitment of Atg9 to the preautophagosomal structure by Atg11 is essential for selective autophagy in budding yeast. *J Cell Biol*. 175:925-35.

Hong, W., and S. Lev. 2014. Tethering the assembly of SNARE complexes. *Trends Cell Biol*. 24:35-43.

Hosokawa, N., T. Hara, T. Kaizuka, C. Kishi, A. Takamura, Y. Miura, S. Iemura, T. Natsume, K. Takehana, N. Yamada, J.L. Guan, N. Oshiro, and N. Mizushima. 2009. Nutrient-dependent mTORC1 association with the ULK1-Atg13-FIP200 complex required for autophagy. *Mol Biol Cell*. 20:1981-91.

Huang, J., C.L. Birmingham, S. Shahnazari, J. Shiu, Y.T. Zheng, A.C. Smith, K.G. Campellone, W.D. Heo, S. Gruenheid, T. Meyer, M.D. Welch, N.T. Ktistakis, P.K. Kim, D.J. Klionsky, and J.H. Brumell. 2011. Antibacterial autophagy occurs at PI(3)P-enriched domains of the endoplasmic reticulum and requires Rab1 GTPase. *Autophagy*. 7:17-26.

Hutagalung, A.H., and P.J. Novick. 2011. Role of Rab GTPases in membrane traffic and cell physiology. *Physiol Rev*. 91:119-49.

Ishihara, N., M. Hamasaki, S. Yokota, K. Suzuki, Y. Kamada, A. Kihara, T. Yoshimori, T. Noda, and Y. Ohsumi. 2001. Autophagosome requires specific early Sec proteins for its formation and NSF/SNARE for vacuolar fusion. *Mol Biol Cell*. 12:3690-702.

Jahn, R., and R.H. Scheller. 2006. SNAREs--engines for membrane fusion. *Nat Rev Mol Cell Biol*. 7:631-43.

Jiang, P., T. Nishimura, Y. Sakamaki, E. Itakura, T. Hatta, T. Natsume, and N. Mizushima. 2014. The HOPS complex mediates autophagosome-lysosome fusion through interaction with syntaxin 17. *Mol Biol Cell*. 25:1327-37.

Jin, M., D. He, S.K. Backues, M.A. Freeberg, X. Liu, J.K. Kim, and D.J. Klionsky. 2014. Transcriptional regulation by Pho23 modulates the frequency of autophagosome formation. *Curr Biol*. 24:1314-22.

Joo, J.H., B. Wang, E. Frankel, L. Ge, L. Xu, R. Iyengar, X. Li-Harms, C. Wright, T.I. Shaw, T. Lindsten, D.R. Green, J. Peng, L.M. Hendershot, F. Kilic, J.Y. Sze, A. Audhya, and M. Kundu. 2016. The Noncanonical Role of ULK/ATG1 in ER-to-Golgi Trafficking Is Essential for Cellular Homeostasis. *Mol Cell*. 62:491-506.

Jung, C.H., C.B. Jun, S.H. Ro, Y.M. Kim, N.M. Otto, J. Cao, M. Kundu, and D.H. Kim. 2009. ULK-Atg13-FIP200 complexes mediate mTOR signaling to the autophagy machinery. *Mol Biol Cell*. 20:1992-2003.

Juris, L., M. Montino, P. Rube, P. Schlotterhose, M. Thumm, and R. Krick. 2015. PI3P binding by Atg21 organises Atg8 lipidation. *EMBO J*. 34:955-73.

Kakuta, S., H. Yamamoto, L. Negishi, C. Kondo-Kakuta, N. Hayashi, and Y. Ohsumi. 2012. Atg9 vesicles recruit vesicle-tethering proteins Trs85 and Ypt1 to the autophagosome formation site. *J Biol Chem*. 287:44261-9.

Kamada, Y., T. Funakoshi, T. Shintani, K. Nagano, M. Ohsumi, and Y. Ohsumi. 2000. Tor-mediated induction of autophagy via an Apg1 protein kinase complex. *J Cell Biol*. 150:1507-13.

Kawamata, T., Y. Kamada, Y. Kabeya, T. Sekito, and Y. Ohsumi. 2008. Organization of the pre-autophagosomal structure responsible for autophagosome formation. *Mol Biol Cell*. 19:2039-50.

Kirisako, T., M. Baba, N. Ishihara, K. Miyazawa, M. Ohsumi, T. Yoshimori, T. Noda, and Y. Ohsumi. 1999. Formation process of autophagosome is traced with Apg8/Aut7p in yeast. *J Cell Biol*. 147:435-46.

Klionsky, D.J. 2007. Monitoring autophagy in yeast: the Pho8Delta60 assay. *Methods Mol Biol*. 390:363-71.

Klionsky, D.J., K. Abdelmohsen, A. Abe, M.J. Abedin, H. Abeliovich, A. Acevedo Arozena, H. Adachi, C.M. Adams, P.D. Adams, K. Adeli, P.J. Adhihetty, S.G. Adler, G. Agam, R. Agarwal, M.K. Aghi, M. Agnello, P. Agostinis, P.V. Aguilar, J. Aguirre-Ghiso, E.M. Airoldi, S. Ait-Si-Ali, T. Akematsu, E.T. Akporiaye, M. Al-Rubeai, G.M. Albaiceta, C. Albanese, D. Albani, M.L. Albert, J. Aldudo, H. Algul, M. Alirezaei, I. Alloza, A. Almasan, M. Almonte-Beceril, E.S. Alnemri, C. Alonso, N. Altan-Bonnet, D.C. Altieri, S. Alvarez, L. Alvarez-Erviti, S. Alves, G. Amadoro, A. Amano, C. Amantini, S. Ambrosio, I. Amelio, A.O. Amer, M. Amessou, A. Amon, Z. An, F.A. Anania, S.U. Andersen, U.P. Andley, C.K. Andreadi, N. Andrieu-Abadie, A. Anel, D.K. Ann, S. Anoopkumar-Dukie, M. Antonioli, H. Aoki, N. Apostolova, S. Aquila, K. Aquilano, K. Araki, E. Arama, A. Aranda, J. Araya, A. Arcaro, E. Arias, H. Arimoto, A.R. Ariosa, J.L. Armstrong, T. Arnould, I. Arsov, K. Asanuma, V. Askanas, E. Asselin, R. Atarashi, S.S. Atherton, J.D. Atkin, L.D. Attardi, P. Auberger, G. Auburger, L. Aurelian, R. Autelli, L. Avagliano, M.L. Avantaggiati, L. Avrahami, S. Awale, N. Azad, T. Bachetti, J.M. Backer, D.H. Bae, J.S. Bae, O.N. Bae, S.H. Bae, E.H. Baehrecke, S.H. Baek, S. Baghdiguian, A. Bagniewska-Zadworna, et al. Guidelines for the use and interpretation of assays for monitoring autophagy (3rd edition). *Autophagy*. 12:1-222.

Klionsky, D.J., A.M. Cuervo, and P.O. Seglen. 2007. Methods for monitoring autophagy from yeast to human. *Autophagy*. 3:181-206.

Knaevelsrud, H., K. Soreng, C. Raiborg, K. Haberg, F. Rasmuson, A. Brech, K. Liestol, T.E. Rusten, H. Stenmark, T.P. Neufeld, S.R. Carlsson, and A. Simonsen. 2013. Membrane remodeling by the PX-BAR protein SNX18 promotes autophagosome formation. *J Cell Biol*. 202:331-49.

Knippschild, U., A. Gocht, S. Wolff, N. Huber, J. Lohler, and M. Stoter. 2005. The casein kinase 1 family: participation in multiple cellular processes in eukaryotes. *Cell Signal*. 17:675-89.

Kondo-Okamoto, N., N.N. Noda, S.W. Suzuki, H. Nakatogawa, I. Takahashi, M. Matsunami, A. Hashimoto, F. Inagaki, Y. Ohsumi, and K. Okamoto. 2012. Autophagy-related protein 32 acts as autophagic degron and directly initiates mitophagy. *J Biol Chem*. 287:10631-8.

Kuma, A., N. Mizushima, N. Ishihara, and Y. Ohsumi. 2002. Formation of the approximately 350-kDa Apg12-Apg5.Apg16 multimeric complex, mediated by Apg16 oligomerization, is essential for autophagy in yeast. *J Biol Chem*. 277:18619-25.

Kurihara, T., S. Hamamoto, R.E. Gimeno, C.A. Kaiser, R. Schekman, and T. Yoshihisa. 2000. Sec24p and Iss1p function interchangeably in transport vesicle formation from the endoplasmic reticulum in Saccharomyces cerevisiae. *Mol Biol Cell*. 11:983-98.

LaGrassa, T.J., and C. Ungermann. 2005. The vacuolar kinase Yck3 maintains organelle fragmentation by regulating the HOPS tethering complex. *J Cell Biol*. 168:401-14.

Lamb, C.A., S. Nuhlen, D. Judith, D. Frith, A.P. Snijders, C. Behrends, and S.A. Tooze. 2016. TBC1D14 regulates autophagy via the TRAPP complex and ATG9 traffic. *EMBO J*. 35:281-301.

Lamb, C.A., T. Yoshimori, and S.A. Tooze. 2013. The autophagosome: origins unknown, biogenesis complex. *Nat Rev Mol Cell Biol*. 14:759-74.

Legakis, J.E., W.L. Yen, and D.J. Klionsky. 2007. A cycling protein complex required for selective autophagy. *Autophagy*. 3:422-32.

Lemus, L., J.L. Ribas, N. Sikorska, and V. Goder. 2016. An ER-Localized SNARE Protein Is Exported in Specific COPII Vesicles for Autophagosome Biogenesis. *Cell Rep*. 14:1710-22.

Loewith, R., and M.N. Hall. 2011. Target of rapamycin (TOR) in nutrient signaling and growth control. *Genetics*. 189:1177-201.

Longatti, A., C.A. Lamb, M. Razi, S. Yoshimura, F.A. Barr, and S.A. Tooze. 2012. TBC1D14 regulates autophagosome formation via Rab11- and ULK1-positive recycling endosomes. *J Cell Biol*. 197:659-75.

Lord, C., D. Bhandari, S. Menon, M. Ghassemian, D. Nycz, J. Hay, P. Ghosh, and S. Ferro-Novick. 2011. Sequential interactions with Sec23 control the direction of vesicle traffic. *Nature*. 473:181-6.

Lord, C., S. Ferro-Novick, and E.A. Miller. 2013. The highly conserved COPII coat complex sorts cargo from the endoplasmic reticulum and targets it to the golgi. *Cold Spring Harb Perspect Biol*. 5.

Lorente-Rodriguez, A., and C. Barlowe. 2011. Entry and exit mechanisms at the cis-face of the Golgi complex. *Cold Spring Harb Perspect Biol*. 3.

Lynch-Day, M.A., D. Bhandari, S. Menon, J. Huang, H. Cai, C.R. Bartholomew, J.H. Brumell, S. Ferro-Novick, and D.J. Klionsky. 2010. Trs85 directs a Ypt1 GEF, TRAPPIII, to the phagophore to promote autophagy. *Proc Natl Acad Sci U S A*. 107:7811-6.

Lynch-Day, M.A., and D.J. Klionsky. 2010. The Cvt pathway as a model for selective autophagy. *FEBS Lett*. 584:1359-66.

McEwan, D.G., D. Popovic, A. Gubas, S. Terawaki, H. Suzuki, D. Stadel, F.P. Coxon, D. Miranda de Stegmann, S. Bhogaraju, K. Maddi, A. Kirchof, E. Gatti, M.H. Helfrich, S. Wakatsuki, C. Behrends, P. Pierre, and I. Dikic. 2015. PLEKHM1

regulates autophagosome-lysosome fusion through HOPS complex and LC3/GABARAP proteins. *Mol Cell*. 57:39-54.

Meyer, J.G., S. Kim, D. Maltby, M. Ghassemian, N. Bandeira, and E.A. Komives. 2014. Expanding proteome coverage with orthogonal-specificity alpha-lytic proteases. *Mol Cell Proteomics*.

Miller, E., B. Antonny, S. Hamamoto, and R. Schekman. 2002. Cargo selection into COPII vesicles is driven by the Sec24p subunit. *EMBO J*. 21:6105-13.

Miller, E.A., T.H. Beilharz, P.N. Malkus, M.C. Lee, S. Hamamoto, L. Orci, and R. Schekman. 2003. Multiple cargo binding sites on the COPII subunit Sec24p ensure capture of diverse membrane proteins into transport vesicles. *Cell*. 114:497-509.

Miller, E.A., Y. Liu, C. Barlowe, and R. Schekman. 2005. ER-Golgi transport defects are associated with mutations in the Sed5p-binding domain of the COPII coat subunit, Sec24p. *Mol Biol Cell*. 16:3719-26.

Miller-Fleming, L., H. Cheong, P. Antas, and D.J. Klionsky. 2014. Detection of Saccharomyces cerevisiae Atg13 by western blot. *Autophagy*. 10:514-7.

Mizuno-Yamasaki, E., F. Rivera-Molina, and P. Novick. 2012. GTPase networks in membrane traffic. *Annu Rev Biochem*. 81:637-59.

Mizushima, N., T. Yoshimori, and Y. Ohsumi. 2011. The role of Atg proteins in autophagosome formation. *Annu Rev Cell Dev Biol*. 27:107-32.

Mochida, K., Y. Ohsumi, and H. Nakatogawa. 2014. Hrr25 phosphorylates the autophagic receptor Atg34 to promote vacuolar transport of alpha-mannosidase under nitrogen starvation conditions. *FEBS Lett*. 588:3862-9.

Mochida, K., Y. Oikawa, Y. Kimura, H. Kirisako, H. Hirano, Y. Ohsumi, and H. Nakatogawa. 2015. Receptor-mediated selective autophagy degrades the endoplasmic reticulum and the nucleus. *Nature*. 522:359-62.

Moreau, K., B. Ravikumar, M. Renna, C. Puri, and D.C. Rubinsztein. 2011. Autophagosome precursor maturation requires homotypic fusion. *Cell*. 146:303-17.

Moskalenko, S., D.O. Henry, C. Rosse, G. Mirey, J.H. Camonis, and M.A. White. 2002. The exocyst is a Ral effector complex. *Nat Cell Biol*. 4:66-72.

Moskalenko, S., C. Tong, C. Rosse, G. Mirey, E. Formstecher, L. Daviet, J. Camonis, and M.A. White. 2003. Ral GTPases regulate exocyst assembly through dual subunit interactions. *J Biol Chem*. 278:51743-8.

Mossessova, E., L.C. Bickford, and J. Goldberg. 2003. SNARE selectivity of the COPII coat. *Cell*. 114:483-95.

Motley, A.M., J.M. Nuttall, and E.H. Hettema. 2012. Pex3-anchored Atg36 tags peroxisomes for degradation in Saccharomyces cerevisiae. *EMBO J*. 31:2852-68.

Munson, M., and P. Novick. 2006. The exocyst defrocked, a framework of rods revealed. *Nat Struct Mol Biol*. 13:577-81.

Murakami, A., K. Kimura, and A. Nakano. 1999. The inactive form of a yeast casein kinase I suppresses the secretory defect of the sec12 mutant. Implication of negative regulation by the Hrr25 kinase in the vesicle budding from the endoplasmic reticulum. *J Biol Chem*. 274:3804-10.

Nair, U., A. Jotwani, J. Geng, N. Gammoh, D. Richerson, W.L. Yen, J. Griffith, S. Nag, K. Wang, T. Moss, M. Baba, J.A. McNew, X. Jiang, F. Reggiori, T.J. Melia, and D.J. Klionsky. 2011. SNARE proteins are required for macroautophagy. *Cell*. 146:290-302.

Nakamura, N., M. Lowe, T.P. Levine, C. Rabouille, and G. Warren. 1997. The vesicle docking protein p115 binds GM130, a cis-Golgi matrix protein, in a mitotically regulated manner. *Cell*. 89:445-55.

Nakatogawa, H., Y. Ichimura, and Y. Ohsumi. 2007. Atg8, a ubiquitin-like protein required for autophagosome formation, mediates membrane tethering and hemifusion. *Cell*. 130:165-78.

Nakatogawa, H., K. Suzuki, Y. Kamada, and Y. Ohsumi. 2009. Dynamics and diversity in autophagy mechanisms: lessons from yeast. *Nat Rev Mol Cell Biol*. 10:458-67.

Nishimura, T., T. Kaizuka, K. Cadwell, M.H. Sahani, T. Saitoh, S. Akira, H.W. Virgin, and N. Mizushima. 2013. FIP200 regulates targeting of Atg16L1 to the isolation membrane. *EMBO Rep*. 14:284-91.

Noda, N.N., Y. Fujioka, T. Hanada, Y. Ohsumi, and F. Inagaki. 2013. Structure of the Atg12-Atg5 conjugate reveals a platform for stimulating Atg8-PE conjugation. *EMBO Rep*. 14:206-11.

Obara, K., T. Sekito, K. Niimi, and Y. Ohsumi. 2008. The Atg18-Atg2 complex is recruited to autophagic membranes via phosphatidylinositol 3-phosphate and exerts an essential function. *J Biol Chem*. 283:23972-80.

Ohashi, Y., and S. Munro. 2010. Membrane delivery to the yeast autophagosome from the Golgi-endosomal system. *Mol Biol Cell*. 21:3998-4008.

Orsi, A., M. Razi, H.C. Dooley, D. Robinson, A.E. Weston, L.M. Collinson, and S.A. Tooze. 2012. Dynamic and transient interactions of Atg9 with autophagosomes, but not membrane integration, are required for autophagy. *Mol Biol Cell*. 23:1860-73.

Pagant, S., A. Wu, S. Edwards, F. Diehl, and E.A. Miller. 2015. Sec24 is a coincidence detector that simultaneously binds two signals to drive ER export. *Curr Biol*. 25:403-12.

Papinski, D., M. Schuschnig, W. Reiter, L. Wilhelm, C.A. Barnes, A. Majolica, I. Hansmann, T. Pfaffenwimmer, M. Kijanska, I. Stoffel, S.S. Lee, A. Brezovich, J.H. Lou, B.E. Turk, R. Aebersold, G. Ammerer, M. Peter, and C. Kraft. 2014. Early Steps in Autophagy Depend on Direct Phosphorylation of Atg9 by the Atg1 Kinase. *Mol Cell*.

Phillips, M.J., and G.K. Voeltz. 2014. Structure and function of ER membrane contact sites with other organelles. *Nat Rev Mol Cell Biol*. 17:69-82.

Popovic, D., and I. Dikic. 2014. TBC1D5 and the AP2 complex regulate ATG9 trafficking and initiation of autophagy. *EMBO Rep*. 15:392-401.

Ptacek, J., G. Devgan, G. Michaud, H. Zhu, X. Zhu, J. Fasolo, H. Guo, G. Jona, A. Breitkreutz, R. Sopko, R.R. McCartney, M.C. Schmidt, N. Rachidi, S.J. Lee, A.S. Mah, L. Meng, M.J. Stark, D.F. Stern, C. De Virgilio, M. Tyers, B. Andrews, M. Gerstein, B. Schweitzer, P.F. Predki, and M. Snyder. 2005. Global analysis of protein phosphorylation in yeast. *Nature*. 438:679-84.

Puri, C., M. Renna, C.F. Bento, K. Moreau, and D.C. Rubinsztein. 2013. Diverse autophagosome membrane sources coalesce in recycling endosomes. *Cell*. 154:1285-99.

Qi, S., J. Kim do, G. Stjepanovic, and J.H. Hurley. 2015. Structure of the Human Atg13-Atg101 HORMA Heterodimer: an Interaction Hub within the ULK1 Complex. *Structure*. 23:1848-57.

Ragusa, M.J., R.E. Stanley, and J.H. Hurley. 2012. Architecture of the Atg17 complex as a scaffold for autophagosome biogenesis. *Cell*. 151:1501-12.

Rao, Y., M.G. Perna, B. Hofmann, V. Beier, and T. Wollert. 2016. The Atg1-kinase complex tethers Atg9-vesicles to initiate autophagy. *Nat Commun*. 7:10338.

Ravikumar, B., K. Moreau, L. Jahreiss, C. Puri, and D.C. Rubinsztein. 2010. Plasma membrane contributes to the formation of pre-autophagosomal structures. *Nat Cell Biol*. 12:747-57.

Reddi, A.R., and V.C. Culotta. 2013. SOD1 integrates signals from oxygen and glucose to repress respiration. *Cell*. 152:224-35.

Reggiori, F., K.A. Tucker, P.E. Stromhaug, and D.J. Klionsky. 2004. The Atg1-Atg13 complex regulates Atg9 and Atg23 retrieval transport from the pre-autophagosomal structure. *Dev Cell*. 6:79-90.

Rieder, S.E., and S.D. Emr. 1997. A novel RING finger protein complex essential for a late step in protein transport to the yeast vacuole. *Mol Biol Cell*. 8:2307-27.

Sanchez-Wandelmer, J., N.T. Ktistakis, and F. Reggiori. 2015. ERES: sites for autophagosome biogenesis and maturation? *J Cell Sci*. 128:185-92.

Schneider, J.L., and A.M. Cuervo. 2014. Autophagy and human disease: emerging themes. *Curr Opin Genet Dev*. 26:16-23.

Scrivens, P.J., B. Noueihed, N. Shahrzad, S. Hul, S. Brunet, and M. Sacher. 2011. C4orf41 and TTC-15 are mammalian TRAPP components with a role at an early stage in ER-to-Golgi trafficking. *Mol Biol Cell*. 22:2083-93.

Sekito, T., T. Kawamata, R. Ichikawa, K. Suzuki, and Y. Ohsumi. 2009. Atg17 recruits Atg9 to organize the pre-autophagosomal structure. *Genes Cells*. 14:525-38.

Shindiapina, P., and C. Barlowe. 2010. Requirements for transitional endoplasmic reticulum site structure and function in Saccharomyces cerevisiae. *Mol Biol Cell*. 21:1530-45.

Shirahama-Noda, K., S. Kira, T. Yoshimori, and T. Noda. 2013. TRAPPIII is responsible for vesicular transport from early endosomes to Golgi, facilitating Atg9 cycling in autophagy. *J Cell Sci*. 126:4963-73.

Shorter, J., M.B. Beard, J. Seemann, A.B. Dirac-Svejstrup, and G. Warren. 2002. Sequential tethering of Golgins and catalysis of SNAREpin assembly by the vesicle-tethering protein p115. *J Cell Biol*. 157:45-62.

Sica, V., L. Galluzzi, J.M. Bravo-San Pedro, V. Izzo, M.C. Maiuri, and G. Kroemer. 2015. Organelle-Specific Initiation of Autophagy. *Mol Cell*. 59:522-39.

Stadel, D., V. Millarte, K.D. Tillmann, J. Huber, B.C. Tamin-Yecheskel, M. Akutsu, A. Demishtein, B. Ben-Zeev, Y. Anikster, F. Perez, V. Dotsch, Z. Elazar, V. Rogov, H. Farhan, and C. Behrends. 2015. TECPR2 Cooperates with LC3C to Regulate COPII-Dependent ER Export. *Mol Cell*. 60:89-104.

Stalder, D., and P.J. Novick. 2016. The casein kinases Yck1p and Yck2p act in the secretory pathway, in part, by regulating the Rab exchange factor Sec2p. *Mol Biol Cell*. 27:686-701.

Stolz, A., A. Ernst, and I. Dikic. 2014. Cargo recognition and trafficking in selective autophagy. *Nat Cell Biol*. 16:495-501.

Suzuki, K., M. Akioka, C. Kondo-Kakuta, H. Yamamoto, and Y. Ohsumi. 2013. Fine mapping of autophagy-related proteins during autophagosome formation in Saccharomyces cerevisiae. *J Cell Sci*. 126:2534-44.

Suzuki, K., Y. Kubota, T. Sekito, and Y. Ohsumi. 2007. Hierarchy of Atg proteins in pre-autophagosomal structure organization. *Genes Cells*. 12:209-18.

Suzuki, S.W., H. Yamamoto, Y. Oikawa, C. Kondo-Kakuta, Y. Kimura, H. Hirano, and Y. Ohsumi. 2015. Atg13 HORMA domain recruits Atg9 vesicles during autophagosome formation. *Proc Natl Acad Sci U S A*. 112:3350-5.

Swaney, D.L., P. Beltrao, L. Starita, A. Guo, J. Rush, S. Fields, N.J. Krogan, and J. Villen. 2013. Global analysis of phosphorylation and ubiquitylation cross-talk in protein degradation. *Nat Methods*. 10:676-82.

Takahashi, Y., N. Tsotakos, Y. Liu, M.M. Young, J. Serfass, Z. Tang, T. Abraham, and H.G. Wang. 2016. The Bif-1-Dynamin 2 membrane fission machinery regulates Atg9-containing vesicle generation at the Rab11-positive reservoirs. *Oncotarget*. 7:20855-68.

Takats, S., K. Pircs, P. Nagy, A. Varga, M. Karpati, K. Hegedus, H. Kramer, A.L. Kovacs, M. Sass, and G. Juhasz. 2014. Interaction of the HOPS complex with Syntaxin 17 mediates autophagosome clearance in Drosophila. *Mol Biol Cell*. 25:1338-54.

Tan, D., Y. Cai, J. Wang, J. Zhang, S. Menon, H.T. Chou, S. Ferro-Novick, K.M. Reinisch, and T. Walz. 2013. The EM structure of the TRAPPIII complex leads to the identification of a requirement for COPII vesicles on the macroautophagy pathway. *Proc Natl Acad Sci U S A*. 110:19432-7.

Tanaka, C., L.J. Tan, K. Mochida, H. Kirisako, M. Koizumi, E. Asai, M. Sakoh-Nakatogawa, Y. Ohsumi, and H. Nakatogawa. 2014. Hrr25 triggers selective autophagy-related pathways by phosphorylating receptor proteins. *J Cell Biol*. 207:91-105.

Tracy, K., P.D. Velentzas, and E.H. Baehrecke. 2016. Ral GTPase and the exocyst regulate autophagy in a tissue-specific manner. *EMBO Rep*. 17:110-21.

Wang, J., S. Davis, S. Menon, J. Zhang, J. Ding, S. Cervantes, E. Miller, Y. Jiang, and S. Ferro-Novick. 2015. Ypt1/Rab1 regulates Hrr25/CK1delta kinase activity in ER-Golgi traffic and macroautophagy. *J Cell Biol*. 210:273-85.

Wang, J., S. Menon, A. Yamasaki, H.T. Chou, T. Walz, Y. Jiang, and S. Ferro-Novick. 2013. Ypt1 recruits the Atg1 kinase to the preautophagosomal structure. *Proc Natl Acad Sci U S A*. 110:9800-5.

Wang, X., M.F. Hoekstra, A.J. DeMaggio, N. Dhillon, A. Vancura, J. Kuret, G.C. Johnston, and R.A. Singer. 1996. Prenylated isoforms of yeast casein kinase I, including the novel Yck3p, suppress the gcs1 blockage of cell proliferation from stationary phase. *Mol Cell Biol*. 16:5375-85.

Weimbs, T., S.H. Low, S.J. Chapin, K.E. Mostov, P. Bucher, and K. Hofmann. 1997. A conserved domain is present in different families of vesicular fusion proteins: a new superfamily. *Proc Natl Acad Sci U S A*. 94:3046-51.

Weinberger, A., F. Kamena, R. Kama, A. Spang, and J.E. Gerst. 2005. Control of Golgi morphology and function by Sed5 t-SNARE phosphorylation. *Mol Biol Cell*. 16:4918-30.

Willett, R., D. Ungar, and V. Lupashin. 2013. The Golgi puppet master: COG complex at center stage of membrane trafficking interactions. *Histochem Cell Biol*. 140:271-83.

Xie, Z., U. Nair, and D.J. Klionsky. 2008. Atg8 controls phagophore expansion during autophagosome formation. *Mol Biol Cell*. 19:3290-8.

Yamamoto, H., S. Kakuta, T.M. Watanabe, A. Kitamura, T. Sekito, C. Kondo-Kakuta, R. Ichikawa, M. Kinjo, and Y. Ohsumi. 2012. Atg9 vesicles are an important membrane source during early steps of autophagosome formation. *J Cell Biol*. 198:219-33.

Yamasaki, A., S. Menon, S. Yu, J. Barrowman, T. Meerloo, V. Oorschot, J. Klumperman, A. Satoh, and S. Ferro-Novick. 2009. mTrs130 is a component of a mammalian TRAPPII complex, a Rab1 GEF that binds to COPI-coated vesicles. *Mol Biol Cell*. 20:4205-15.

Yen, W.L., T. Shintani, U. Nair, Y. Cao, B.C. Richardson, Z. Li, F.M. Hughson, M. Baba, and D.J. Klionsky. 2010. The conserved oligomeric Golgi complex is involved in double-membrane vesicle formation during autophagy. *J Cell Biol*. 188:101-14.

Young, A.R., E.Y. Chan, X.W. Hu, R. Kochl, S.G. Crawshaw, S. High, D.W. Hailey, J. Lippincott-Schwartz, and S.A. Tooze. 2006. Starvation and ULK1-dependent cycling of mammalian Atg9 between the TGN and endosomes. *J Cell Sci*. 119:3888-900.

Yu, S., and M.G. Roth. 2002. Casein kinase I regulates membrane binding by ARF GAP1. *Mol Biol Cell*. 13:2559-70.

Zanetti, G., K.B. Pahuja, S. Studer, S. Shim, and R. Schekman. 2011. COPII and the regulation of protein sorting in mammals. *Nat Cell Biol*. 14:20-8.

Zhen, Y., and W. Li. 2015. Impairment of autophagosome-lysosome fusion in the buff mutant mice with the VPS33A(D251E) mutation. *Autophagy*. 11:1608-22.

Zoppino, F.C., R.D. Militello, I. Slavin, C. Alvarez, and M.I. Colombo. 2010. Autophagosome formation depends on the small GTPase Rab1 and functional ER exit sites. *Traffic*. 11:1246-61.